Role of TNFα and hepatic glutamine synthetase in pathogenesis of hepatic encephalopathy.

Inaugural-Dissertation

zur Erlangung des Doktorgrades
der Mathematisch-Naturwissenschaftlichen Fakultät
der Heinrich-Heine-Universität Düsseldorf

vorgelegt von

Vitaly Pozdeev
aus Pavlograd, USSR

Düsseldorf, October 2018

aus dem Institut für Molekulare Medizin II
der Heinrich-Heine-Universität Düsseldorf

Gedruckt mit der Genehmigung der
Mathematisch-Naturwissenschaftlichen Fakultät der
Heinrich-Heine-Universität Düsseldorf

Berichterstatter:

1.Prof. Dr. Philipp Lang

2. Prof. Dr. Eckhard Lammert

Tag der mündlichen Prüfung: 11.10.2018
(bitte bei der Abgabe Ihrer Dissertation noch offen lassen)
(bitte bei der Abgabe Ihrer Dissertation noch offen lassen)

Table of content

Table of figures

List of tables

Abstract

Hepatic encephalopathy is neurological complication frequently observed during acute or chronic liver injury. Up to 60% of patients with cirrhosis develop symptoms of hepatic encephalopathy. Hepatic encephalopathy is a clinical manifestation of a low-grade cerebral edema associated with astrocyte swelling, oxidative/nitrosative stress in brain tissue, alterations in gene expression, and signal transduction, neurotransmission, impaired motor functions, and altered behavioral patterns. Importantly, ammonia is known to be the main precipitating factor of hepatic encephalopathy.

The main hepatic mechanism to detoxify ammonia is the urea cycle. Ammonia not used by the urea cycle is taken up by periveneous hepatocytes and detoxified by conjugation to glutamate, resulting in glutamine. This reaction is catalyzed by hepatic glutamine synthetase.

In order to investigate role of hepatic glutamine synthetase in the pathogenesis of hepatic encephalopathy, we created conditional knockout mice that lacked glutamine synthetase only in the liver. We demonstrated that absence of hepatic glutamine synthetase in the perivenous area of liver is sufficient to trigger systemic hyperammonemia *in vivo*. Hyperammonemia in hepatic glutamine synthetase deficient mice was associated with enhanced RNA oxidation in the brain, increased locomotion, impaired memory of fear, and a slightly reduced lifespan.

Concentrations of tumor necrosis factor in patients' blood correlate with the severity of hepatic encephalopathy, however, the exact mechanism by which TNFα is involved in the pathogenesis of hepatic encephalopathy remains unknown. We found that ammonia metabolism is impaired in TNFα-deficient mice as well as in TNFR1 &

TNFR2 double knockout mice. On the other side TNFα-deficient mice and TNFR1-deficient mice were protected against acute ammonia intoxication. Protection of TNFα-deficient mice against an NH_4^+ intoxication was associated with decreased cerebral expression of the ammonia permeable $Na^+,K^+,2Cl^-$ cotransporter. In addition, pharmacological inhibition of the $Na^+,K^+,2Cl^-$ cotransporter reduced duration of coma during ammonia intoxication.

Taken together, the findings presented in this Ph.D. thesis decipher the role of hepatic glutamine synthetase and TNFα in ammonia homeostasis and pathogenesis of hepatic encephalopathy.

Zusammenfassung

Die hepatische Enzephalopathie (HE) ist eine neurologische Erkrankung, die häufig während eines akuten oder chronischen Leberschaden auftritt. Bis zu 60% der Patienten mit einer Leberzirrhose entwickeln die Symptome einer hepatischen Enzephalopathie. Die hepatische Enzephalopathie ist eine klinische Manifestation eines geringgradigen Hirnödems, das mit Astrozytenschwellung, zerebralem oxidativem / nitrosativem Stress im somatosensorischen Kortex assoziiert ist. Daraus folgend ist die HE mit Veränderungen in der Genexpression, Signaltransduktion und Neurotransmission sowie einer Beeinträchtigung von Lokomotion und Verhalten assoziiert. Ammoniak ist als wichtiger Faktor identifiziert worden, der die hepatische Enzephalopathie induziert. In der Leber wird Ammoniak hauptsächlich über den Harnstoffzyklus entgiftet. Ammoniak, der nicht im Harnstoffzyklus entfernt wurde, wird von perivenös-lokalisierten Hepatozyten aufgenommen und dort für die Glutaminsynthese genutzt, wobei Ammoniak durch die Kopplung an Glutamat entgiftet wird. Diese Reaktion wird von der Glutaminsynthetase katalysiert.

Um die Rolle der hepatischen Glutaminsynthetase in der Pathogenese der hepatischen Enzephalopathie zu untersuchen, haben wir konditionale Knockout-Mäuse hergestellt, denen die Glutaminsynthetase leberspezifisch fehlt. Wir konnten zeigen, dass das Fehlen von der hepatischen Glutaminsynthetase im perivenösen Bereich der Leber ausreicht, um eine systemische Hyperammonämie *in vivo* auszulösen. Die Hyperammonämie in leberspezifischen Glutaminsynthetase-defizienten Mäusen war mit einer verstärkten RNA-Oxidation, sowie mit einer erhöhten Fortbewegung, einem beeinträchtigten Angstgedächtnis und einer leicht verringerten Lebensdauer verbunden.

Die Konzentrationen des Tumornekrosefaktors im Blut von Patienten korreliert mit dem Schweregrad der hepatischen Enzephalopathie, jedoch ist der genaue Mechanismus, durch den TNFα an der Pathogenese der hepatischen Enzephalopathie beteiligt ist, unbekannt. Wir konnten feststellen, dass der Ammoniak-Metabolismus in TNFα -defizienten Mäusen sowie in TNFR1 & TNFR2 Doppel-Knockout-Mäusen beeinträchtigt ist.

Auf der anderen Seite waren TNFα -defiziente Mäuse und TNFR1-defiziente Mäuse gegen eine akute Ammoniakintoxikation geschützt. Der Schutz von TNFα-defizienten Mäusen gegen eine NH_4^+ -Vergiftung war mit einer verminderten zerebralen Expression von Ammoniak-durchlässigen Na^+, K^+, $2Cl^-$ Co-Transporter assoziiert. Pharmakologische Inhibierung von Na^+, K^+, $2Cl^-$ Co-Transporter während der Ammoniakintoxikation reduzierte die Dauer des Ammoniak-induzierten Komas.

Zusammengefasst, entschlüsselt diese Doktorarbeit die Rolle der leberspezifischen Glutaminsynthetase und TNFα in der systemischen Ammoniakhomöostase und der Pathogenese der hepatischen Enzephalopathie.

Acknowledgment

First, I would like to thank my supervisor Prof. Dr. Philipp Lang for his help and useful discussions during my thesis work and especially for his help with publishing our results. Working in your lab allowed me to be a part of very inspiring team and to participate in multiple exciting projects and publications.

I would also like to thank Prof. Dr. Eckhard Lammert for being my supervisor and finding time for me and my thesis.

I want to thank Prof. Karl Lang, Prof. Florian Lang, Prof. Dieter Haussinger, Dr. Boris Goerg, and Dr. Hans Bidmon for fruitful discussions and collaborations, experimental help, and sharing ideas and reagents.

Dr. Elizabeth Lang, thank you for our collaboration. I am very happy that we worked together and could publish several papers.

Prashant Shinde, you were an awesome lab-mate as well as the best Best Man.

Bala, Chris, Dave, Eugene, George, Jun, Junnat, Marina, Krissy, Marc, Renan, Sathish, and Yuan, I want to thank you all for your help with the experiments and fun we had together.

I would particularly like to acknowledge my wife Melanie. Thank you for your everyday support and help. Meeting you was the best thing that ever happened to me.

Я хочу сказать спасибо моей семье: маме Ирине, папе Игорю, бабушке Люде, дедушке Виталию и Марине. Без вашей помощи я бы никогда не оказался там где я сейчас, спасибо за вашу поддержку и помощь во всем. Я всегда помню и думаю о вас.

List of abbreviations

8-H(d)G	8-Hydroxydeoxyguanosine 8-Oxo- 2´- deoxyguanosine
8-OHG	8-Hydroxyguanosine
A	Adenine
ALF	Acute liver failure
APAF-1	Apoptotic protease activating factor 1
APC	Antigen presenting cell
APC(wnt)	Adenomatous polyposis coli
AQP	Aquaporin
ARG	Arginase 1
ASL	Argininosuccinate lyase
ASS	Argininosuccinate synthetase
ATP	Adenosine triphosphate
BBB	Blood–brain barrier
BCAA	Branched-chain amino acid
Bcl-2	B-cell lymphoma 2
BDL	Bile duct ligation
BID	BH3 interacting-domain death agonist
C	Cytosine
C3	Complement component 3
CCL	C-C chemokine ligand
CCR	C-C chemokine receptors
CD	Cluster of differentiation
CFF	Critical flicker frequency
cFLIP	Cellular FLICE inhibitory protein
cIAP	Cellular Inhibitor of Apoptosis Protein 1
CNS	Central nervous system
CPS-1	Carbamoyl phosphate synthase I
CRIg	Complement Receptor of the Immunoglobulin superfamily
CTL	Cytotoxic T lymphocyte
CTLA-4	Cytotoxic T-lymphocyte-associated protein 4
CXCL	Chemokine (C-X-C motif) ligand
DcR	Decoy receptor
DISC	Death-inducing signaling complex
DKK1	Dickkopf-related protein 1
DNA	Deoxyribonucleic acid
DR	Death receptor
ER	Endoplasmic reticulum
FAD	Flavin adenine dinucleotide
FADD	Fas-associated protein with death domain
Fas	First apoptosis signal
FasL	Fas ligand
Fc	Fragment crystallizable
G	Guanine
GABA	Gamma-Aminobutyric acid
D-Gal	D-Galactosamine
GLAST	Glutamate aspartate transporter
GLT-1	Glutamate transporter 1
GS	Glutamine synthetase

HBV	Hepatitis B virus
HCC	Hepatocellular carcinoma
HCV	Hepatitis C virus
HE	Hepatic encephalopathy
HIF-1alpha	Hypoxia-inducible factor 1-alpha
HSC	Hepatic stellate cells
ICAM-1	Intercellular Adhesion Molecule 1
IFNa	Interferon alfa
IFNγ	Interferon gamma
IkBa	Nf-kB inhibitor alpha
Ikk	IκB kinase
IL	Interleukin
iNKT	Invariant natural killer
KC	Kupffer cells
Lag-3	Lymphocyte-activation gene 3
LOLA	L-ornithine l aspartate
LPS	Lipopolysaccharide
LSEC	Liver sinusoidal endothelial cells
MHC	Major histocompatibility complex
MMP	Matrix metalloproteinase
mRNA	Messenger RNA
MTF-1	Metal regulatory transcription factor 1
NADPH	Nicotinamide adenine dinucleotide phosphate
NAFDL	Non-alcoholic fatty liver disease
NASH	Non-alcoholic fatty liver disease
Nf-kB	Nuclear factor kappa-light-chain-enhancer of activated B cells
NK	Natural killer
NKCC	Na-K-Cl co-transporter
NKT	Natural killer T cells
NMDA	N-methyl-D-aspartate receptor
OPG	Osteoprotegerin
ORNT1	Ornithine translocase
OTC	Ornithine transcarbamylase
PD-1	Programmed cell death protein 1
PD-L1	Programmed death-ligand 1
PRR	Pattern recognition receptor
PTN	Protein tyrosine nitration
RIPK	Receptor-interacting serine/threonine-protein kinase 1
RNA	Ribonucleic acid
RNOS	Reactive Nitrogen Oxide Species
rRNA	Ribosomal ribonucleic acid
Sp1	Specificity protein 1
T	Thymine
TACE	Tumor necrosis factor-alpha-converting enzyme
TGFb	Transforming growth factor beta
Th	T helper
TIM-3	T-cell immunoglobulin and mucin-domain containing-3
TCR	T-cell receptor
TLR	Toll-like receptor
TNFα	Tumor necrosis factor alpha

TNFR	Tumor necrosis factor receptor
TRADD	TNFR1-associated death domain protein
TRAF	TNF receptor associated factor
TRAIL	TNF-related apoptosis-inducing ligand
VEGF	Vascular endothelial growth factor

1. Introduction

1.1 Liver anatomy.

1.1.1 Gross anatomy.

Mouse liver occupies the anterior third of the abdominal cavity and consists of four lobes: the undivided left lateral lobe, the caudate lobe subdivided into dorsal and ventral parts, the right lobe divided horizontally into anterior and posterior parts, and the median lobe subdivided into right and left parts.[1] Blood is supplied through branches of the hepatic artery and hepatic portal vein. The portal vein delivers blood from the spleen and gastrointestinal tract. The gall bladder is located in the bifurcation of the median lobe. The cystic duct from the gall bladder joins the hepatic duct from the liver and together, they form a common bile duct.[1]

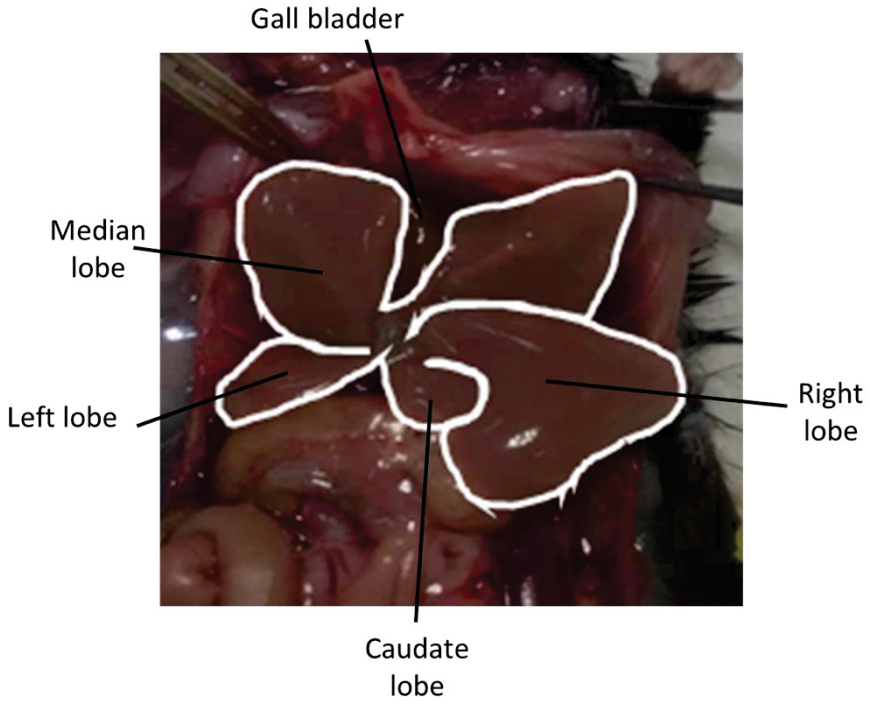

Figure 1.1: Liver anatomy [2]

1.1.2 Cellular anatomy.

The liver is formed by the following cell types: parenchymal cells (hepatocytes), which form 60% of the total amount of cells in the liver and 80% of liver volume and non-parenchymal cells (epithelial cells, stellate cells, Kupffer cells, hepatic dendritic cells, etc.), which form 40% of the liver cells but only 6.5% of liver volume.[3]

The functional unit of the liver is the hexagonal hepatic lobule and these lobules consist of three to six portal triads (hepatic artery, hepatic portal vein, and common bile duct). Portal vein venules from each triad branch further and these branches run around each lobule as well as to the centre of a lobule to form sinusoids. The blood flows from periphery of the lobule to its centre. Sinusoids are fenistrated blood vessels, are positioned radially, and join at the centre of a lobule into the central vein.[4]

Hepatocytes are the building blocks of liver lobules; they are located in parallel to liver sinusoids but separated from them by the space of Disse.[5] Localization of hepatocytes together with the space of Disse and fenistration allows effective exchange of materials between hepatocytes and blood.[5] Such liver architecture also allows non-parenchymal cells such as immune cells to infiltrate through fenistrates and perform their functions.

1.1.2.1 Parenchymal cells.

1.1.2.1.1 Hepatocytes.

The metabolic functions of liver rely on hepatocytes, which are involved in blood protein synthesis, glucose metabolism, ammonia detoxification, lipid metabolism, drugs, and xenobiotics metabolism.[6] These functions are not uniformly distributed among hepatocytes. According to the localization of hepatocytes in the liver lobule,

hepatocytes can be divided in two populations: periportal hepatocytes and perivenous hepatocytes. The border between periportal and perivenous areas cannot be defined in anatomical terms, but can be described in functional terms as different metabolic processes are located in distinct zones of the liver lobule.[6,7]

Ammonia and glutamine metabolism.

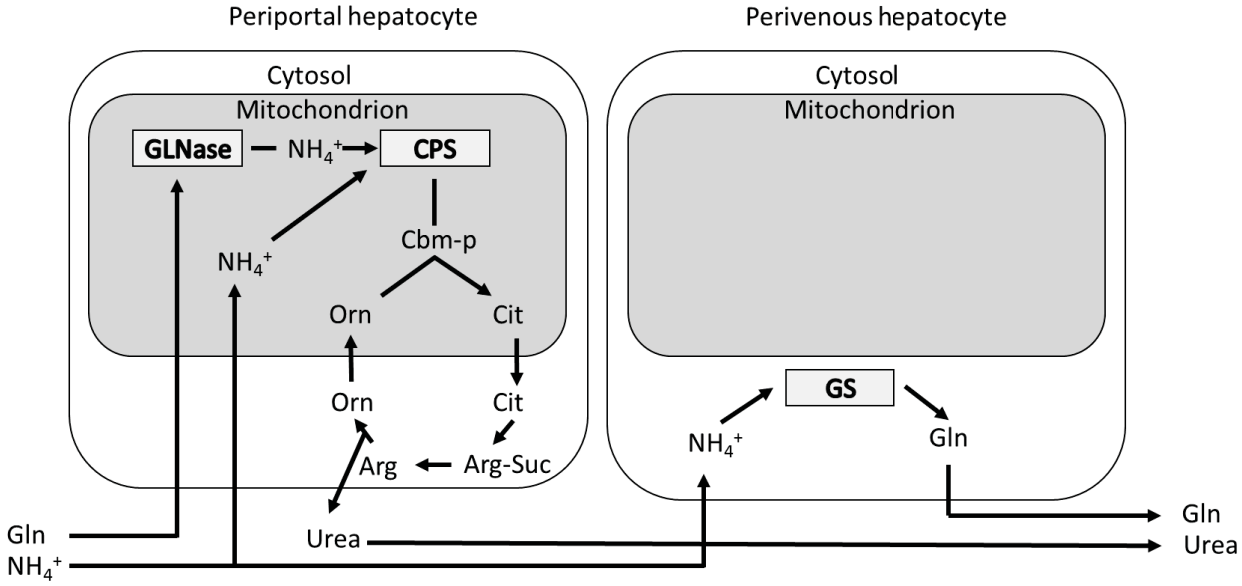

Figure 1.2: Ammonia and glutamine metabolism[7]

To efficiently metabolize ammonia, glutamine and ammonia metabolism are embedded into a structural/functional zonation in the liver lobule. Hepatic urea synthesis occurs in periportal hepatocytes.[8] The urea cycle is comprised of five enzymes: carbamoil phosphate synthetase-1 (CPS-1), ornithine transcarbamylase (OTC), argininosuccinate synthetase (ASS), arginosuccinate lyase (ASL), and arginase (ARG). CPS-1 and OTC are located in the mitochondrial matrix, whereas other urea cycle enzymes are cytosolic.[9] Expression of transporters is required for the functioning of the urea cycle, namely, the mitochondrial ornithine/citrulline transporter ORNT1 and the mitochondrial aspartate/glutamate transporter. [10,11]

The first step in urea production is synthesis of carbamoyl phosphate from ammonia and bicarbonate by the Carbamoylphosphate synthetase.[9]

Carbamoylphosphate synthetase requires adenosine triphosphate, free Mg^{2+}, and N-acetyl-Glutamate as an allosteric activator.[12,13] Importantly, CPS-1 has low affinity to ammonia and high concentration of ammonia is required for activity of the urea cycle in periportal hepatocytes.[7] Ammonia comes from the portal vein and additional elevation of ammonia concentration is achieved through mitochondrial glutaminase activity, which turns glutamine into glutamate and ammonia.[14] Carbamoylphosphate synthetase is rate limiting enzyme for urea synthesis.[15]

The next step in the urea cycle is also conducted by mitochondrial enzyme, ornithine transcarbamoylase, which converts carbamoyl phosphate and ornithine to citrulline.[9] The proceeding steps of the urea cycle occur in cytosol where citrulline is combined with asparate by arginosuccinate synthetase, resulting in arginosuccinate. In this process, arginosuccinate is cleaved to form arginine and fumarate by the action of arginosuccinate lyase.[9] In the last step of the urea cycle, arginine is cleaved by arginase resulting in urea and ornithine; the urea is released into circulation and ornithine can be recycled by urea synthesis.[9]

Ammonia not used by urea cycle is taken up by perivenous hepatocytes and detoxified by conjugation to glutamate, resulting in glutamine. This reaction is catalysed by the glutamine synthetase, which is expressed only in small populations of hepatocytes surrounding the hepatic venule (perivenous hepatocytes).[7,16] The glutamine synthetase pathway is a high-affinity system, which ensures that ammonia does not reach the systemic circulation in high concentrations, in contrast to the urea cycle, which is a low-affinity but high-capacity system.[17]

Ammonia demonstrates neurotoxicity. Disturbances in the ammonia metabolizing pathways in humans lead to severe disease outcomes. For example, new-borns with urea cycle deficiency demonstrate gradual development of symptoms starting from somnolence to lethargy and coma.[18] Inherited GS deficiency leads to glutamine deficiency and consequently, to a lethal outcome.[19]

Liver damage can also disturb ammonia metabolizing pathways, leading to increased ammonia concentrations in the blood.[20] For example, during lipopolysaccharide induced liver injury, nitration and a decrease of the enzymatic activity of the hepatic glutamine synthetase is observed.[21] Also, rats with bile duct ligation demonstrate fibrosis of the liver followed by the decrease in urea production, which can further decrease after induction of septic shock. [22]

Blood protein synthesis.

Liver is the main source of plasma proteins. Albumin, fibrinogen, prothrombin, Factor V, Factor VI, Factor IX, and Factor X are among serum proteins produced by the liver.[23,24] Albumin is the most abundant protein produced by liver, and approximately 10.5 grams of albumin is produced by a human liver daily.[25] During injury, the liver is able to produce acute phase reaction proteins including the C-reactive protein, serum amyloid A, α1-antichymotrypsin, α1-antitrypsin, α2-macroglobulin, and complement factors.[26]

Drugs and xenobiotics metabolism.

Liver is the main organ involved in detoxification of xenobiotics and the kidney and intestine play a minor role in this process.[27,28] Xenobiotic metabolism can be divided in two phases: PhaseI, which includes reactions of oxidation, reduction, and hydrolysis, and PhaseII, which includes reactions of conjugation. PhaseI enzymes

include cytochrome P450, flavin containing monooxygenase, aldehyde, and alcohol dehydrogenase enzymes. PhaseII enzymes conduct conjugation, i.e., glucuronidation, glutathione conjugation, sulfation, methylation, acetylation, and amino acid conjugation.[29]

The cytochrome P450 family is one of the most important PhaseI systems and consist of 57 different isoforms in humans.[30] CYP450 enzymes contain heme with helated Fe^{2+}/Fe^{3+}, and these enzymes catalyse reactions of mono-oxigenation for a variety of exogenous and endogenous substrates. [31] The second most important family of drug metabolizing enzymes is flavin monooxigenase, which is responsible for the oxidation of a variety of nucleophilic agents such as amines, thiols, thioesters and phosphines, nicotine, and hydrazines. [32]

After oxidation, the next step of drug metabolism is conjugation. The most prominent reactions of conjugation are glucuronidation and sulfation. These reactions are catalysed by different isoforms of UDP- glucuronosyltransferases and sulfotransferases, respectively.[29]

Monooxygenation and conjugation with glucuronic acid appear to happen in the perivenous area, while conjugation with sulfuric acid happens mainly in the periportal area.[6]

Lipid metabolism.

The liver plays a major role in the synthesis and oxidation of fatty acids. Lipids are a main component of cellular membrane and also act as energy storing molecules. Additionally, the liver is a key player in energy homeostasis, which converts excess glucose into fatty acids and then exports them for storage as triglycerides as lipid

droplets.[6] Under chronicle energy overload, triglycerides can also accumulate in the liver, leading to the development of hepatic steatosis and steatohepatitis.[33]

Liver zonation.

Functional segregation of hepatocytes is shown to be dependent on the Wnt/beta-catenin pathway. For example, liver specific beta-catenin knockout mice have been demonstrated to lack GS and GLT-1 in the perivenous area.[34] Moreover, liver zonation is tightly regulated by the expression of the inhibitor of Wnt/beta-catenin signalling – APC. Importantly, liver-specific tamoxifen inducible knocking down of APC leads to the perivenous-like liver phenotype, expressing GS and GLT-1 in all hepatocytes. Infection of the liver with DKK1 expressing arenavirus leads to periportal-like phenotype, expressing CPS-1in all hepatocytes.[35]

1.1.2. Nonparenchymal cells.

1.1.2.2 Sinusoidal endothelial cells.

Liver sinusoidal endothelial cells (LSECs) comprise 50% of all nonparenchymal cells in the liver.[36] LSECs separate hepatocytes from the sinusoidal lumen blood. LSECs have limited contact, forming a gap between endothelial cells and hepatocytes, referred to as the space of Disse.[5] However, endothelial cells do not completely separate parenchymal cells from the sinusoids, rather, LSECs organize special pores in the endothelium, also called fenestrated endothelium. These pores have an approximate diameter of around 100nm, which allows the exchange of material between parenchyma and blood.[37] Also, LSECs are able to transfer antigens in the space of Disse by transcytosis, allowing hepatocytes and HSCs to contact antigens from blood.[38] Fenestration allows direct contact between hepatocytes and T cells, and these T cells form membrane extensions, which can directly make contact with

hepatocytes. Simultaneously, the hepatocyte membranes appear to be polarized and express MHCI and ICAM-1 molecules predominantly on perisinusoidal cell membrane, facilitating $CD8^+$ T cell functions.[39] LSECs also express a variety of pattern recognition receptors such as TLR3, TLR4, TLR7, and TLR9.[40]

Additionally, LSECs play an important role as antigen-presenting cells (APC) and also express MHCI and MHCII molecules, together with co-stimulatory molecules CD80 and CD86. LSECs can directly activate T cells. [40,41,42,43] LSECs can also internalize antigens from blood and effectively present them through MHCI and MHCII molecules to circulatinging and liver resident T Cells. [44,41,45,46,47]

However, antigen presentation of blood-derived antigens by LSECs can induce tolerance in T cells.[47,48]

Upon activation, $CD8^+$ T cells rapidly proliferate. However, LSEC-activated T cells demonstrate reduced cytokine production (such as IFNγ and TNFα) and demonstrate reduced cytotoxicity.[47] This phenomenon occurs because of the expression of high levels of PD-L1 by LSECs, which induces T cell exhaustion and tolerance.[49] In addition to the expression of PD-L1, upon activation of LSECs by LPS, LSECs down-regulate co-stimulatory molecules.[50] At the same time, Kupffer cells, stimulated with LPS, produce IL-10 and contribute to the development of T cell tolerance.[51] IL-10 can also directly affect LSECs and down-regulate their ability to uptake antigens and expression of co-stimulatory molecules CD80 and CD86. [42]

On the other hand LSECs can inhibit the antigen presenting function of dendritic cells by direct cell-cell contact and consequently, down-regulate the T cell response.[52]

1.1.2.3 Kupffer cells.

Kupffer cells are residential liver macrophages. These cells recognize, engulf, and digest cellular debris and pathogens and play a central role in the production of inflammatory cytokines in the liver.[6] Kupffer cells represent approximately 35% of the liver's non-parenchymal cells and approximately 80% of all tissue macrophages in the organism.[53]

The main roles of Kupffer cells are to protect the organism from bacterial infections and uptake bacteria translocated from the gut. To perform these functions, Kupffer cells are strategically located through the sinusoids and express PRR, Fc-receptors, and complement receptors.[40,54,55,56,57] These receptors drive the activation of Kupffer cells and induce production of cytokines. Kupffer cells also express the unique complement receptor CRIg, which is required for uptake of C3-opsonised pathogens.[58] Notably, CRIg knockout mice are susceptible to Lysteria monocytogenes infection. CRIg is also important during early anti-viral response.[58,59.]

Kupffer cells play an important tolerogenic role in liver homeostasis by producing anti-inflammatory cytokines, such as IL-10, and inducing immune tolerance against antigens delivered through the portal vein.[51,60,61]

Kupffer cells also act as antigen-presenting cells and express MHCI, MCHII, and co-stimulatory molecules. During HCV infection, Kupffer cells up-regulate expression of CD80, CD86, and CD40, however, KC expresses lower amounts of co-stimulatory molecules than hepatic dendritic cells.[62,63] Additionally, Kupffer cells act as potent activators of invariant NKT cells (iNKT), which recognize lipid antigens through CD1d and are important for anti-bacterial immunity.[64]

1.1.2.4 Stellate cells.

Hepatic stellate cells (HSC) are non-parenchymal cells located in the liver, specifically in the space of Disse, and comprise 5-8% of total liver cells.[65] HSCs play a central role in the storage of vitamin A and can be identified by lipid droplets in cytosol.

HSCs are quiescent long-living cells, however, during liver injury, HSCs lose retinoid droplets and become highly proliferative matrix-secreting myofibroblasts[66].

HSCs can be activated by a variety of cytokines secreted by other hepatic cell populations. Kupffer cells play important role in the activation of HSC, i.e., Kupffer cells can stimulate cell proliferation, matrix synthesis, and the release of retinoids from HSCs through the release of TNFα, TGFb, and MMP-9.[67] TGFb is the most prominent signal, inducing matrix synthesis. [67]

On the other side IFNγ reduces activation of HSCs *in vitro* and *in vivo,* and can induce apoptosis of activated HSCs. [68,69] Moreover, the adenovirus mediated expression of interferon-gamma can inhibit progression of liver fibrosis *in vitro*.[70]

HSCs demonstrate antigen-presenting properties and express MHCI, MHCII, CD80, and CD86.[71,72] Moreover, microscopical studies have demonstrated direct interactions between T cells and HSCs, further supporting the antigen-presenting role of HSCs.[73]

1.1.2.5 Dendritic cells.

Hepatic dendritic cells are professional antigen-presenting cells, constitutively expressing MHCII on their surface, and are typically found in the portal area. [74,75,76] Strategical localization allows DCs to effectively capture and process antigens. DCs can be recruited to the inflamed liver by Kupffer cells.[77,78]

DCs promote both immune response and immune tolerance. Immature hepatic dendritic cells induce tolerance, while mature DCs, expressing CD80 and CD86, promote immune response. [79] Two major subtypes of DCs have been distinguished: myeloid and plasmacytoid dendritic cells.[80]

Myeloid dendritic cells are $CD11c^+$ $MHCII^+$ cells and can produce cytokines such as IL-12, IL-10, and small amounts of IFNa in response to stimulation. In naïve conditions, myeloid dendritic cells demonstrate immature phenotypes and express low levels of CD80, CD86 and CD40 co-stimulatory molecules.[81]

Plasmacytoid dendritic cells are potent producer of interferon-alpha.[82]

Dendritic cells express multiple pattern recognition receptors, for example, TLR7 and TLR9.[83]

DCs from the liver demonstrate a reduced ability to activate T cells compared with DCs from other organs. These phenotypes are attributed to lower antigen uptake and higher production of immunosuppressive IL-10 and reduced production of IL-12 by hepatic dendritic cells.[84,85,86]

1.1.2.6 Lymphocytes.

NK cells.

One-third of liver lymphocytes are NK cells.[36]

Upon activation, NK cells secrete granules containing perforin and granzyme, both of which induce death of target cells.[87] NK cells also play a role in the modulation of immune responses by other cells. NK cells secrete IFNγ in response to TLR stimulation, which induces expression of MHCII molecules by macrophages and

inhibits hepatocytes proliferation.[88,89,90] Moreover, NK cells regulate anti-viral immunity by modulating T cell response.[91]

NKT cells.

NKT cells form an important immune population in the liver. These cells express a restricted TCR repertoire and recognize lipid antigens, presented via the CD1d molecule.[92] NKT cells are rapidly activated and produce large quantity of cytokines, e.g., TNFα, IFNγ, IL-4, and IL-13.[93]

NKT cells are important for the immune response against bacteria and lipid-coated viruses such as HBV. In response to HBV infection, NKT cells produce IFNγ, which blocks virus replication.[94] Moreover, activation of NKT cells occurs after anti-HBV vaccination and is important for mounting an immune response.[95]

Stimulation of NKT cells and transplantation of ex-vivo activated NKT cells protect mice from hepatocellular carcinoma after transfer of hepatoma cells *in vivo*.[96,97] Partially, these effects are attributed to the activation of NK cells by NKT cells.[96] NKT cells may play a controversial role during liver regeneration as they infiltrate the liver after partial hepaectomy and promote hepatocytes proliferation.[98] However, in HBV transgenic mice, NKT cells inhibit liver regeneration by producing interferon gamma, which inhibits hepatocytes proliferation.[99]

T cells.

T cells represent an adaptive immune system. In general, T cells can be divided into cytotoxic T cells, which express CD8 and T helper cells, which are positive for CD4.

CD8 and CD4 positive cells recognize antigen peptides presented on the cell surface by MHCI and MHCII molecules, respectively.[100] Antigen presentation to T cells in the liver often leads to the induction of tolerance rather than activation of T cells.[101]

Th cells.

$CD4^+$ lymphocytes or T helper cells regulate immunity by cell-cell contact and the production of cytokines. $CD4^+$ lymphocytes can be further divided into many subsets: Th1, Th2, Th17, Th22, Tfh, and Treg cells.[102]

Th1 response is characterized by the production of IL-2, IFNγ and TNFα and is important for pro-inflammatory responses and killing intracellular pathogens.[103] Th2 cells produce IL-4 and IL-5 cytokines, which are important for IgE production, activation of mast cells and eosinophils, and anti-helmint immunity.[104]

$CD4^+$ T cells are important for resolution of HCV infection.[105] A strong $CD4^+$ T cell response is associated with clearance of infection, however, patients with persisting infection demonstrate diminished $CD4^+$ response and IL-2 production.[106]

Th17 cells are associated with liver damage during alcoholic liver disease and contribute to liver injury during HBV infection.[107,108] Moreover, HCV and HBV infections promote Th17 cells response. [108,109]

Cytotoxic T-cells.

The main function of $CD8^+$ cytotoxic lymphocytes is to eliminate tumor cells and infected cells. CTL can induce apoptosis in the transformed and infected cells by perforin/granzyme apoptosis or by using FasL-induced apoptosis.[110] CTL can also produce high quantities of cytokines, e.g., IFNγ, TNFα, and IL-2.[111]

$CD8^+$ T cells are essential for the clearance of HCV and HBV.[112,113,114] Prolonged exposure of $CD8^+$ T cells to antigens lead to T cell exhaustion, during which, exhausted T cells lose their effector functions, e.g., killing ability and expression of IFNγ and TNFα. During exhaustion, T cells up-regulate expression of inhibitory molecules, namely, programed cell death protein (PD-1), T-cell immunoglobulin and mucin-domain containing-3(TIM3), lymphocyte-activation gene 3 (Lag-3), and cytotoxic T-lymphocyte-associated protein 4 (CTLA-4).[115,116] CTL are also responsible for liver damage during viral hepatitis, which is manifested by elevated activity of liver enzymes (e.g., transaminases) in serum. [117]

1.2 Liver damage

Based on duration or persistence liver injury could be divided in acute and chronic. Acute liver injury can be resolved by the elimination of injurious agents with no long-term consequences and a full recovery of liver architecture and functions. However, continuous exposure to the harmful agents can lead to progressive liver fibrosis and potentially result in cirrhosis, hepatocellular carcinoma, or liver failure.

1.2.1 Chemokines and cytokines.

Chemokines.

Infiltration of leukocytes contributes to the development and progression of liver injury. Chemokines are cytokines specialized in the recruitment of cells to the site of inflammation and injury. Following hepatic injury, different hepatic cell types secrete chemokines such as CCL5 and CCL2, resulting in the attraction of T cells, NK, NKT cells, and neutrophils.[118,119,120]

Leukocyte migration into liver tissue is observed during LPS-induced liver injury, alcoholic liver disease, and HCV and HBV infections. Activated stellate cells during liver fibrosis secret CCL2 and CCL5, which attract macrophages and leukocytes and therefore, lead to further activation of HSCs and progression of fibrosis.[121] Blocking chemokine receptors CCR1, CCR5, and CCR2 can protect mice from liver fibrosis during BDL-induced liver fibrosis and CCl4-mediated liver damage. [122,123] These chemokine receptors are essential for the migration of HSC and macrophages and up-regulation of the expression of other cytokines, e.g., TNFα, IL-6 and IL-1β.[122,123]

Cytokines.

Pro-inflammatory cytokines including TNFα, IL-6, and IL-1β are up-regulated in most types of liver injuries.[124]

Tumor necrosis factor.

TNFα plays a major role in liver homeostasis because of its ability to activate both pro-apoptotic and anti-apoptotic signal pathways.

TNFα is produced as part of the liver's response to hepatotoxins such as LPS and carbon tetrachloride.[125] Most liver damage inflicted during carbon tetrachloride liver injury is induced by TNFα. A blockade of TNFα by soluble receptor of TNFα has been demonstrated to decrease mortality *in vivo* and reduce liver damage, as assessed by levels of transaminases and histology.[126] Moreover, TNFα- and TNFR1-deficient mice are less susceptible to carbon tetrachloride liver damage.[127] Toxicity of LPS is also mediated by TNFα and TNFR1 and therefore, TNFR1-deficient mice are protected against septic shock, but succumb to L. monocytogenes infection.[128] Importantly, intravenous administration of TNFα alone does not cause liver damage,

but the blocking of translation by administration of D-galactosamine sensitizes the liver to TNFα-induced apoptosis.

TNFα is also involved in alcoholic liver injury. Long-term alcohol feeding induces liver damage in WT- and TNFR2-deficient mice, whereas TNFR1-deficient mice are protected from alcohol-induced liver damage.[129] Notably, levels of TNFα positively correlates with disease severity in alcoholic hepatitis.[130]

TNFα is also known to be up-regulated in the serum of patients with NASH.[131,132] TNFα is considered as one of the precipitating factors of hepatic encephalopathy. Concentration of TNFα in the serum of patients positively correlates with the severity of hepatic encephalopathy. Moreover, in patients with cirrhosis during HE stage I or II, ammonia concentrations in the blood of patients are not elevated, but TNFα concentrations are significantly up-regulated, suggesting, that TNFα is involved in triggering HE pathogenesis.[133,134]

Additionally, TNFα has been shown to be up-regulated in brain tissue during acute liver failure in mice, and deletion of TNFR1 delays onset of HE, however, detailed molecular mechanism remains unclear.[135]

IL-6.

IL-6 is a main inducer of the acute phase response in liver and is secreted mainly by monocytes and macrophages. [136]

IL-6 in liver can signal through its specific membrane bound receptor IL-6R, complex IL-6/IL-6R recruit additional protein gp130 and induce downstream signaling. This process happens in cells that express IL-6R such as hepatocytes, Kupffer cells, and stellate cells.[137] Cells that do not express IL-6R can sense IL-6 through „trans-

signaling“, for example, when soluble IL-6R binds to IL-6 and this complex binds to gp130, downstream signaling is induced.[138]

During an acute phase response, various proteins are expressed including C-reactive protein, serum amyloid A, haptoglobin, and fibrinogen. In IL-6-deficient mice, acute phase response is impaired.[139] IL-6 is important for liver regeneration after partial hepatectomy or liver damage; importantly, activation of Kupffer cells lead to expression of TNFα and further promotes expression of IL-6.[140] *IL-6*$^{-/-}$ mice demonstrate impaired liver regeneration, which could be reverted by administrating IL-6.[141]

A blockade of IL-6 trans signaling leads to increased liver damage in the model of CCl4-induced liver damage.[142]

High levels of IL-6 in serum is associated with increased risk of developing hepatocellular carcinoma caused by viral infections and alcoholic cirrhosis.[143,144,145]

Transforming growth factor-β.

Transforming growth factor-β (TGFb) is a major regulator contributing to liver fibrosis during chronic liver disease and the progression from liver injury to cirrhosis and hepatocellular carcinoma. During liver injury, TGFb is secreted by granulocytes, Kupffer cells, and HSC.[146,147] TGFb is a potent inhibitor of hepatocytes proliferation, and acts as a negative regulator of liver mass. It can inhibit proliferation as well as induce apoptosis of hepatocytes.[148,149] TGFb expression is up-regulated during the end stage of liver regeneration.[150] TGFb plays an important role in the activation of HSC and therefore, liver fibrosis. TGFb promotes HSC activation, differentiation of HSC into myofibroblasts, expression of collagens, suppression of matrix

metalloproteinases, and increases of tissue inhibitors of metalloproteinases(TIMPs).[151]

1.2.2 Infectious disease

1.2.2.1 HBV

Hepatitis B virus (HBV) infection is one of the most common chronic infections and small amount of virus particles (1-10) are sufficient to cause infection. The virus is transmitted via blood and body fluids as well as vertically from mother to child. Infection in adults results in acute infections; specifically, less than 5% of infected subjects develop chronic infection.[155] HBV is not cytopathic and therefore, liver damage is mediated by the immune system. HBV can promote development of HCC directly and indirectly by promoting inflammation, liver injury, and fibrosis.[156] Protein coded by the hepatitis B x gene (HBx) is associated with activation of the Ras-Raf-MAP kinase pathway and can interact with p53 and suppress its antitumor activity.[155] The genome of HBV can integrate into the human genome, however, integration is not essential for virus replication. Integration of HBV genome promotes genomic instability and carcinogenesis.[157]

1.2.2.2 HCV

Chronic infection with hepatitis C virus (HCV) is a common cause of cirrhosis and chronic liver failure. HCV is a single-stranded RNA virus from the Flaviviridae family.[158] HCV is transmitted via intravenous drug abuse and rarely from mother to child.[159] Acute HCV infection is often asymptomatic; only 15% of cases are demonstrate to cause symptoms such as fatigue, nausea, joint pain, or signs of liver damage such as jaundice and increased liver enzymes.[160] Seventy-five to eighty-five

per cent of infected adults develop chronic infection.[160] Chronic HCV infection is associated with chronic hepatic inflammation which can drive liver fibrosis.[161] HCV infection also promotes HCC via indirect (chronic inflammation, cell death, proliferation, and cirrhosis) and direct (modulating metabolic and intracellular signaling pathways) mechanisms.[162,163]

1.2.3 Non-alcoholic fatty liver disease.

Non-alcoholic fatty liver disease (NAFDL) affects up to 19% of the population in the United States.[164] It is characterized by the accumulation of triglycerides in the liver. The proportion of people with NAFDL that progresses into more severe disease non-alcoholic steatohepatitis (NASH) is approximately 6% of the adult population in the US.[165] Development of NASH is described by the multiple hits theory and requires lipotoxicity, pro-inflammatory cytokines, oxidative stress, and endoplasmic reticulum stress.[166] There are no noninvasive diagnostic tests available for differentiating NAFDL from NASH. Up to 20% of cirrhosis cases are developed from NASH.[167]

1.2.4 Liver cirrhosis.

Liver cirrhosis occurs in response to chronic liver injury and is characterized by the development of regenerative liver nodules surrounded by fibrotic tissue.[168] The transition from chronic liver disease to cirrhosis requires inflammation and activation of hepatic stellate cells followed by fibrinogenesis.[169] Cirrhosis at the advanced stage is accompanied by distortion of hepatic vasculature, which leads to shunting of the portal into central vein. [168] Liver fibrosis leads to impaired hepatocytes functions, portal hypertension, and ultimately, to the development of hepatocellular carcinoma. Reduced function of liver parenchyma and portal hypertension could lead to jaundice,

coagulopathy, ascites, hepatic encephalopathy, and esophageal and gastric varices with the risk of hemorrhage.[170]

1.2.5 Hepatic encephalopathy.

Hepatic encephalopathy (HE) is a neurological complication frequently observed during acute or chronic liver injury. This condition is characterized by low-grade cerebral edema with oxidative/nitrosative stress followed by alterations in gene expression, signal transduction, synaptic plasticity, and neurotransmission.[171,172,173]

For a long time, HE was considered a reversible disease, however, recent reports demonstrated long-term impairment of cognitive functions after resolving HE.[174]

1.2.5.1 Symptoms.

More than 60% of patients with cirrhosis are reported to demonstrate signs of HE.[175]

HE is characterized by impaired cognition, motor functions, emotional regulation, and altered behavioral patterns. In clinical practice, four different stages of overt HE are distinguished according to the severity of manifestation. Additionally, minimal hepatic encephalopathy is considered as HE even without obvious clinical symptoms.[176]

Minimal HE requires special psychometric tests to be identified. These tests usually include several paper-pen tests or computerized tests measuring reaction time and rate of appropriate reactions.[177] Patients with minimal HE tend to exhibit longer reaction times and lower rates of correct answers.[178] Alternatively, electroencephalography or measurement critical flicker frequency could be utilized. Critical flicker frequency (CFF) measurement requires patient to observe a light pulsing starting at 60Hz and slowing during the test; in this test, patients should identify when the light starts flickering. If the identified CFF is below 39Hz, the patient

is diagnosed with HE.[179] Symptoms of overt hepatic encephalopathy initially include tremors, disturbance in sleep-wake rhythmicity, irritability, drastic changes in personality, and progress to stupor and coma during high-grade HE.

Symptoms of HE are summarized in the Table 2.

	Grade	Symptoms
Low grade	Minimal HE	No overt symptoms
	Grade I	Short attention span, disturbed sleep-wake-rhythm, tremors, changes in personality
	Grade II	Lethargy, fatigue, disorientation, flapping tremors, memory malfunction
High grade	Grade III	Somnolence, stupor
	Grade IV	Coma

Table 1. Severity grades of hepatic encephalopathy.

1.2.5.2 Pathogenesis.

Ammonia plays a central role in the pathogenesis of hepatic encephalopathy.[180] Ammonia as pathogenic factor of HE was identified at the end of nineteenth century by the team of Nobel prize winning Prof. Pavlov. They observed that a shunt bypassing blood from portal vein directly into vena Cava after six weeks lead to

abnormal behavior in dogs.[181] Specifically, the dogs demonstrated aggression, ataxia, i.e., seizures and coma, especially after ingesting ammonia-rich food. Feeding ammonia to these dogs was later shown to induce coma and death, adding support to original observations of ammonia neurotoxicity in cases of bypassing liver.[181] Moreover, it has been demonstrated that administration of different nitrogen-containing substances such as ammonia chloride, protein, or ammonium citrate to patients with advanced cirrhosis results in the patient developing symptoms similar to an impending hepatic coma.[182]

Ammonia is mainly produced by gut microbiota, which demonstrate high urease activity, and glutaminase expressed by enterocytes in the small intestine and colon.[181] Ammonia from the gut is absorbed and delivered by the portal vein into the liver, where it is normally detoxified by a high-capacity and low-affinity urea cycle to urea and excreted by the kidneys; ammonia spilled over from urea cycle is utilized by low-capacity and high-affinity hepatic glutamine synthetase to glutamine.[17] However, other organs such as muscles, kidneys, and the brain can metabolize ammonia.[183,184,185] Acute or chronic liver injury reduces the ability of liver to metabolize ammonia. Inherited defects in the urea cycle genes as well as in glutamine synthetase genes lead to hyperammonemia and can cause severe neurological symptoms such as lethargy, coma, and death. [18,19] LPS-induced liver damage is associated with nitration and inactivation of hepatic glutamine synthetase in rats, which also contributes to accumulation of ammonia.[21]

The correlation between ammonia concentration and severity of hepatic encephalopathy has been observed in ALF patients, where 55% of patients with ALF and a blood ammonia concentration higher than 200 mmol/L developed both HE and intracranial hypertension.[186] Elevated concentration of blood ammonia, higher than

150 mmol/L, was demonstrated to predict a higher chance of death in patients with ALF.[187]

Notably, during chronic liver failure, levels of ammonia do not always correlate with the severity of HE and additional precipitating factors play an important role in the pathogenesis of HE, such as hyponatraemia, pro-inflammatory cytokines, and benzodiazepines.[133,173]

Astrocytes dysfunction.

Excess ammonia that has not metabolized in the liver is delivered with the blood stream to central nervous system (CNS). The most abundant cells in the CNS are astrocytes, which have several functions such as providing mechanical support to neurons, providing nutrients, the uptake of neurotransmitters, and maintenance of ion balance in extracellular space.[188,189]

Astrocytes are susceptible to ammonia toxicity due to high levels of expression of glutamine synthetase.[185,190]

Astrocytes provide neuron protection against ammonia, neurons co-cultured with astrocytes are protected from ammonia toxicity, whereas neurons alone are sensitive to ammonia intoxication and undergo apoptosis after treatment with ammonia chloride for 48 hours.[191]

Kato et. al have demonstrated swelling of astrocytes and endothelial cells in post mortem brain analysis in patients succumbing to fulminant liver failure.[192]

Astrocytes chronically exposed to ammonia *in vivo* and *in vitro* develop Alzheimer type II phenotype, which includes swollen nucleus, margination of the chromatin, and significant swelling of the cytoplasm. These phenotypes can be observed *in vivo,*

e.g., in rats fed with ammonia-rich food and with a portocaval shunt and *in vitro* after exposure of cultured astrocytes to ammonia.[193,194]

Ammonia induces senescence in cultured astrocytes; elevated expression of senescence associated genes has been detected in post-mortem human cerebral cortex samples with HE.[195]

Astrocytes express high levels of glutamine synthetase and during exposure to elevated levels of ammonia, astrocytes produce high amounts of glutamine, which could be detected by MRI in the brains of patients with HE.[196] Excess glutamine produced by astrocytes appear to cause an osmotic stress and promote astrocyte swelling in HE and contribute to the subsequent astrocyte and CNS dysfunction. Astrocyte swelling can be inhibited by pharmacological inhibition of glutamine synthetase with methionine sulfoximine.[197]

Osmotic activity of glutamine can be compensated by the depletion of myo-inositol and taurine.[198] Concentration of myo-inositol has reverse correlation with concentrations of glutamine and memory functions during hyperammonemia induced by amino acid load in patients with cirrhosis. [199]

According to the Trojan horse theory postulated by Norenberg, glutamine synthesized in astrocytes is translocated in mitochondria, where it is converted back to glutamate and ammonia by glutaminase.[200] In mitochondria, ammonia interferes with energy metabolism, depletion of ATP has been observed in *in vivo* and *in vitro* exposure of astrocytes to high ammonia concentrations.[201] Elevated levels of lactate has been observed in the blood of patients with paracetamol-induced liver failure and these data further support the theory of energy failure during ammonia intoxication.[202]

Hepatic encephalopathy can also be precipitated by inflammatory cytokines, benzodiazepines, and hyponatraemia.[173] In cultured rat astrocytes, ammonia induces swelling and production of free radicals (reactive oxygen and reactive nitrogen species) and induction of oxidative stress.[203,204] Benzodiazepines and hypoosmotic conditions also contribute to oxidative stress in astrocytes.[205,206] Induction of oxidative stress occurs through N-methyl-D-aspartate (NMDA) receptor-dependent mechanisms and can be inhibited by the NMDA receptor inhibitor MK-801.[207,204] Astrocyte swelling and oxidative stress are interconnected: astrocyte swelling induces oxidative stress through NMDA receptors. NMDA receptor activation and oxidative stress, on the other hand, induce astrocyte swelling, resulting in a self-amplificating loop.[208] Production of ROS during swelling is mediated by the activation of NADPH oxidase and Ca^{2+}/calmodulin-dependent isoforms of nitric oxide synthase are responsible for synthesis of nitric oxide.[206,204]

Protein nitration.

RNOS produced during astrocyte swelling causes direct damage to neurons by disturbing the mitochondrial respiratory chain.[209]

RNOS can covalently modify proteins through the reaction of an addition in the third position of the phenolic ring in tyrosine.[210] Protein tyrosine nitration (PTN) can be induced by different factors acting synergistically during HE. Ammonia alone, benzodiazepines, and inflammatory cytokines are able to induce protein tyrosine nitration *in vitro* in cultured astrocytes.[207,205,211]

PTN can induce astrocyte swelling that can be abrogated by antioxidants. PTN in astrocytes can be induced *in vitro* by HE precipitating factors, benzodiazepines, and inflammatory cytokines (TNFα, IL-1β, and IFNγ).[212]

Benzodiazepines induced nitration is mediated by the activation of peripheral benzodiazepine receptors, whereas PTN induced by ammonia and cytokines is NMDA receptor dependent.[204,205,211]

PTN in astrocytes is also observed *in vivo* in rats intoxicated with ammonium acetate, LPS, or with a portocaval shunt bypassing liver. PTN is especially prominent in astrocytes located close to the cerebral blood vessels and could potentially affect the blood brain barrier.[213]

PTN only affects distinct proteins: Erk-1, the peripheral benzodiazepine receptor; glyceraldehyde-3-phosphate dehydrogenase; and glutamine synthetase.[213] Nitration can inhibit protein function, nitration of glutamine synthetase and glyceraldehyde-3-phosphate dehydrogenase suppresses their activity.[21,214,215]

In a human post-mortem brain study, patients with cirrhosis and HE demonstrated elevated brain PTN compared with a cirrhosis-only group. Increased PTN in the brain was associated with decreased GS activity, while expression of GS was not altered; also of note, expression of glutamate/aspartate co-transporter was up-regulated in the tissue of patient's with HE.[216]

RNA oxidation.

Production of ROS can lead to the oxidation of the nucleic acids DNA and RNA. Deoxyguanosine in DNA can be oxidized to 8-Hydroxydeoxyguanosine 8-Oxo-2´-deoxyguanosine (8-OH(d)G) and guanosine in RNA can be oxidized to 8-Hydroxyguanosine (8-OHG). Cytoplasmic RNA is more susceptible to oxidation than DNA, probably due to the histon-provided protection of DNA. Oxidation of DNA can lead to the transversion of G:C to A:T during replication. Oxidation of RNA

downregulates protein expression and can be observed during Alzheimer‘s disease.[217]

Ammonia triggers RNA oxidation in cultured rat astrocytes and brains *in vivo*. In particular, ribosomal 18s rRNA and mRNA coding glutamate/aspartate transporter (GLAST) has been identified as susceptible to oxidation.[218] Notably, RNA oxidation *in vivo* is reversible. RNA oxidation is NMDA receptor dependent and can be increased by TNFα and benzodiazepines.[218] Significantly higher oxidation of RNA has been observed in human post-mortem brain sections from humans with cirrhosis and HE compared with humans with cirrhosis but without HE.[216]

The exact role of RNA oxidation in pathogenesis of HE is unknown, however, disturbed protein synthesis and folding can participate in memory formation and learning.[173,217]

Zn homeostasis.

Hypoosmolarity and ammonia affects Zn^{2+} homeostasis in cultured rat astrocytes and causes intranuclear Zn^{2+} release. An increase in $[Zn^{2+}]_i$ is accompanied by the translocation of MTF-1 and Sp1 transcription factors into the nucleus.[219,220]

MTF-1 regulates the expression of metallothioneins mRNA. Metallothioneins protect astrocytes from Zn^{2+} toxicity and oxidative stress as well as preventing astrocyte swelling.[221,222]

Sp1 regulates expression of the peripheral-type benzodiazepine receptor (PBR).[223] PBR is up-regulated in HE and mediates the oxidative stress response towards benzodiazepines.[205]

Neuroinflammation.

Acute liver failure can lead to cerebral production of pro-inflammatory cytokines, e.g., *TNFα*, *IL-1β,* and *IL-6* on mRNA and protein levels.[224] In a rat model of acute liver failure (portocaval shunt), the amount of activated microglial cells, as measured by the amount of CD11b and MHCII positive microglial cells, correlated with the severity of liver damage and expression of pro-inflammatory cytokines. [225] Expression of IL-1β, IL-6, and TNFα were elevated 2.3-fold, 3.0-fold, and 2.1-fold, respectively.[225] Similar up-regulation of IL-1β expression in brain tissues has been reported in bile duct ligated rats and ammonia fed animals.[226]

These findings indicate that hyperammonemia alone can induce the activation of microglia and expression of inflammatory cytokines by microglia.

In post-mortem samples of patients with cirrhosis and HE, activation of microglia was detected, however, no up-regulation of inflammatory cytokines was reported in comparison with patients with cirrhosis but without HE.[227]

In another study, elevated expressions of mRNA coding IL-R1 (receptor for IL-1) and receptors of anti-inflammatory cytokines IL-4 and IL-10 were observed in patients with cirrhosis and HE compared to patients with cirrhosis only. [228]

Overview of the pathogenesis model.

Hepatic encephalopathy is the result of astrocyte swelling, which is triggered by ammonia and can be precipitated by other factors e.g. inflammatory cytokines, benzodiazepines, and hyponatremia. Astrocytes detoxify ammonia by converting it to glutamine. Accumulation of glutamine cause osmotic stress and swelling of astrocytes. Osmotic stress mediates the formation of reactive nitrogen and oxygen radicals (ROS/RNS), while ROS/RNS induces cell swelling. Therefore, astrocyte

swelling and oxidative stress form a self-amplificating loop. Oxidative stress induces RNA oxidation and protein tyrosine nitration and malfunction of astrocytes. As a result, disturbances of oscillatory cerebral networks occur, which leads to the onset of HE. An overview of pathogenesis model is presented in Figure 1.3.

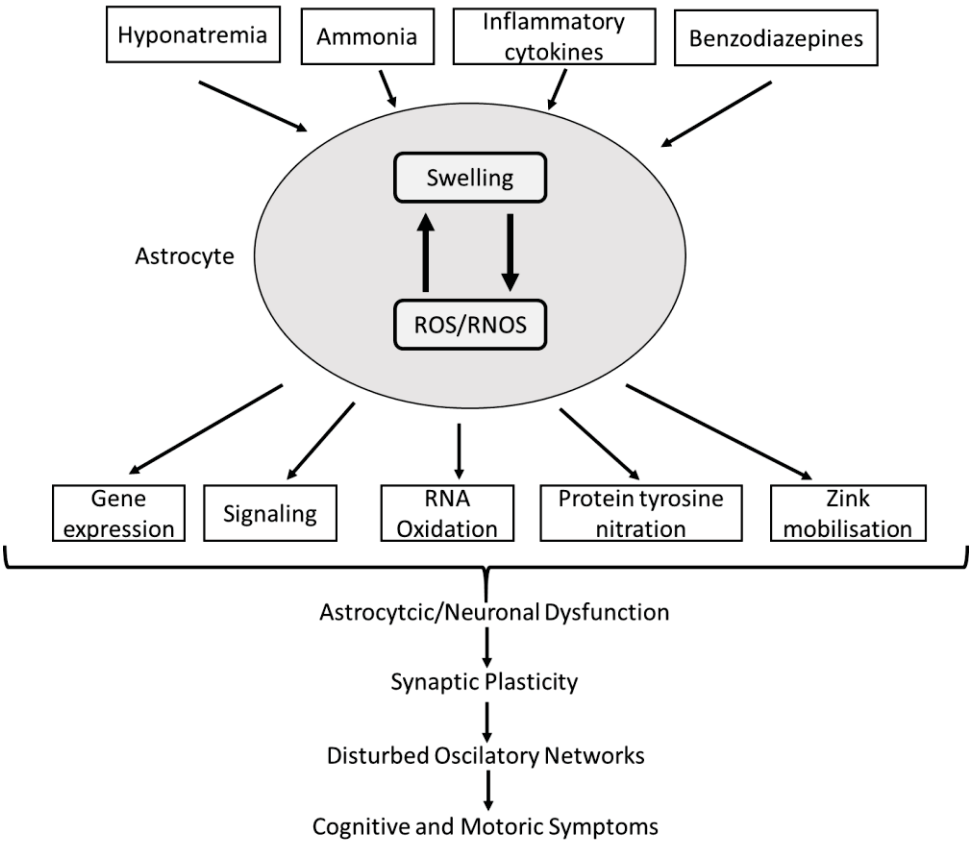

Figure 1.3 *Pathophysiological model of hepatic encephalopathy.*[171]

Blood brain barrier.

The role of blood brain barrier (BBB) in the onset of HE is debatable and controversial data are available. In experimental acute liver failure induced by D-galastosamine in rats and rabbits, no disturbance in the integrity of blood brain barrier was reported.[229,230]

The inflammatory cytokines TNFα and IL-1β, involved in pathogenesis of HE, can permeabilize the blood brain barrier. Additonally, administration of D-galactosamine and lipopolysaccharide or D-Gal and TNFα down-regulate expression of tight-junction protein occludin and lead to leakage of BBB. The permeability of the BBB was detected by Evans blue penetration into the brain and was TNFR1 dependent.[231] In humans with acute liver failure, tight junctions forming the blood brain barrier appeared to be physically intact, however, endothelial cells were swollen, with increased numbers of vesicles and vacuoles.[192] IL-1β is reported to induce expression of HIF-1alpha and VEGF-A and regulate BBB permeability.[232]

Inflammatory cytokines can induce expression of MMP-9, which plays a major role in the regulation of BBB permeability by degradation of the tight junction proteins claudin and occludin.[233,234] During azoxymethane-induced liver failure, activity of MMP-9 in systemic circulation is up-regulated, and inhibition of MMP-9 activity by specific inhibitor GM6001 or monoclonal antibodies attenuates the onset of astrocyte swelling, brain edema, and extravasation of Evans blue.[235]

In the mouse model of allergic encephalomyelitis, disturbance of the BBB is RNOS dependent and can be prevented by the scavenger of peroxynitrite-uric acid, suggesting potential BBB disturbance during hyperammonemia-induced oxidative stress.[236,237]

Ammonia can also reach the brain by passing through ion channels such as the Na-K-Cl co-transporter 1 or utilizing water channels such as aquaporins.

Na-K-Cl co-transporter.

Na-K-Cl co-transporters (NKCC) are a class of transmembrane proteins that transport Na^+, K^+ and Cl^- across cell membranes in variety of cells. NKCC mediate

the stoichiometric transport of Na^+, K^+ and $2Cl^-$, and therefore, NKCC-mediated ion transport is electro neutral.[238]

NKCC exist in two isoforms: NKCC1 and NKCC2. NKCC1 is ubiquitously expressed, whereas NKCC2 is expressed only in the kidneys.[239] NKCC1 is involved in brain edema formation after ischemia and traumatic brain injury and can be inhibited by bumetanide.[240,241,242]

In a study conducted by Jaykumar et al., NKCC1 is shown to mediate the swelling of astrocytes during ammonia intoxication. Astrocytes cultured with ammonium acetate demonstrated increased activity of NKCC1 associated with induction of NKCC1 expression by ammonia. Ammonia treatment caused nitration and oxidation of NKCC1, anti-oxidant treatment diminished NKCC1 activation and decreased astrocytes swelling, and bumetanide was able to prevent astrocyte swelling.[243]

Ammonia *in vivo* disturbs potassium buffering by astrocytes, leading to an increase of extracellular potassium concentration and overactivating NKCC1 in neurons. These events lead to depolarization of neuronal GABA potential and impaired cortical inhibitory networks. Inhibition of NKCC1 activity by bumetanide prevents neuronal dysfunction and decreases mortality of ammonia-intoxicated mice.[244]

Aquaporins.

Aquaporins are small transmembrane proteins responsible for water homeostasis. Eleven aquaporins are currently known and most of them exclusively transport water.[245] However, AQP3, AQP7, and AQP9 also transport glycerin and ammonia.[246] Treatment of astrocytes with ammonia induces expression of aquaporin 4 on the cell membrane.[247] Mice treated with LPS, D-galactoseamine, and additionally treated with ammonia acetate, demonstrate elevated expressions of Aqp-4, but not Aqp-1.[248]

Aquaporin 4 deficient mice demonstrate reduced brain edema after acute water intoxication and ischemia.[249] Aquaporin 4 is highly abundant in astrocytes and could regulate the transport of water across the blood brain barrier.[250] A direct correlation between the expression of aquaporin 4 and brain edema has been demonstrated in ischemia and traumatic brain injury. [251,252,253]

1.2.5.3 Therapy

Ninety per cent of patients with HE have at least one of precipitating factors. Resolving the precipitating factors is the first priority of treatment, the second is managing the patient's mental status, and third is preventing of recurrence of HE.[254]

There are few treatment options available for hepatic encephalopathy: nonabsorbable disaccharides (lactulose), antibiotics (rifaximin), nutrition management, probiotics, zinc, branched chain amino acids (BCAAs), and ammonia scavengers.[254]

Nutrition.

Protein malnutrition, particularly the restriction of dietary protein, is associated with a poor prognosis during HE.[255] Restriction of protein intake leads to muscle wasting and accumulation of circulating ammonia levels.[256] In addition, skeletal muscles express high levels of glutamine synthetase and contribute to ammonia detoxification.

Nonabsorbable disaccharides.

Nonabsorbable disaccharides (lactulose and lactitol) are standard treatment for HE. Lactoluse is not absorbed in intestine, but it can be metabolized by gut microbiota into acetic acid, propionic acid, butyric acid, and lactic acid.[257] Acidic metabolites of

lactulose contribute to acidification of the gut and therefore, by converting NH_3 into the non-absorbable NH_4^+ form, leading to a lowering of ammonia levels in the bloodstream and helping to resolve HE.

Antibiotics.

Since majority of ammonia is generated by gut microbiota, treatment with antibiotics is efficient against HE. Currently, rifaximin is the antibiotic of choice for treating HE. Rifaximin is shown to be effective in blood ammonia lowering and produce less adverse effects then neomycin.[258] Additionally, rifaximin is a non-absorbable antibiotic, and this property allows it to reach high concentrations in the gut. Combination therapy, using lactoluse and rifaximin, is demonstrated to be highly effective, 76% of patients treated with a combination of these drugs showed complete recovery from HE compared to 50.8% in the lactoluse-treated group.[259]

Ammonia scavengers.

Ammonia scavengers facilitate the reduction of ammonia concentration in the blood and increase ammonia clearance. Glycerol phenylbutyrate and ammonia are converted to phenylacetylglutamine *in vivo*, which can be excreted via the kidneys. During clinical trials, glycerol phenylbutyrate has demonstrated to reduce the amount of HE events from 36% in a placebo group to 21% and lowered concentrations of circulating ammonia.[260] Another ammonia lowering agent is ornithine phenylacetate, which uses the same pathway as glycerol phenylbutyrate and promotes the excretion of ammonia in urine. Also, ornithine phenylacetate can reduce plasma ammonia levels in patients with decompensated cirrhosis. [261]

L-ornithine l aspartate.

L-ornithine l aspartate (LOLA) promotes activity of the urea cycle by increasing glutamate synthesis and up-regulating urea synthesis by increasing flux via ornithine transcarbamylase (OTC), leading to increased ammonia clearance from patients' blood.[262] LOLA has significantly improved clinical outcomes of patients with HE compared with those in placebo- or no-treatment groups. Moreover, no significant difference has been observed between lactoluse- and LOLA-treated groups.[263]

Polyethilene glycol.

Before the discovery of lactoluse efficacy against HE, laxatives were commonly used in treatment, suggesting that simple bowel evacuation could be efficient against HE. Polyethilene glycol is common, safe, and efficient laxative. In clinical trials, 91% of patients who received polyethylene glycol showed an improvement in HE compared to 52% in patients treated with lactoluse. Moreover, HE resolution in the polyethylene glycol group occurred faster than in the lactoluse-treated group. [264]

Probiotics.

As gut microbiota plays central role in the production of ammonia, alteration of gut bacteria composition can be beneficial. During clinical trials, comparing lactoluse, probiotics, and no treatment, lactoluse and probiotics were shown to be effective whereas no significant difference in recurrence of HE was observed between the lactoluse- and probiotic-treated groups.[265,266]

N-acetylcisteine.

N-acetylcysteine, is a potent antioxidant with hepatoprotective and neuroprotective properties, prevents hepatic damage caused by azoxymethane, and contributes to

the normalization of levels of glutathione in the brain.[267] This antioxidant can also prevent the onset of hepatic encephalopathy and brain edema in mice with acute liver failure induced by azoxymethane.[268]

Albumin dialysis.

Albumin dialysis with molecular adsorbent recirculating system decreases ammonia, bilirubin, and creatinine concentrations in the plasma of patients with liver failure.[269,270] Interestingly, dialysis has also shown decreased portal pressure in patients with severe alcoholic hepatitis.[271] Additionally, albumin dialysis decreases concentration of NO and TNFα, leading to facilitation of HE symptoms.[272]

Minocyclin.

Minocyclin is a semi-synthetic tetracycline, which in addition to anti-microbial activity, has been demonstrated to have anti-inflammatory effects and can limit activation of microglia.[273] Minocycline also attenuates production of TNFα in acute liver failure, thereby lowering oxidative and nitrosative stress *in vivo* in rat brains.[225,274]

1.3 Death receptor-mediated apoptosis and liver.

Apoptosis is programed cell death characterized by cell blebbing, shrinkage, fragmentation of the nucleus, chromatin condensation, and chromosomal DNA fragmentation.[275]

Apoptosis plays a major role in both liver injury and its subsequent fibrosis. Apoptosis may occur via two fundamental pathways: extrinsic (induced through death receptors) or an intrinsic or mitochondrial pathway. Activation of the extrinsic pathway requires ligation and oligomerisation of death receptors on the cell surface. In

contrast, the intrinsic pathway is induced by a variety of intracellular stress responses, e.g., DNA damage, ER stress, or oxidative stress.[276]

1.3.1 CD95.

CD95, or Fas, was the first death receptor to be discovered. Fas was identified using monoclonal antibodies, which can crosslink Fas and induce cell death by the induction of apoptosis.[277] Fas has one natural ligand: FasL, which is a transmembrane protein expressed predominantly by activated T cells and NK cells.[278] Stimulation with LPS or IFNγ leads to significant up-regulation of FasL expression in Kupffer cells.[279] Fas is expressed by a variety of liver cells, including hepatocytes, cholangiocytes, and activated HSC. [280,281,282]

Upon ligation, Fas undergo trimerisation, which leads to the recruitment of the cytoplasmic adaptor protein called Fas associated death domain protein (FADD) and procaspase 8. The resulting complex is referred to as Death Inducing Signaling Complex (DISC). [283]

Downstream signaling of DISC differs between different cells types: type I and type II cells. In type I cells, formation of DISC leads to the auto-activation of procaspase 8, thereby converting it into caspase 8. Activated caspase 8 can directly activate effector caspases such as -3 and -7 and induce mitochondria independent cell death[284]. In type II cells such as hepatocytes, activated caspase 8 cleaves BID protein, truncated t-BID protein translocate to mitochondria, and induces the release of Cytochrome c.[285,286] Cytosolic cytochrome c interact with apoptotic protease activating factor 1 (APAF-1) and activate caspase-9; the latter activates effector caspase 3, which then induces cell death by cleaving multiple substrates.[287] Fas-

induced apoptosis in type II cells can be inhibited by overexpression of BCL-2 and BCL-X_L proteins.[288]

Role in liver disease.

Inhibition of apoptosis leads to diseases associated with excessive cell growth, e.g., hepatocellular carcinoma. On the other side apoptosis of hepatocytes is commonly associated with acute liver failure, cholestasis, alcoholic hepatitis, and non-alcoholic steatohepatitis.

Administration of anti-Fas antibodies leads to hepatocyte apoptosis and fulminant hepatic failure in mice.[289]

Down-regulation of Fas has been reported in hepatocellular carcinoma and Fas expression negatively correlates with the survival of patients.[290] Notably, alcoholic patients exhibit higher expression of both Fas and FasL in their livers than healthy humans.[291] Similarly, up-regulation of Fas and FasL expression has been observed during Wilson disease.[292]

Incubation of HepG2 cells with fatty acids induces expression of Fas and sensitivity of cells to Fas-induced apoptosis occurs in a similar manner to NASH.[280] Expression of Fas in mouse hepatocytes is up-regulated during hepatic steatosis and consequently, increased sensitivity of hepatocytes to Fas-induced apoptosis is observed.[293]

Chronic viral hepatitis, caused by HCV or HBV, activates the Fas-FasL signaling pathway.[294] High levels of FasL are detected in infiltrating T cells in human liver biopsies and both Fas and FasL are found in hepatocytes during HBV.[295]

1.3.2 TNFα.

Tumor necrosis factor (TNFα) is mainly produced by activated macrophages, however, activated T cells, DCs, adipocytes, and endothelial cells can also produce TNFα.[296,297] TNFα is produced as transmembrane protein type II and can be cleaved by the metalloprotienase TNFα converting enzyme (TACE), which belongs to the ADAM family, resulting in a soluble 17kDa form of TNFα.[298] Both membrane-bound and soluble forms of TNFα demonstrate biological activity.[299]

TNFα signals via two receptors: TNFR1(p55/65, CD120a) and TNFR2 (p75/80, CD120b). Both soluble and membrane-bound forms of TNFα can induce activation of TNFR1 signaling, however, only membrane-bound TNFα is able to fully activate TNFR2-dependent signaling.[300] The expression of receptor for TNFα is cell type dependent, i.e., TNFR1 appear to be ubiquitously expressed while expression of TNFR2 is restricted to immune cells.[301]

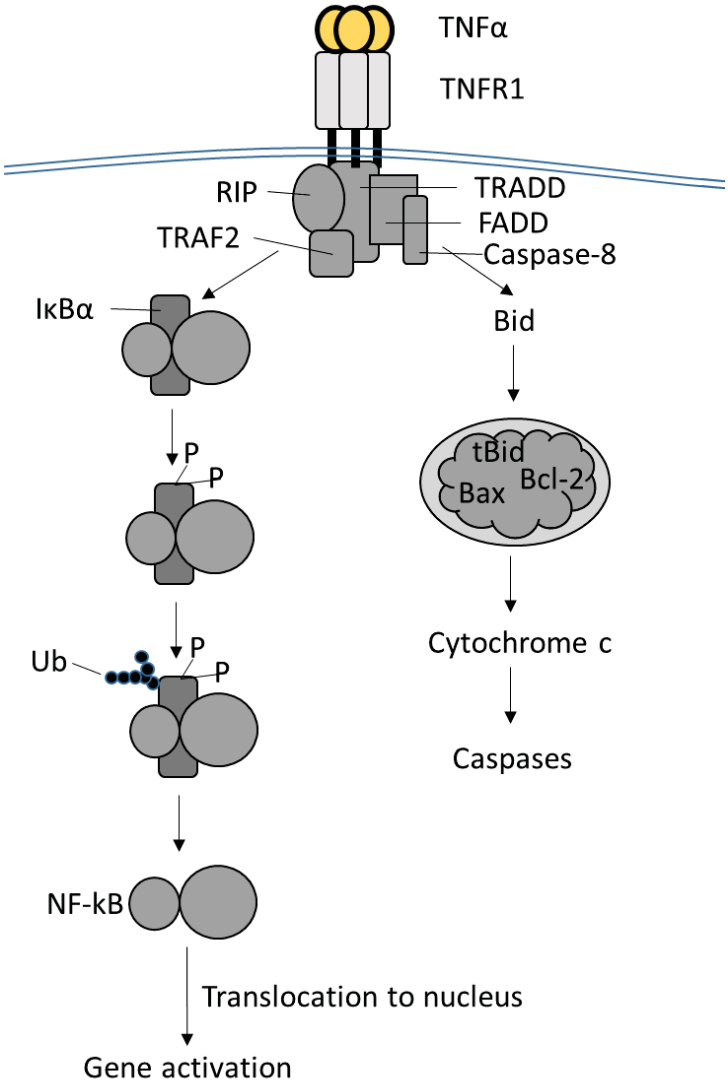

Figure 1.4 Scheme of TNFα signaling through TNFR1.[302]

NF-kb activation.

The binding of TNFα to TNFR1 or TNFR2 can cause activation of NF-kB through different molecular pathways; in addition, activation of TNFR1 can also induce apoptosis. During activation, TNFR2 recruits TNFR-associated factor 1 (TRAF1) and TRAF2.[303] Upon engagement with TNFα, TNFR1 is translocated to the lipid raft and the intracellular domain undergoes conformational changes which allows death

domain (DD) of TNFR1 to recruit TNFR1-associated death domain protein (TRADD) and further recruit receptor-interacting serine/threonine-protein kinase 1 (RIPK1).[304,305]

A complex of TNFR1-TRADD-RIPK1 (Complex 1) in next step recruits TRAF2.[306,307] From this point, downstream signaling of the TNFR1-TRADD-RIPK1-TRAF2 complex and TNFR2-TRAF2 complex becomes similar.

Ubiquitin chains attached to the RIPK1 recruits the IKK complex (IKK-alpha, IKK-beta, and NEMO) to complex 1.[308] Upon activation, IKK phosphorylates NF-κB inhibitor-α (IκBα), which under steady-state conditions, binds to NF-kB and arrests its activation. Phosphorylated IκBα then dissociates from NF-kB and undergoes degradation, allowing NF-kB to be translocated into the nucleus and activate transcription of target genes including expression.[309]

Apoptosis.

After activation through TNFR1, RIPK1 can form a complex 2a with TRADD, FADD, pro-Caspase 8 homodimers and pro-Caspase 8, and FLICE-like inhibitory protein ($FLIP_L$) heterodimers, or complex 2b, which includes RIPK3 instead of TRADD. Once complex 2a or 2b is assembled, pro-caspase 8 undergoes autocatalytic cleavage. These events lead to the release of activated caspase 8 into cytosol and triggering of the classical apoptosis program.[307,310]

$FLIP_L$ is crucial for counterbalancing apoptosis induction by the activation of Nf-kB.[311] Notably, the expression of $FLIP_L$ is up-regulated upon activation of Nf-kB.[312] Formation of heterodimer $FLIP_L$ – caspase-8 can alter substrate specificity from Caspase 8 and inhibit the formation of caspase-8 homodimers and therefore, auto-

activation of caspase 8 and induction of apoptosis. This complex is also important for cleaving RIP1 and preventing the induction of necrosis.[313, 314]

Moreover, TNFα can trigger activation of several kinases such as MAPK, MKK4, and MKK7 and lead to the activation of c-Jun N-terminal kinase (JNK), which prompts apoptosis.[315]

1.3.3 TRAIL

TRAIL is type 2 transmembrane protein belonging to the TNFα family. Originally it was cloned because of its high homology with TNFα (23% identical) and CD95L (28% identical).[316]

Functional studies have demonstrated the ability of TRAIL to induce apoptosis in a variety of cancer cell lines.

In humans, TRAIL interacts with at least four membrane receptors, all of which belong to the TNFα receptor family: DR4, DR5, DcR1, DcR3, and soluble osteoprotegerin (OPG).[316] DR4 and DR5 have functional death domains and can induce apoptosis. DcR1, DcR2, and OPG act as decoy receptors and are able to block apoptosis when overexpressed.

Ligation of TRAIL to its death receptors causes the trimerisation of the receptor followed by changes in the conformation of intracellular domains and formation of death-inducing signaling complex (DISC). DISC includes FADD and pro-caspase 8 molecules and the formation of DISC leads to auto-activation of caspase 8 and classical apoptosis program.

Importantly, TRAIL does not induce apoptosis in most primary cells including primary hepatocytes in physiological conditions.[317] However, transformed hepatocytes

undergo apoptosis after treatment with TRAIL and different factors can sensitize hepatocytes to TRAIL, e.g., viral infections, bile acids, and fatty acids.[318,319,320]

TRAIL-deficient mice and mice treated with TRAIL receptor 2 blocking antibodies are protected against Con-A-induced liver damage.[321]

It has also been shown that TRAIL deficiency leads to reduced levels of aminotransferases during L. monocytogenes infection, reduced amounts of apoptotic hepatocytes, and improved survival compared with wild-type animals.[322]

TRAIL expression is up-regulated by 6-folds during bile duct ligation in mice.[323] In animals, expression of TRAIL leads to enhanced hepatocytes apoptosis, fibrosis, and decreased survival. In the mouse BDL model, TRAIL is mainly expressed by hepatic NK and NKT cells and therefore, depletion of these cells significantly down-regulates expression of hepatic TRAIL.[323]

Analysis of HBV-infected patients has revealed increased expression of TRAIL death receptors by infected hepatocytes and increased amounts of activated NK cells, producing TRAIL in the liver of infected individuals.[324]

Fatty acids can sensitize hepatocytes to TRAIL-induced death, making TRAIL one of the pathogenic factors involved in nonalcoholic fatty liver disease.[319]

Aim of the study

Hepatic encephalopathy is a neurological complication frequently observed during acute or chronic liver injury. The main factor triggering HE is ammonia. For a long time, the importance of hepatic glutamine synthetase in the maintenance of ammonia homeostasis and onset of hepatic encephalopathy was discussed. Hepatic glutamine synthetase is one of pathways involved in ammonia detoxification, nitration and the inhibition of enzymatic activity of hepatic glutamine synthetase during HE has also been reported. However, the importance of hepatic glutamine synthetase in ammonia homeostasis remains unclear due to the low enzymatic capacity of GS.

Pro-inflammatory cytokines are acknowledged as one of precipitating factors during hepatic encephalopathy. Particularly, concentrations of TNFα correlate with the severity of hepatic encephalopathy. However, the detailed role and molecular mechanism of action of TNFα's action during HE is still unclear.

The aim of the present research is to analyze the role of the hepatic glutamine synthetase and TNFα in the maintenance of ammonia homeostasis *in vivo* and in pathogenesis of hepatic encephalopathy.

2.1 Materials

2.1.1 Instruments

Instrument Details	Manufacture
Centrifuge (Eppi)	Eppendorf
Centrifuge	Themo Fisher
ECL Developer Curix 60	AGFA
ELISA plate 96-well	Nunc
ELISA-Reader	Thermo Fisher
Amersham Hyperfilm ECL	GE Healthcare
Cell-Observer (Microscope)	Zeiss
Freezer -20°C	Samsung
Freezer -80°C	Thermo Fisher
Fume hood	Vinitex
Gel chamber Novex Mini Cell	Thermo Fisher
Heating block Thermostat 5320	Eppendorf
Pasteur Pipettes	Welabo
Immersol	Zeiss
Incubator	Thermo Fisher
Microscope, convex	VWR International GmbH
Nanodrop ND-1000	Peqlab
Nitrocellulose membrane	GE Healthcare
NuPAGE 4-12% Bis-Tris Gel	Thermo Fisher
Pipetboy	VWR International GmbH
Pipettes 1000 µL, 200 µL, 20 µL, 10 µL	Brand
Plastic Pipettes 5 ml, 10 ml, 25 ml	Costar
Power supply power pack 200	BioRad
Vaccum Pump	Welch
Reaction vessels 0.2 ml, 1.5 ml, 2 ml	Eppendorf
Roller Mixer	Progen Scientific
Shaker (rocking shaker)	Edmund Bühler
Sterile Bench	Welabo
Steril filter-bottle	Nalgene

Test tubes	VWR International GmbH
Tips 1000 µl, 200 µl, 20 µl	Star Lab
Tissue	Wep
Tubes, 15 ml, 50ml	BD Falcon
Vortex	Scientific Industries
Waterbath	Medingen
Whatman Paper	GE Healthcare
Ammonia checker II	Arkray

2.1.2 Chemicals

Chemicals	Manufactures
Ammonia acetate	Sigma-Aldrich
2N sulfuric acid	VWR
Bradford reagent	Bio-Rad
Bumetanide	Sigma-Aldrich
BSA	GE Healthcare
Dimethylsulfoxide	Sigma
EDTA	Merck KGaA
Ethanol	VWR
Sample Buffer x4	life technologies
Sodium chloride	Merck KGaA
Super Signal Western Blot Enhancer	Thermo Scientific
Recombinant mouse TNFα	R&D Systems
Tween®-20	Merck KGaA
TX-100	Roth
β-Mercaptoethanol	Sigma
Fetal Bovine Serum	Biochrome
Formaldehyde	Sigma
Glycerol	Merck
Methanol	VWR
NuPage MOPS Buffer	Invitrogen
PBS Powder	Panbiotech
Protease Inhibitor cocktail	Sigma
Protein marker	life technologies

2.2 Methods

The Method section was adapted from the published manuscripts:

Hyperammonemia in gene-targeted mice lacking functional hepatic glutamine synthetase

Natalia Qvartskhava, Philipp A. Lang, Boris Görg, Vitaly I. Pozdeev, Marina Pascual Ortiz, Karl S. Lang, Hans J. Bidmon, Elisabeth Lang, Christina B. Leibrock, Diran Herebian, Johannes G. Bode, Florian Lang, and Dieter Häussinger

Proc Natl Acad Sci U S A. 2015 Apr 28;112(17):5521-6. doi: 10.1073/pnas.1423968112.

TNFα induced up-regulation of Na+, K+ ,2Cl- cotransporter NKCC1 in hepatic ammonia clearance and cerebral ammonia toxicity

Vitaly Pozdeev, Elisabeth Lang, Boris Görg, Hans Bidmon, Prashant Shinde, Gerald Kircheis, Diran Herebian, Klaus Pfeffer, Florian Lang, Dieter Häussinger, Karl S. Lang, and Philipp A. Lang

Sci Rep. 2017 Aug 11;7(1):7938. doi: 10.1038/s41598-017-07640-8.

Animals.

Tnfa $^{-/-}$, *Tnfrsf1b* $^{-/-}$ *mice* were purchased from Jackson Laboratories. *Tnfrsf1a* $^{-/-}$ were previously described.[20] Gene-targeted mice lacking functional hepatic GS were generated by inserting a loxP site, together with a flip-recombinase target flanked neomycin resistance cassette. Resulting mice were crossed with deleter mice

expressing the flippase recombinase to remove the resistance cassette. *Glul*$^{fl/fl}$ mice were backcrossed to C57BL/6J background more than 10 times. Next, mice were crossed to a mouse expressing the Cre recombinase under the albumin promotor[325], resulting in liver-specific deletion of GS. Animals appeared viable and fertile, and showed no signs of distress. Animals were kept under specific pathogen-free conditions. Age- and sex-matched animals weighing over 20 g were used for experiments. Most experiments were carried out with littermate controls of mice aged between 8 and 12 wk. For determination of locomotor activity, animals between 3 and 75 wk of age were transferred into a light barrierequipped cage monitored by a computer system (ActiMot/MoTil; TSESystems). Animals were allowed to adapt to the new environment for 24 h prior to starting the measurement for another 24 h. For ammonia challenge animals were injected with 12 mmol/kg or 14 mmol/kg body weight ammonium acetate (Sigma-Aldrich, Deisenhofen, Germany) followed by monitoring of the animals over time, normalization of reflexes and spontaneous movements were considered as recovery from coma. 30 mg/kg of bumetanide or control vehicle was administrated intraperitoneally 5 minutes prior to injection of 14 mmol/kg body weight ammonium acetate. 200 ng of TNFα (RandD systems, UK) was administrated intravenously; D-Gal was injected i.p. 15 minutes prior to TNFα. All animal experiments were reviewed and approved by the appropriate authorities, and were performed in accordance with the German animal protection law (Landesamt für Natur, Umwelt und Verbraucherschutz Recklinghausen, Regierungspräsidium Tübingen, Tierveruchsanlage Düsseldorf).

Genotyping.

Genotyping of mice was performed by PCR assay on DNA isolated from mouse tail using a commercial kit (DNeasy Blood & Tissue Kit; Qiagen). PCR amplification was

performed with 1 μg of purified DNA on a PTC200 Gradient Cycler (MJ Research) using the following PCR settings: 33 cycles, 3 min of denaturation at 94 °C, 60 s of annealing at 60 °C, and 60 s of extension at 72 °C. The following primer pairs were used: GS-forward (for): 5′-GCT TAG GAT GGG TTA CTC TTC CAA GG-3′ and GS-reverse (rev): 5′-ATC ATC ATC TCC CTT CTC CCA TTC C-3′, and albumin promoter-controlled Cre recombinase gene (Alb-Cre) for: 5′-CTG TCA CTT GGT CGT GGC AGC-3′ and Alb-Cre rev: GTC CAA TTT ACT GAC CGT ACA-3′. PCR products were visualized on a 1.5% (wt/vol) ethidium bromidecontaining agarose gel using a gel documenter (Vilbert Lourmat).

O-Maze.

A 5.5-cm-wide annular runway was constructed using gray PVC. It had an outer diameter of 46 cm and was placed 40 cm above the floor. The two opposing 90° closed sectors were protected by 11-cm-high inner and outer walls of gray PVC, whereas the remaining two open sectors had a border of 5 mm. Animals were released in one of the closed sectors and observed for 10 min. Mice were allowed to adapt to the new environment before they advanced onto an unprotected runway. Time spent in protected and unprotected zones and number of transitions between the areas were assessed.

Tissue Sampling.

Brain tissue was prepared from the cerebellum, hippocampus, and cerebral cortex. The cerebral cortex was further dissected into somatosensory and piriform cortical areas, which can be separated accurately due to visible morphological characteristics. For this procedure, the forebrain hemisphere was placed in ice-cold PBS (pH 7.2, spiked with frozen pellets of saline) in a Petri dish under a dissecting

microscope (Olympus SZX 10). While holding the hemisphere at the remaining brainstem, the forebrain was cut in several frontal slices, and the desired brain regions were microdissected from these slices according to Hof et al.[326] The dissected cortical regions were sampled in precooled Eppendorf cups and frozen in liquid nitrogen until further processing. For measuring GS expression in muscle tissue, we dissected the ischiocrural and anterior thigh muscle bellies.

Slice Preparation for Immunofluorescence Analysis.

For immunofluorescence analysis of liver and brain tissue, animals were killed by i.p. injection of pentobarbital (70 mg/kg) and perfused with 20 mL of physiological saline, followed by perfusion with 250 mL of buffered paraformaldehyde [4% (wt/vol), pH 7.2, 4–6 °C] or Zamboni's fixative [4% (wt/vol) paraformaldehyde and 15% (vol/vol) saturated picric acid in 0.1 M PBS, pH 7.2, 4–6 °C]. Tissue was immediately dissected, submerged in 20% (wt/vol) sucrose in PBS (24 h at 4 °C) until complete saturation, and finally frozen in precooled 2-methylbutane (Sigma–Aldrich) at −40 °C before being sliced into 50-μm-thick sections on a cryotome (Frigomobil; Leica).

Immunofluorescence Analysis.

For immunofluorescence of mouse brain or liver, the following primary antibodies were used for immunostaining: anti-NKCC1 (rabbit, polyclonal; Cell signaling), 8-OH(d)G (mouse, monoclonal; QED Bioscience), GFAP (rabbit, polyclonal; Sigma–Aldrich), GS (mouse, monoclonal; BD Biosciences), Iba1 (rabbit, polyclonal; WAKO Chemicals GmbH), rhesus family B glycoprotein (goat, polyclonal; Abcam), ornithine aminotransferase (rabbit, polyclonal; Abcam), or calbindin 28k (Sigma–Aldrich), GLT1 (rabbit polyclonal, Abcam). All antibodies, except anticalbindin (1:10,000), were diluted 1:500 in PBS containing 0.1% saponin (Sigma–Aldrich) and 2% goat serum

(Vector Laboratories) or 5% (wt/vol) BSA. Primary antibodies were labeled with fluorochrome-coupled anti-mouse or anti-goat Cy3 and anti-rabbit FITC antibodies (1:500). Brain slices were incubated in antibody solution for 2 d at 4 °C under gentle agitation, followed by repeated washing with PBS, and were finally mounted on microscope slides using Fluoromount-G (Southern Biotech). Confocal laser scanning microscopy was performed using an LSM510meta microscope (Zeiss). Wide-field fluorescence microscopy was performed using a Cell Observer Z1 microscope (Zeiss).

Histochemistry.

For H&E staining, cryofixed liver slices (7 μm) were treated twice with xylol, each for 10 min, followed by three consecutive incubations in ethanol [100% (vol/vol), 90% (vol/vol), and 70% (vol/vol), respectively]. Slices were stained using Haematoxylin Solution Gill Nr. 3 (Sigma–Aldrich) for 1.5 min. After staining, slices were briefly washed in HCl (0.1% for 20 s) followed by water (10 min). Slices were then stained with Eosin Y solution (Sigma–Aldrich) for 3 min and briefly washed with water. Finally, slices were incubated consecutively in ethanol [70% (vol/vol), 90% (vol/vol), and 100% (vol/vol); each for 3 min] and xylol (5 min) and mounted using Fluoromount-G mounting media.

Video-Tracking.

For data acquisition, animals were video-tracked by a 302050-SW-KIT-2-CAM camera (TSE-Systems) at a resolution of 0.62–0.72 pixel and analyzed using the tracking software VideoMot2 (TSE-Systems).

Western Blot Analysis.

For protein analysis, brain or liver samples were homogenized with a pestle-homogenizer using 10 mmol/L Tris·HCl buffer (pH 7.4) containing 1% Triton X-100, 150 mmol/L NaCl, 10 mmol/L Na4P2O7, 1 mmol/L EDTA, 20 mmol/L NaF, 1 mmol/L sodium vanadate, 20 mmol/L β-glycerophosphate, and protease inhibitor mixture (Boehringer Mannheim). The lysates were centrifuged at 20,000 × g at 4 °C. Protein concentration of the supernatant was determined by Bradford assay (BioRad). For SDS gel electrophoresis and Western blot analysis, the supernatant was added to an identical volume of 2× gel-loading buffer containing 200 mmol/L DTT (pH 6.8). After heating at 95 °C for 5 min, the protein samples were subjected to gel electrophoresis (150–170 mg of protein per lane, 10% gels). Following electrophoresis, gels were equilibrated with transfer buffer [39 mmol/L glycine, 48 mmol/L Tris·HCl, 0.03% SDS, 20% (vol/vol) methanol]. Proteins were transferred to nitrocellulose membranes using a semidry transfer apparatus (Pharmacia). After the membrane was blocked with 5% (wt/vol) BSA in TBST [20 mmol/L Tris·HCl (pH 7.5) containing 150 mmol/L NaCl and 0.1% Tween 20], the membrane was incubated with the indicated primary antibody (3′-nitrotyrosine monoclonal and GS monoclonal, 1:5,000; anti-NKCC1 1:1000; HRP-conjugated anti-β-ACTIN 1:2000; GAPDH, 1:10,000) followed by a secondary HRP-coupled antibody (1:5000 or 1:10,000). Finally, blots were washed with Tris-buffered saline and developed using Western-Lightning Chemiluminescence Reagent Plus (PerkinElmer). Densitometric analysis was performed with the Kodak Image Station 4400, using Kodak Molecular Imaging software.

Northwestern Blot Analysis.

Blood-free perfused and frozen brain tissue was homogenized with a pestle-homogenizer using lysis buffer from an RNeasy Mini Kit (Qiagen). Total RNA was purified from mice brain areas according to the manufacturer's protocol. RNA concentration was estimated using a NanoDrop spectrophotometer. Northwestern blot analysis was performed using formaldehyde [2% (vol/vol)] containing agarose (0.8%) gels loaded with 1–2 mg of isolated total RNA. After electrophoresis, the RNA 1 of 4 was transferred overnight to a nitrocellulose membrane (Schleicher & Schuell) by capillary transfer. The gel was then soaked for 15 min in freshly prepared 50 mmol/L NaOH, followed by washing for 5 min in diethylpyrocarbonate-treated water before incubating the gel for 45 min in 20× SSC transfer buffer [3 M sodium acetate, 0.3 M sodium citrate (pH 7.0)]. At the end of the transfer, the membrane was baked for 2 h at 70 °C. To control the loading of RNA transfer, the membrane was stained with methylene blue solution [0.2% methylene blue in 0.3 mmol/L NaAc (pH 5.5)]. For detection of 8-OH(d)G immunoreactivity, the membrane was blocked in 5% (wt/vol) BSA solubilized in 20 mmol/L Tris·HCl (pH 7.5) containing 150 mmol/L NaCl and 0.1% Tween 20, and then incubated for 2 h with the anti–8-OH(d)G antibody (1:5,000) at room temperature after washing and incubation with HRP-coupled anti-mouse IgG antibody diluted 1:10,000 at room temperature for 2 h. Blots were developed and analyzed by densitometry on the Kodak Image Station 4400 as described above.

Real-Time PCR.

Total RNA was isolated using an RNA extraction kit (Qiagen). The cDNA was generated using a QuantiTect Reverse Transcription Kit (Qiagen). Quantitative real-

time PCR analysis was accomplished in 40 cycles on an AB7500 Sequence Detection System (Applied Biosystems) using SYBR Green as a reporter dye. Real-time PCR was performed using the following primer sequences (MWG Biotech): argininosuccinate lyase (ASL) rev: 5′-CCA GTG GCT ACT TGG AGG ACA G-3′ and ASL for: 5′-CC TCA AGG GAC TTC CAA GCA C-3′, carbamoyl phosphate synthetase 1 (CPS-1) rev: 5′-GAT ACT GGA GAC AGC ACA CCA ATC-3′ and CPS-1 for: 5′-TAT GTT ACC TAC AAT GGC CAG GAG-3′, ornithine transcarbamylase (OTC) rev: 5′-TAA GGA TTT CCC TTG CAA TAA AGG-3′ and OTC for: 5′-CCA GAG TCA AGT ACA GCT GAA AGG-3′, succinate dehydrogenase complex subunit A (SDHA) rev: 5′-GTG GGA ATC CCA CCC ATG T-3′ and SDHA for: 5′-CTT CGC TGG TGT GGA TGT CA-3′. and SDHA for: 5′-CTT CGC TGG TGT GGA TGT CA-3′, Iba1 for: 5′-GTC CTT GAA GCG AAT GCT GG-3′ and Iba1 rev: 5′-CAT TCT CAA GAT GGC AGA TC-3′, and CD14 for: 5′-GGC GCT CCG AGT TGT GAC T-3′ and CD14 rev: 5′-TAC CTG CTT CAG CCC AGT GA-3′. Data were produced in duplicate for each gene. Target gene mRNA expression levels were normalized to mRNA expression levels of SDHA, which served as a housekeeping gene. Gene expression of β-actin, Aqp4, Aqp8, Aqp9 was performed using FAM/VIC probes from Applied Biosystem.

GS Activity Assay.

For measuring GS activity, aliquots of 100 µL of tissue homogenate were incubated with 900 µL of reaction mixture at 37 °C. The reaction mixture contained 60 mmol/L L-Gln, 15 mmol/L hydroxylamine-HCl, 20 mmol/L Na-arsenite, 0.4 mmol/L adenosine diphosphate, 3 mmol/L MnCl2, and 60 mmol/L imidazol-HCl buffer (pH 6.8) in a final volume of 1 mL. The reaction was initiated at 37 °C and terminated by the addition of 1 mL of stop-solution containing 0.2 mol/L trichloroacetic acid, 0.67 mol/L HCl, and

0.37 mol/L FeCl3. The solution was cleared of protein by centrifugation at 20,000 × g at 4 °C, and the formed glutamyl hydroxamate was measured photometrically in the supernatant at 500 nm.

Serum Liver Enzyme Activity.

Activity of Ala aminotransferase and Asp aminotransferase was measured in serum using a serum multiple biochemical analyzer (Ektachem DTSCII; Johnson & Johnson).

Quantification of Urea Nitrogen in Serum and Urine.

Urea nitrogen was quantified using a Spotchem analyzer (Axonlab). Serum samples were prediluted 1:5 and urine samples were prediluted 1:50 in PBS (Panbiotech).

Blood and cerebrospinal fluid ammonia measurement

Ammonia was measured within 3 min after blood sampling from the right heart ventricle or retro-orbital venous sinus or cerebrospinal fluid from the brain using an Ammonia Checker II (Daiichi Kagaku Co. Ltd).

Statistical analysis

Data are expressed as mean ± S.E.M. Statistical significant differences between two different groups were analyzed using students t test. Statistical differences between several groups were tested using one-way ANOVA with additional Bonferroni or Dunnett's post-tests. Statistically significant differences between groups in experiments involving more than one time point were calculated using two-way ANOVA (repeated measurements). Only results with $P < 0.05$ were considered statistically significant.

3. Results

3.1. Hyperammonemia in gene-targeted mice lacking functional hepatic glutamine synthetase

Natalia Qvartskhava*, Philipp A. Lang*, Boris Görg, Vitaly I. Pozdeev, Marina Pascual Ortiz, Karl S. Lang, Hans J. Bidmon, Elisabeth Lang, Christina B. Leibrock, Diran Herebian, Johannes G. Bode, Florian Lang, and Dieter Häussinger

Proc Natl Acad Sci U S A. 2015 Apr 28;112(17):5521-6. doi: 10.1073/pnas.1423968112.

Figures and figure legends were adapted from the published manuscript.

Name of the journal:	*PNAS*
Impact factor:	9.423
Autor:	co-author
Contribution to the paper (%): 5%	Vitaly Pozdeev was involved in sample collection, performing experiments and analysis of data.

Effect of deletion of hepatic glutamine synthetase on the liver architecture, zonation, and ammonia levels in the blood.

Hepatic glutamine synthetase (GS) is one of two hepatic pathways involved in the detoxification of ammonia. Hepatic GS activity can be reduced during liver damage.[327,21] Because the urea cycle demonstrates a high ability to metabolize ammonia to urea, the role of hepatic glutamine synthetase in the regulation of ammonia levels during liver damage remains unclear. To investigate the role of GS, we created conditional knockout mice lacking GS in the liver. We crossed mice expressing Cre recombinase under albumin promoter (*Alb-Cre*) with *Glul*$^{fl/fl}$ mice (Figure 3.1 A). As expected, GS was expressed in livers of the *Glul*$^{fl/fl}$ mice in the absence of Cre recombinase but GS expression was abolished in livers of *Glul*$^{fl/fl}$ *x Alb-Cre*$^{+}$ mice (Figure 3.1 B, C). Expression of GS in the brain or muscles was not affected (Figure 3.1 D, E). Next, we measured enzymatic activity of GS in liver tissues of *Glul*$^{fl/fl}$ mice and *Glul*$^{fl/fl}$ *x Alb-Cre*$^{+}$ mice. GS activity was dramatically reduced in the livers of *Glul*$^{fl/fl}$ *x Alb-Cre*$^{+}$ mice compared with *Glul*$^{fl/fl}$ mice (Figure 3.1 F). Some residual GS activity was still present in the livers of *Glul*$^{fl/fl}$ *x Alb-Cre*$^{+}$ mice, probably due to the GS activity in non-parenchymal cells.[328]

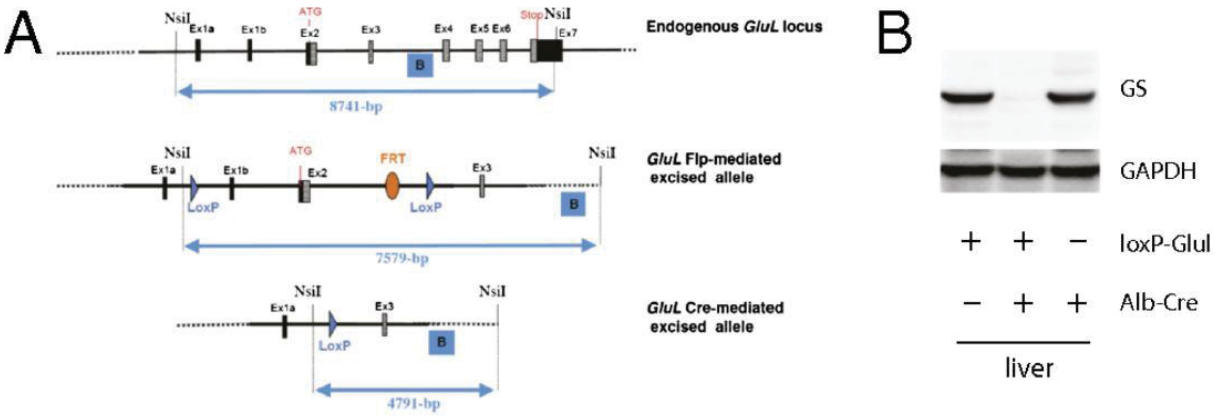
A
NsiI
Ex1a
Ex1b
ATG
Ex2
Ex3
Ex4
Ex5 Ex6
Stop
NsiI
Ex7
B
8741-bp
Endogenous GluL locus
NsiI
Ex1a
Ex1b
ATG
Ex2
FRT
Ex3
NsiI
LoxP
LoxP
B
7579-bp
GluL Flp-mediated excised allele
NsiI
Ex1a
Ex3
NsiI
LoxP
B
4791-bp
GluL Cre-mediated excised allele
B
GS
GAPDH
+ + − loxP-Glul
− + + Alb-Cre
liver

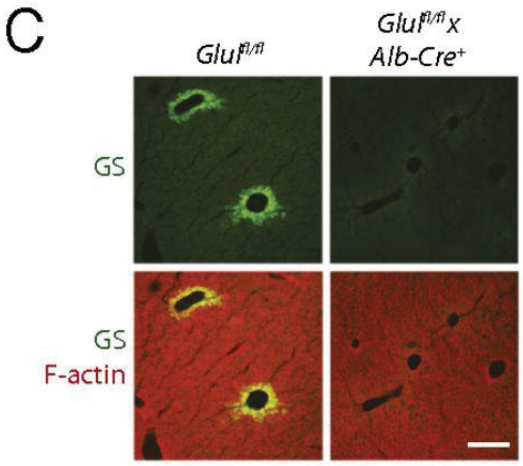
C
Glulfl/fl
Glulfl/fl x Alb-Cre+
GS
GS
F-actin

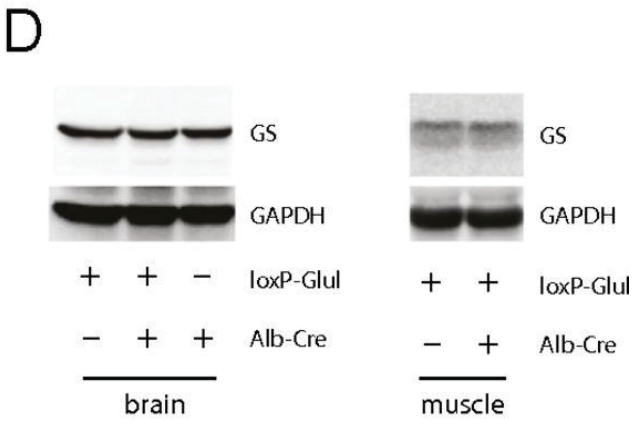
D
GS
GAPDH
+ + − loxP-Glul
− + + Alb-Cre
brain
GS
GAPDH
+ + loxP-Glul
− + Alb-Cre
muscle

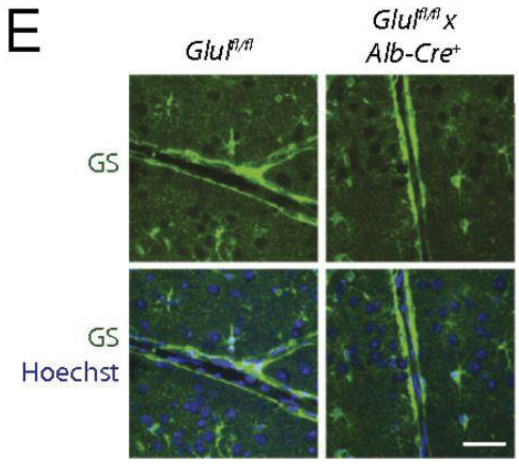
E
Glulfl/fl
Glulfl/fl x Alb-Cre+
GS
GS
Hoechst

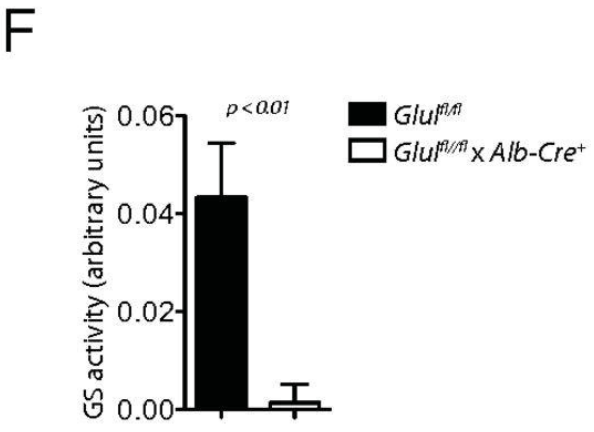
F
p < 0.01
Glulfl/fl
Glulfl/fl x Alb-Cre+
GS activity (arbitrary units)
0.06
0.04
0.02
0.00

Figure 3.1 Organ-specific deletion of GS in the *Glul*$^{fl/fl}$ × *Alb-Cre*$^{+}$ mice.

(*A*) Gene-targeted mice lacking functional hepatic GS were generated as described in *Materials and Methods*. (*B*) GS and GAPDH expression in liver tissue from *Glul*$^{fl/fl}$ × *Alb-Cre*$^{+}$*, Alb-Cre*$^{+}$ and *Glul*$^{fl/fl}$ mice is shown using Western blot analysis. One representative of *n* = 3 is shown. (*C*) Snap-frozen sections from liver tissue harvested from *Alb-Cre*$^{+}$, *Glul*$^{fl/fl}$, and *Glul*$^{fl/fl}$ × *Alb-Cre*$^{+}$ mice were stained with anti-GS (green) and F-actin (red) antibodies. One representative of *n* = 3 is shown. (Scale bar: 200 µm.) (*D*, *Left*) Western blot analysis for GS and GAPDH on protein samples obtained from brain tissue from *Glul*$^{fl/fl}$ × *Alb-Cre*$^{+}$*, Alb-Cre*$^{+}$*,* and *Glul*$^{fl/fl}$ mice was performed. (*D*, *Right*) GS expression and GAPDH expression were assessed in muscle tissue of *Glul*$^{fl/fl}$ × *Alb-Cre*$^{+}$ and *Glul*$^{fl/fl}$ mice by Western blot analysis. One representative of *n* = 3 is shown. (*E*) Immunostaining of snap-frozen sections from brain tissue harvested from *Alb-Cre*$^{+}$, *Glul*$^{fl/fl}$, *and Glul*$^{fl/fl}$ × *Alb-Cre*$^{+}$ mice with an anti-GS antibody (green) and Hoechst 34580 (blue) was performed. One representative of *n* = 3 is shown. (Scale bar: 50 µm.) (*F*) GS activity was assessed in liver tissue harvested from *Glul*$^{fl/fl}$ and *Glul*$^{fl/fl}$ × *Alb-Cre*$^{+}$ mice (*n* = 3–7, respectively).

We observed no difference in liver architecture between *Glul*$^{fl/fl}$ and *Glul*$^{fl/fl}$ *x Alb-Cre*$^{+}$ mice on the histological slides of snap-frozen sections (Figure 3.2 A). Additionally, we observed no significant difference in the activity of ALT and AST in the serum of *Glul*$^{fl/fl}$ and *Glul*$^{fl/fl}$ *x Alb-Cre*$^{+}$ mice, indicating that deletion of the hepatic GS did not cause additional liver damage (Figure 3.2 B). Deletion of GS in the perivenous hepatocytes did not affect expression of Ornitine aminotransferase (OAT-1) and Rhesus family B glycoprotein (RhBg) (Figure 3.2 C,D), which are expressed in the perivenous area.[329,330] These data suggest that deletion of hepatic GS did not affect liver zonation. However, highly up-regulated concentration of ammonia in the blood of *Glul*$^{fl/fl}$ *x Alb-Cre*$^{+}$ mice was detected (Figure 3.2E).

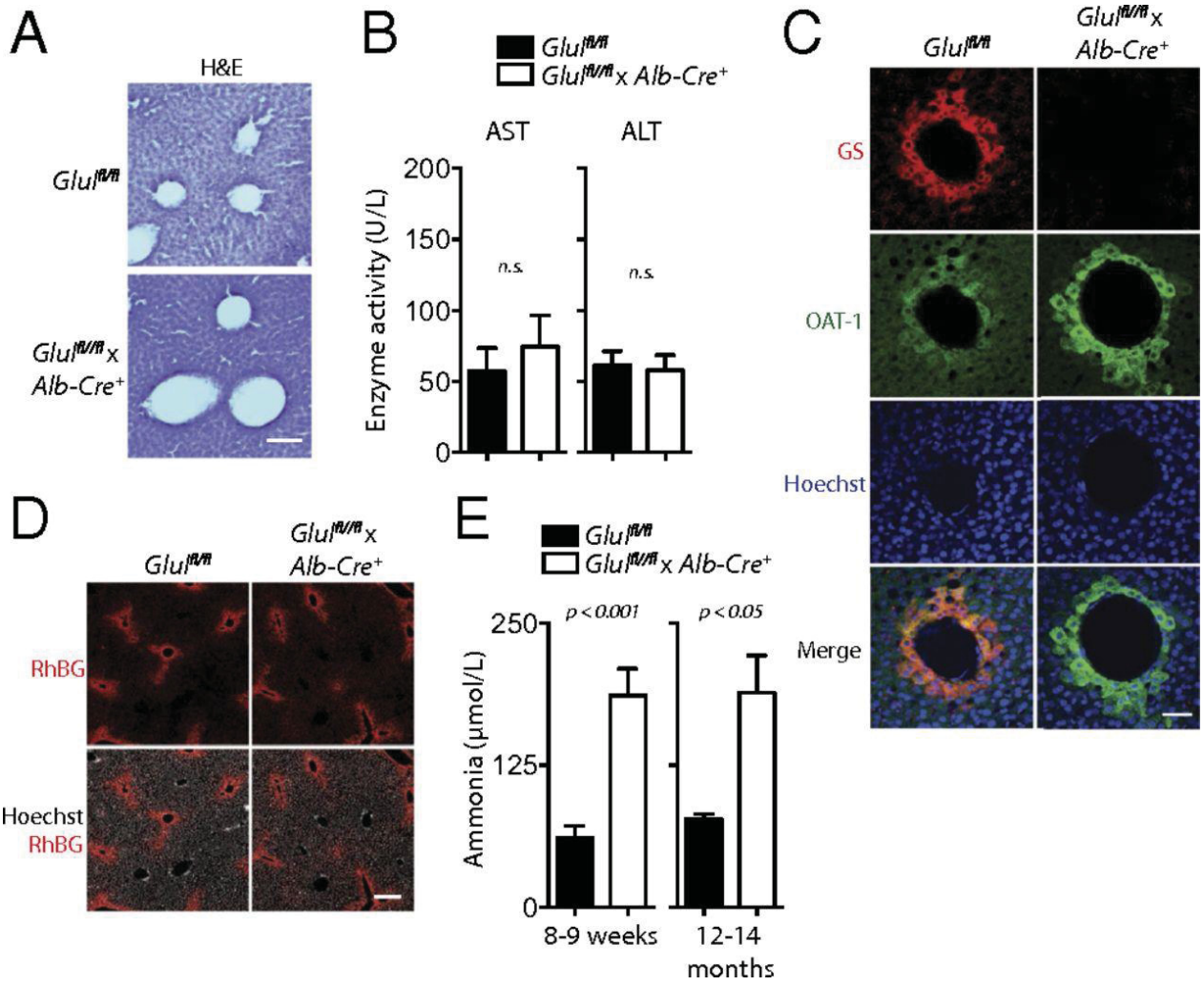
A
H&E
Glul fl/fl
Glul fl/fl x Alb-Cre+
B
Glul fl/fl
Glul fl/fl x Alb-Cre+
AST
ALT
Enzyme activity (U/L)
200
150
100
50
0
n.s.
n.s.
C
Glul fl/fl
Glul fl/fl x Alb-Cre+
GS
OAT-1
Hoechst
Merge
D
Glul fl/fl
Glul fl/fl x Alb-Cre+
RhBG
Hoechst
RhBG
E
Glul fl/fl
Glul fl/fl x Alb-Cre+
Ammonia (µmol/L)
250
125
0
p < 0.001
p < 0.05
8-9 weeks
12-14 months

Figure 3.2 Intact liver architecture/zonation and elevated systemic ammonia levels by liver-specific deletion of GS.

(*A*) Representative H&E-stained sections of snap-frozen liver tissue obtained from *Glul*$^{fl/fl}$ × *Alb-Cre*$^{+}$ and *Glul*$^{fl/fl}$ mice of *n* = 3 is shown. (Scale bar: 100 μm.) (*B*) Asp aminotransferase (AST) and Ala aminotransferase (ALT) activity was determined in the serum of *Glul*$^{fl/fl}$ (*n* = 10) and *Glul*$^{fl/fl}$ × *Alb-Cre*$^{+}$ mice (*n* = 12). n.s., not statistically significantly different. (*C*) Immunofluorescence analyses of snap-frozen liver tissue from *Glul*$^{fl/fl}$ × *Alb-Cre*$^{+}$ (*Lower*) and *Glul*$^{fl/fl}$ (*Upper*) mice were performed for GS (red), ornithine aminotransferase (OAT; green), and Hoechst 34580 (blue). One representative set of images of *n* = 3 is shown. (Scale bar: 20 μm.) (*D*) Immunofluorescence analyses of snap-frozen liver tissue from Glul$^{fl/fl}$ × Alb-Cre^{+} (*Right*) and *Glul*$^{fl/fl}$ (*Left*) mice were performed for ammonia transporter Rh family B glycoprotein (RhBG; red) and Hoechst 34580 (gray). One representative set of images of *n*= 3 (*Glul*$^{fl/fl}$) and *n* = 4 (*Glul*$^{fl/fl}$ × *Alb-Cre*$^{+}$*)* is shown. (Scale bar: 200 μm.) (*E*) Ammonia levels were assessed in blood samples collected by cardiac puncture from 8- to 9-wk-old *Glul*$^{fl/fl}$ × *Alb-Cre*$^{+}$ mice and *Glul*$^{fl/fl}$ mice (*Left*, *n* = 7–8, respectively) and from 12- to 14-month-old animals (*Right*, *n* = 3).

Increase in blood ammonia was probably not due to the urea cycle defect as expression of genes coding urea cycle enzymes was not different between WT and *Glul*$^{fl/fl}$ *x Alb-Cre*$^{+}$ (Figure 3.3 A). Moreover, serum urea nitrogen and serum Gln, Glu, and Ala concentrations were similar between WT and *Glul*$^{fl/fl}$ *x Alb-Cre*$^{+}$ (Figure 3.3 B, C). Taken together, these data show that deletion of hepatic GS does not alter liver architecture, but leads to the upregulation of ammonia concentration in the blood.

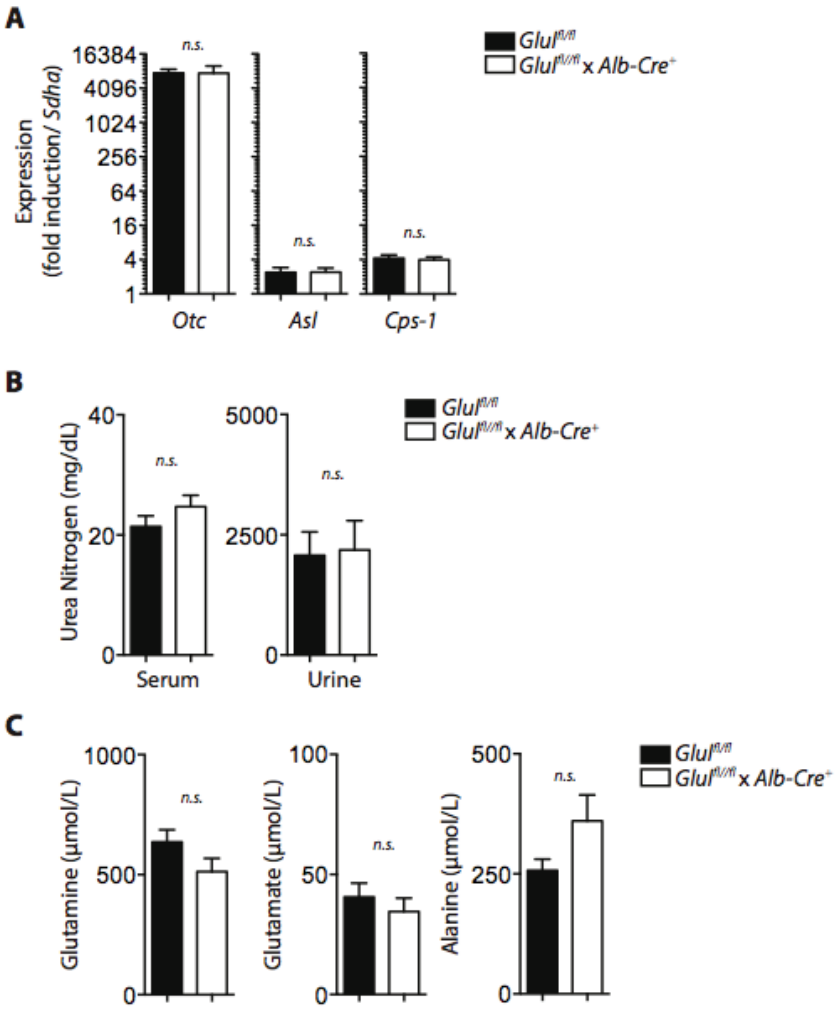

Figure 3.3 *GS is dispensable for the functional urea cycle.*

(A) Real-time PCR analyses of liver tissue harvested from *Glul*$^{fl/fl}$ and *Glul*$^{fl/fl}$ × *Alb-Cre*$^{+}$ mice of OTC (Left, n = 8–9), ASL (Middle, n = 8–12), and CPS-1 (Right, n = 8–9) were performed. (B) Urea nitrogen concentration was determined in *Glul*$^{fl/fl}$ and *Glul*$^{fl/fl}$ × *Alb-Cre*$^{+}$ mice: serum samples (Left, n = 12–14) and urine samples (Right, n = 7–9) from *Glul*$^{fl/fl}$ and *Glul*$^{fl/fl}$ × *Alb-Cre*$^{+}$ mice, respectively. (C) Serum Gln concentrations (Left), Glu concentrations (Middle), and Ala concentrations (Right) were assessed in *Glul*$^{fl/fl}$ and *Glul*$^{fl/fl}$ × *Alb-Cre*$^{+}$ mice (n = 11–13), respectively. n.s., not statistically significantly different.

Liver-Specific GS deficiency triggers RNA oxidation in mouse brain

Both ammonia intoxication and hepatic encephalopathy are associated with oxidative stress and RNA oxidation in the brain tissue.[218,216]

Using immunofluorescence staining of brains from WT and *Glul*$^{fl/fl}$ *xAlb-Cre*$^{+}$ mice, we analysed whether RNA oxidation was happening in brain tissue of *Glul*$^{fl/fl}$ *xAlb-Cre*$^{+}$ mice. Strong induction of RNA oxidation in *Glul*$^{fl/fl}$ *xAlb-Cre*$^{+}$ mice was observed in the cerebellum, hippocampus, and somatosensory cortex (Figure 3.4 A–C) but not in the piriform cortex (Figure 3.4 D). These results were also confirmed by Northwestern blotting (Figure 3.4 E and Fig. 3.5).

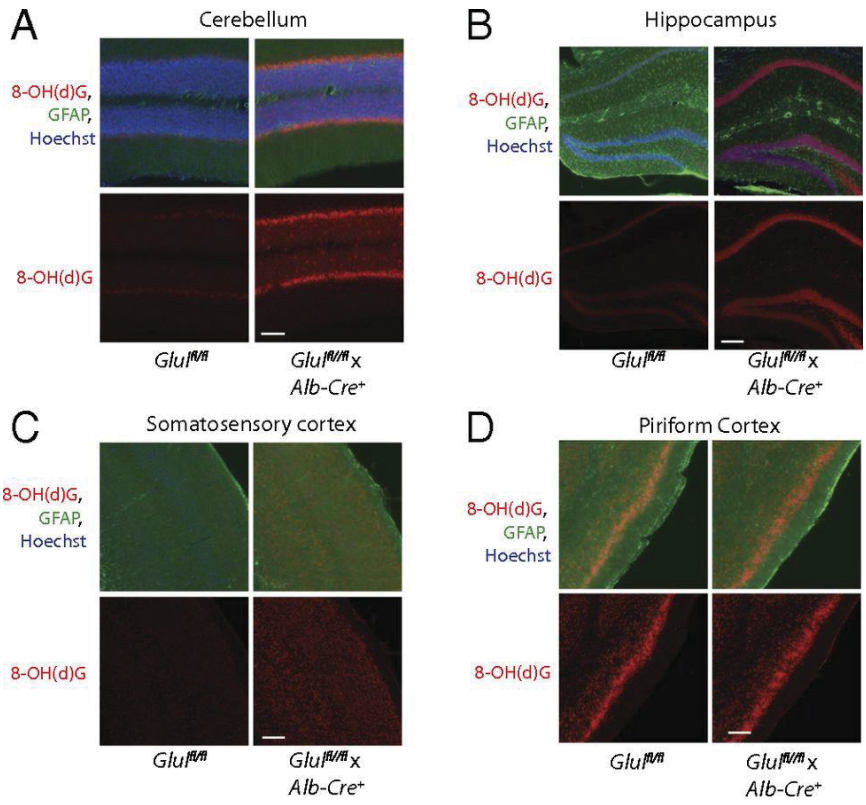
A
Cerebellum
8-OH(d)G, GFAP, Hoechst
8-OH(d)G
Glul fl/fl
Glul fl/fl x Alb-Cre+
B
Hippocampus
8-OH(d)G, GFAP, Hoechst
8-OH(d)G
Glul fl/fl
Glul fl/fl x Alb-Cre+
C
Somatosensory cortex
8-OH(d)G, GFAP, Hoechst
8-OH(d)G
Glul fl/fl
Glul fl/fl x Alb-Cre+
D
Piriform Cortex
8-OH(d)G, GFAP, Hoechst
8-OH(d)G
Glul fl/fl
Glul fl/fl x Alb-Cre+

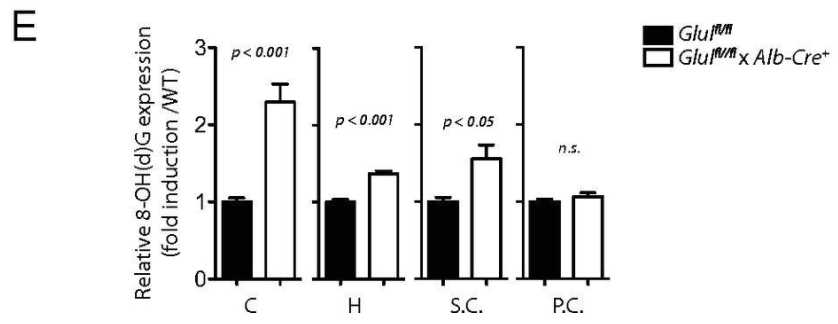
E
Relative 8-OH(d)G expression (fold induction /WT)
Glul fl/fl
Glul fl/fl x Alb-Cre+
p < 0.001
p < 0.001
p < 0.05
n.s.
C
H
S.C.
P.C.

Figure 3.4 Liver-specific deletion of GS induces RNA oxidation in mouse brain.

(*A*–*D*) Survey of 8-OH(d)G immunoreactivity in brain tissue from *Glul*$^{fl/fl}$ (*Left*) and *Glul*$^{fl/fl}$ × *Alb-Cre*$^{+}$ (*Right*) mice is presented in the absence (*Lower*) or presence (*Upper*) of costaining with GFAP (green) and Hoechst 34580 (blue). One representative of the cerebellum (*A*), hippocampus (*B*), somatosensory cortex (*C*), and piriform cortex (*D*) of *n* = 5 is demonstrated. (Scale bars: *A*, 100 μm; *B*–*D*, 200 μm.) (*E*) Samples harvested from brain sections (from left to right: cerebellum, hippocampus, somatosensory cortex, and piriform cortex) of *Glul*$^{fl/fl}$ and Glul$^{fl/fl}$ × Alb-Cre^{+} mice were tested for RNA oxidation expression using Northwestern blotting [*n* = 6 for *Glul*$^{fl/fl}$ mice, *n* = 9 (cerebellum, hippocampus, and piriform cortex) and *n* = 10 (somatosensory cortex) for *Glul*$^{fl/fl}$ × *Alb-Cre*$^{+}$ mice].

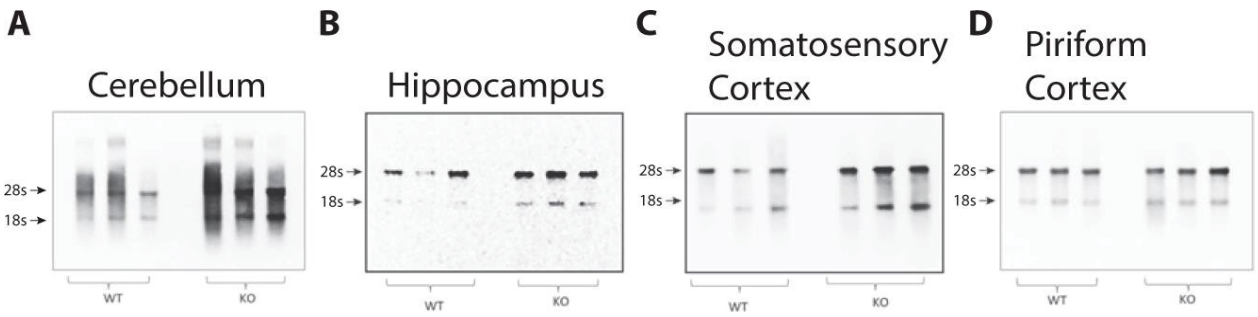

Figure 3.5 Hepatic GS KO triggers RNA oxidation in brain tissue.

Samples harvested from different brain regions of WT and *Glul*$^{fl/fl}$ *x Alb-Cre*$^{+}$ mice were tested for RNA oxidation expression using Northwestern blotting. Representative blots are presented for the cerebellum (A), hippocampus (B), somatosensory cortex (C), and piriform cortex (D).

Treatment of brain slices with RNase abolished RNA oxidation signal, proving that the oxidation was specific for the RNA (Figure 3.6). Interestingly, high levels of oxidation were observed in the Purkinje cells(Figure 3.7), which are important for controlling motor coordination.[331] Taken together, these data show that specific deletion of hepatic glutamine synthetase results in increased ammonia levels followed by biochemical changes in the brain tissue of mice.

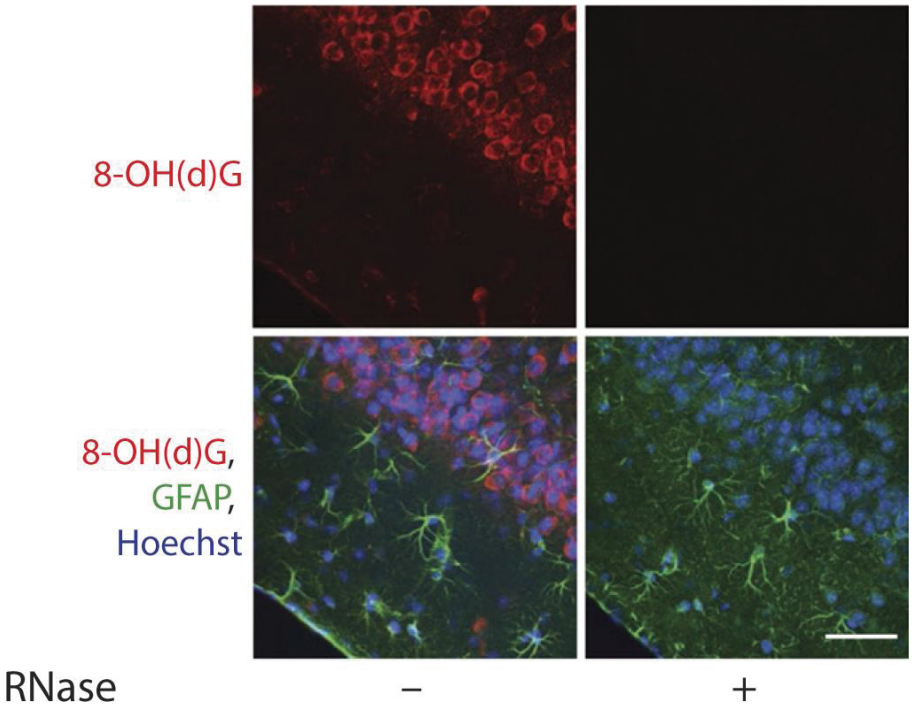

Figure 3.6 *Specificity control for the 8-OH(d)G antibody.*

A survey of 8-OH(d)G immunoreactivity in brain tissue from *Glul*$^{fl/fl}$ *x Alb-Cre*$^{+}$ mice is presented in the absence (Left) or presence (Right) of RNase (one representative of n=3 is shown). (Scale bar: 50μm.)

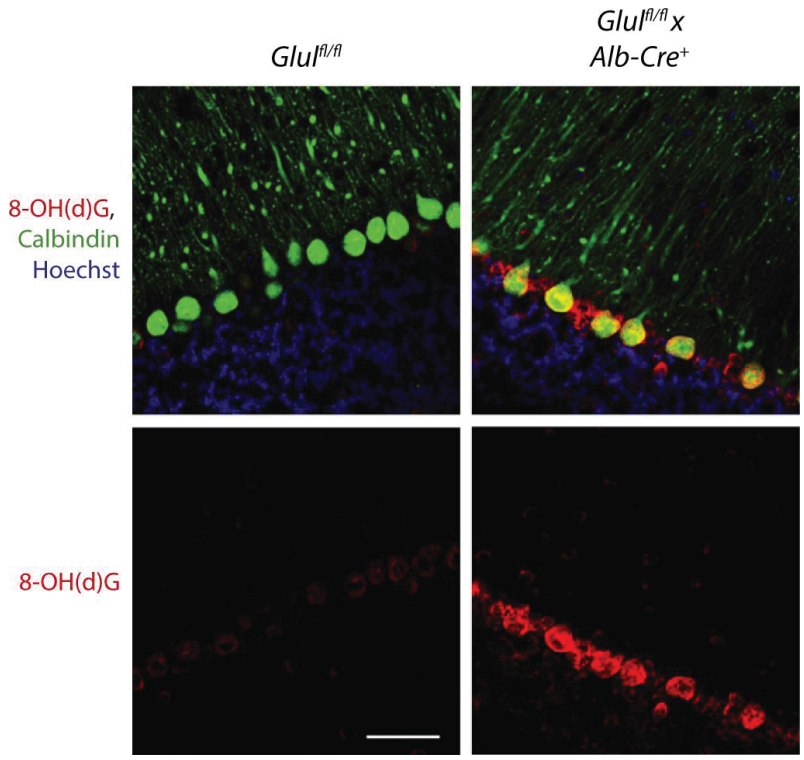

Figure 3.7 Liver-specific deletion of GS induces RNA oxidation in cerebellar Purkinje cells.

Survey of 8-OH(d)G immunoreactivity in mouse cerebellum from WT (Left) and *Glul*$^{fl/fl}$ *x Alb-Cre*$^{+}$ (Right) mice is presented in the absence (Lower) or presence (Upper) of costaining with calbindin (green) and Hoechst 34580 (blue). One representative of n=3 is demonstrated. (Scale bar: 50μm.)

Glul$^{fl/fl}$ *x Alb-Cre*$^{+}$ mice demonstrate no activation of microglia.

Activation of microglia has been observed in the brains of rats during hyperammonemia and in post-mortem brain samples from humans with liver cirrhosis and HE.[226,227] Activated microglia is also known to produce pro-inflammatory cytokines.[332] However, in the cerebral cortex of *Glul*$^{fl/fl}$ *x Alb-Cre*$^{+}$ mice compared with WT, expression of microglia activation marker ionized calcium-binding adaptor protein 1 (Iba1) and microglia morphology were not altered (Figure 3.8 A). Expression of genes coding Iba1 and CD14 were unchanged (Figure 3.8 B) and expression of the mRNA of pro-inflammatory cytokines IL-1β, IL-6, and TNFα in the cerebral cortex of *Glul*$^{fl/fl}$ *xAlb-Cre*$^{+}$ mice was not altered (Figure 3.8 C).

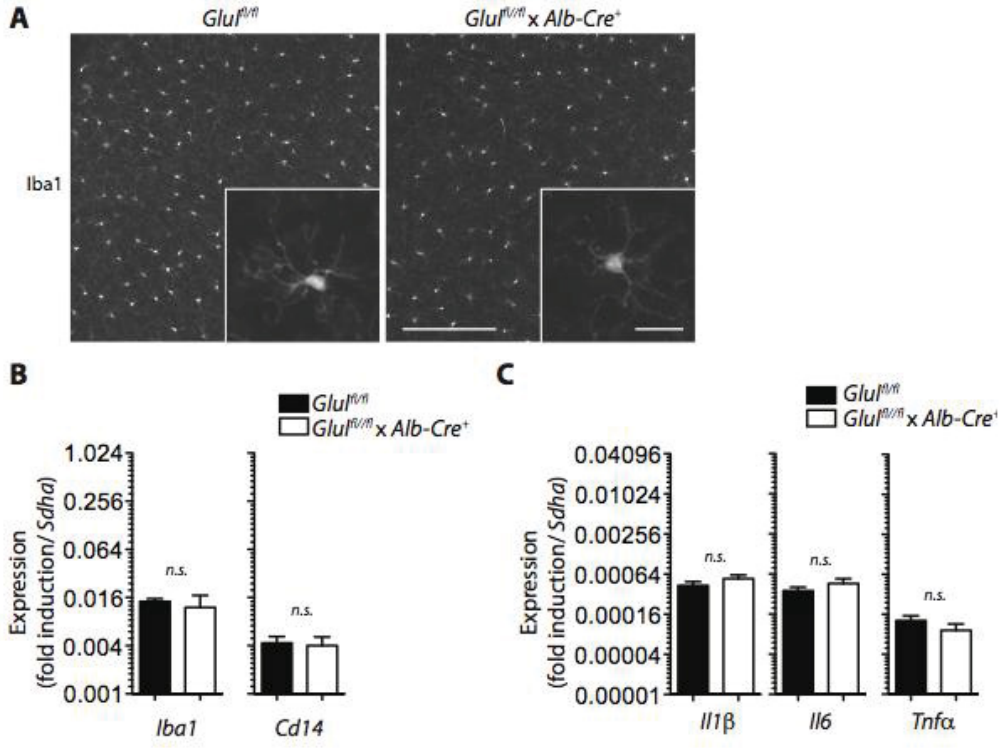

Figure 3.8 *Microglia activation marker and proinflammatory cytokine mRNA expression in the cerebral cortex of WT and* Glul$^{fl/fl}$ × Alb-Cre^{+} *mice.*

(*A*) Detection of Iba1 in mouse cerebral cortex by wide-field fluorescence microscopy. One representative immunofluorescence analysis of three is shown. (Scale bars: 200 μm; *Inset*, 20 μm.) mRNA expression levels in mouse cerebral cortex by RT-PCR of Iba1 and CD14 (*B*, *n* = 3) or IL-1β, I-L6, or TNF-α (*C*, *n* = 8 for *Glul* $^{fl/fl}$ mice and *n* = 6 of for *Glul*$^{fl/fl}$ *x Alb-Cre*$^{+}$ mice) are shown. mRNA expression levels of Iba1, CD14, IL-1β, IL-6, or TNF-α were normalized to succinate dehydrogenase complex subunit A (SDHA) mRNA levels.

Consequently, we observed no difference in the protein expression of CD14, Iba1, IL-1β, IL-6, and TNFα in the cerebral cortex of WT and *Glul*$^{fl/fl}$ *x Alb-Cre*$^{+}$ mice (Figure 3.9 A, B). These data suggest that systemic hyperammonemia in *Glul*$^{fl/fl}$ *x Alb-Cre*$^{+}$ mice is not associated with microglia activation or increased production of pro-inflammatory cytokines in the cerebral cortex.

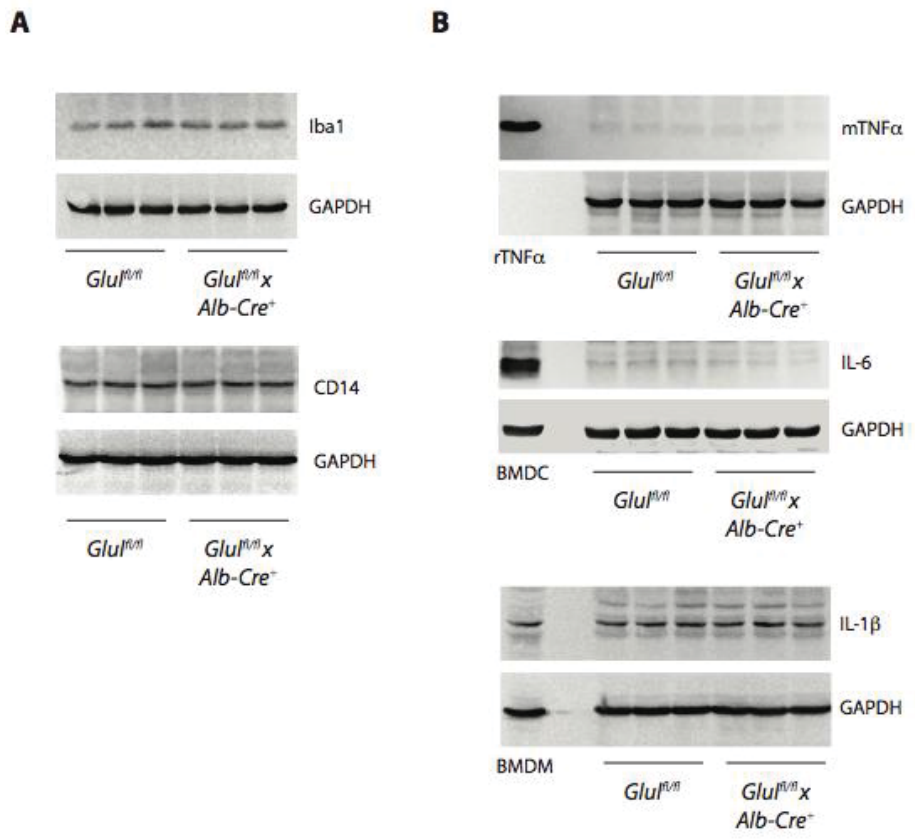

Figure 3.9 *Microglia activation marker and proinflammatory cytokine protein expression in the cerebral cortex of WT and* $Glul^{fl/fl}$ × *Alb-*Cre^{+}*mice.*

Detection of microglia activation markers Iba1 and CD14 (A) or proinflammatory cytokines IL-1β, IL-6, or TNF-α (B) protein levels in mouse cerebral cortex by Western blot analysis is shown. Recombinant mouse TNF-α (Upper, rTNF-α), bone marrow-derived dendritic cells [LPS (30 ng/mL, 3 h)-treated] (Middle, BMDC), or bone marrow-derived mouse macrophages [LPS (10 ng/mL, 24 h)-treated] (Lower, BMDM) was used as a positive control. GAPDH served as a loading control (n = 3 for $Glul^{fl/fl}$ and n = 5 for $Glul^{fl/fl}$ *x Alb-*Cre^{+} mice)

***Glul*$^{fl/fl}$ *Alb-Cre*$^{+}$ mice demonstrate behavioral abnormalities**.

Hyperammonema can trigger behavioural changes in patients.[176] We investigated whether hyperammonemia in *Glul*$^{fl/fl}$ *x Alb-Cre*$^{+}$ mice can cause behavioral abnormalities compared with WT. When light barrier cages were used to monitor activity and distance travelled, we observed increased activity of *Glul*$^{fl/fl}$ *x Alb-Cre*$^{+}$ mice and consequently, longer distances were travelled by *Glul*$^{fl/fl}$ *x Alb-Cre*$^{+}$ mice compared with WT mice (Figure 3.10 A, B). Moreover, during the o-maze test, *Glul*$^{fl/fl}$ *x Alb-Cre*$^{+}$ mice spent significantly more time in the open arms compared with WT mice, also *Glul*$^{fl/fl}$ *x Alb-Cre*$^{+}$ mice spent significantly less time in the closed arms compared with WT mice. (Figure 3.10 C, D)

When we monitored animals over a prolonged period of time, we observed a slight reduction of lifespan of *Glul*$^{fl/fl}$ *x Alb-Cre*$^{+}$ mice compared with *Glul*$^{fl/fl}$ mice. (Figure 3.11)

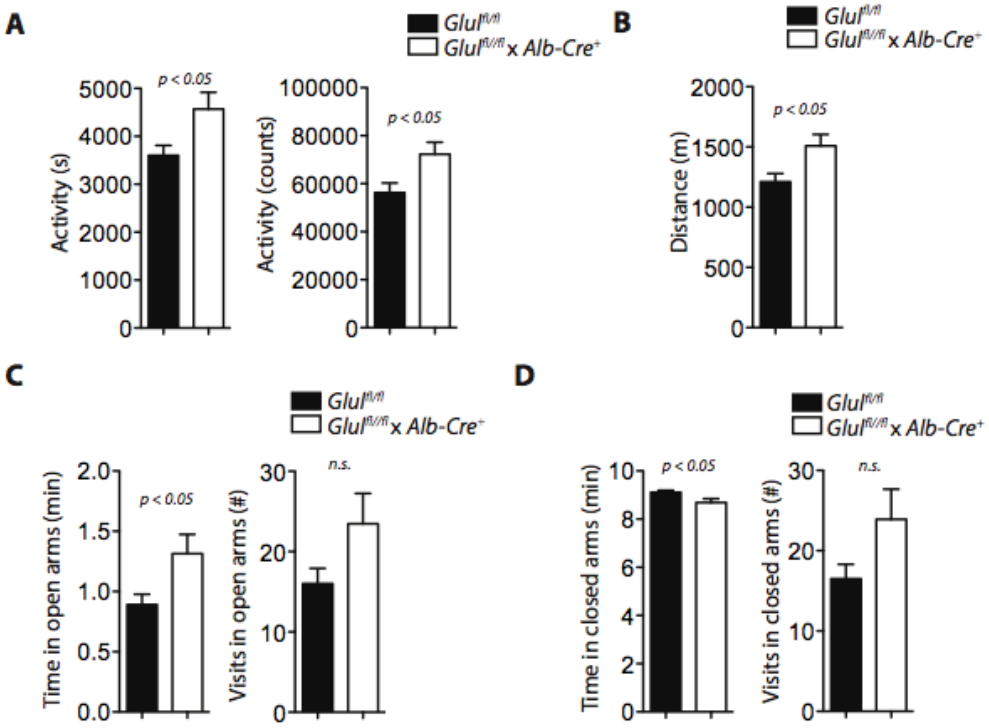

Figure 3.10 Glul$^{fl/fl}$ x Alb-Cre^{+} mice show behavioral abnormalities compared with WT mice.

(*A* and *B*) *Glul*$^{fl/fl}$ and *Glul*$^{fl/fl}$ *xAlb-Cre*$^{+}$ mice were transferred into a light barrier-equipped cage and allowed to adapt to the new environment for 24 h prior to starting the measurement. Total activity time (*Left*, *n* = 22 for *Glul*$^{fl/fl}$ mice and *n* = 23 for *Glul*$^{fl/fl}$ *x Alb-Cre*$^{+}$ mice) and counts (*Right*, *n* = 23 for *Glul*$^{fl/fl}$ mice and *n* = 24 for *Glul*$^{fl/fl}$ *x Alb-Cre*$^{+}$ mice) (*A*) and distance travelled (*n* = 21 for *Glul*$^{fl/fl}$ mice and *n* = 22 for *Glul*$^{fl/fl}$ *x Alb-Cre*$^{+}$ mice) (*B*) were determined after 24 h. Animals were monitored using the O-Maze test. Time (*Left*) and visits (*Right*) in the open arms (*C*) and time (*Left*) and visits (*Right*) in the closed arms (*D*) are presented (*n* = 10 for *Glul*$^{fl/fl}$ mice and *n* = 11 for *Glul*$^{fl/fl}$ *x Alb-Cre*$^{+}$ mice).

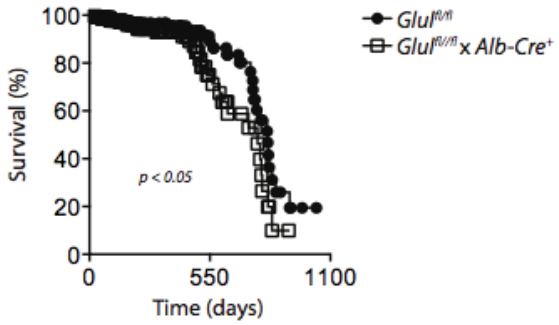

Figure 3.11 *Glul$^{fl/fl}$ x Alb-Cre^{+} mice exhibit a slightly reduced life span compared with Glul$^{fl/fl}$ mice.*

Kaplan–Meier curve of *Glul$^{fl/fl}$* (●) and *Glul$^{fl/fl}$ x Alb-Cre^{+}* (□) mice is shown over time (starting with n = 246–256; P < 0.05 using the Mantel–Cox test)

Taken together, these data demonstrate that deletion of hepatic glutamine synthetase leads to systemic hyperammonemia, phenotypical changes in brain tissues followed by behavioral abnormalities, and shortening of the life span of animals.

3.2. TNFα induced up-regulation of Na+, K+ ,2Cl- cotransporter NKCC1 in hepatic ammonia clearance and cerebral ammonia toxicity

Vitaly Pozdeev*, Elisabeth Lang*, Boris Görg, Hans Bidmon, Prashant Shinde, Gerald Kircheis, Diran Herebian, Klaus Pfeffer, Florian Lang, Dieter Häussinger, Karl S. Lang, and Philipp A. Lang

Figures and figure legends were adapted from the published manuscript.

Name of the journal:	*Scientific reports*
Impact factor:	4.259
Autor:	co-First-author
Contribution to the paper (%):	20%
	Vitaly Pozdeev was involved in designing of study, sample collection, planning and performing experiments and analysis of data.

TNFα knockout mice demonstrate decreased expression of hepatic *Cps-1* and increased levels of ammonia in the blood.

Ammonia levels in the blood are known to correlate with TNFα concentrations in the blood during hepatic encephalopathy[333]. Surprisingly, *Tnfa*$^{-/-}$ mice demonstrate elevated ammonia concentrations in central as well as peripheral blood (Figure 3.12 A, B). TNFα is known to induce signal through TNFR1 and TNFR2.[310] Our data revealed that an increase in ammonia appears to be dependent on both TNFR1 and TNFR2 signaling. In addition, *Tnfrsf1a*$^{-/-}$ *and Tnfrsf1b*$^{-/-}$ mice demonstrated normal levels of ammonia in the blood but only *Tnfrsf1a*$^{-/-}$*Tnfrsf1b*$^{-/-}$ double knockout mice demonstrated elevated ammonia concentrations in peripheral blood (Figure 3.12 B).

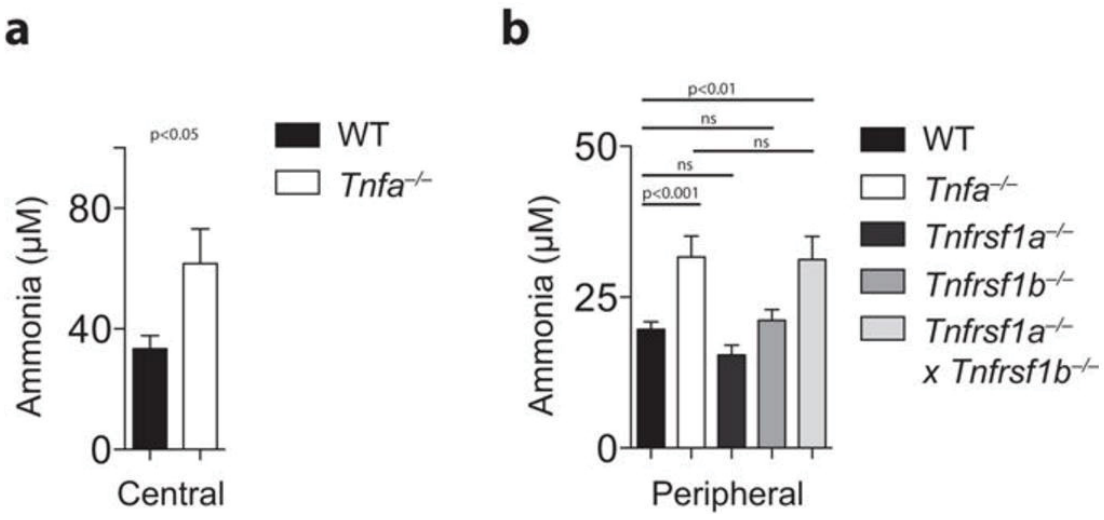

Figure 3.12 Hyperammonia in TNFα- and TNFR1/TNFR2-deficient animals.

(A) Ammonia levels were measured in blood samples harvested by cardiac puncture n=4) of WT and *Tnfa*$^{-/-}$ mice. (B) Ammonia levels were measured in blood samples harvested from the retro orbital vein sinus of WT, *Tnfa*$^{-/-}$, *Tnfrsf1a* $^{-/-}$,*Tnfrsf1b* $^{-/-}$, and *Tnfrsf1a* $^{-/-}$ *Tnfrsf1b* $^{-/-}$ animals (n=4-20).

Next, we investigated the role of TNFα in the regulation of hepatic ammonia. No difference in the localization of hepatic GS in TNFα-deficient animals (Figure 3.13 A) was observed. Moreover, enzymatic activity of hepatic GS in *Tnfa*$^{-/-}$ mice was significantly higher than in WT (Figure 3.13 B). Expression of ornithine aminotransferase, Rhesus family B glycoprotein, and excitatory amino acid transporter 2 (EAAT2/GLT-1) was similar between WT and *Tnfa*$^{-/-}$ livers (Figure 3.13 C).

Expression of the rate-limiting enzyme for the urea cycle Cps-1 was significantly lower in the livers of *Tnfa*$^{-/-}$ mice compared with WT. However, expression of the genes coding other urea cycle enzymes was not altered. (Figure 3.13 D).

These data indicate that TNFα deficiency induces systemic hyperammonemia but does not alter liver zonation. Also, these data show that in the absence of TNFα, reduced expression of the *Cps-1* gene may contribute to the onset of hyperammonemia.

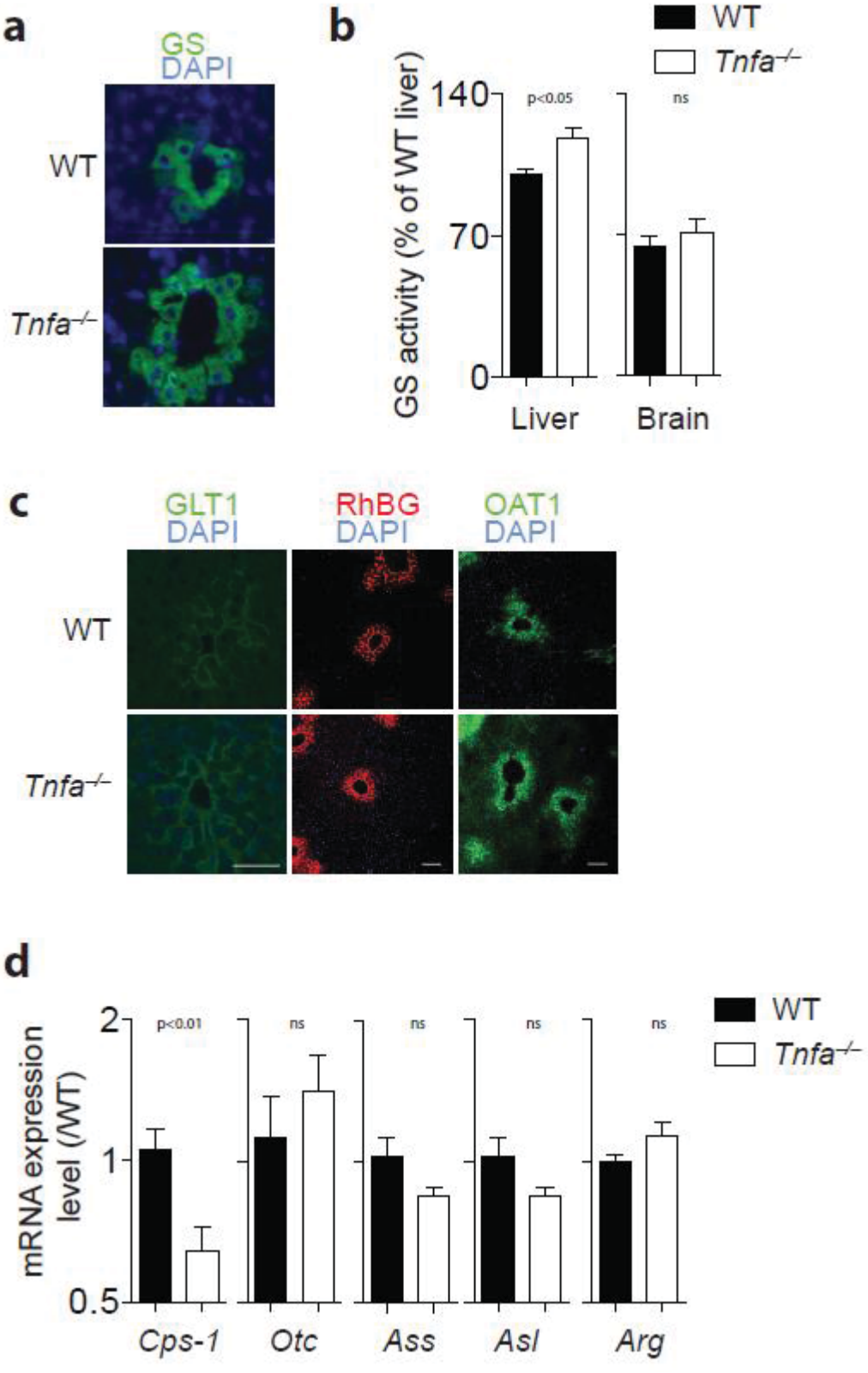
a
GS
DAPI
WT
Tnfa-/-
b
WT
Tnfa-/-
GS activity (% of WT liver)
140
70
0
p<0.05
ns
Liver
Brain
c
GLT1
DAPI
RhBG
DAPI
OAT1
DAPI
WT
Tnfa-/-
d
mRNA expression level (/WT)
2
1
0.5
p<0.01
ns
ns
ns
ns
WT
Tnfa-/-
Cps-1
Otc
Ass
Asl
Arg

Figure 3.13 Intact liver structure but reduced hepatic expression of CPS-1 in TNFα deficient animals. (A) Sections from snap frozen liver tissue harvested from WT and *Tnfa*$^{-/-}$ mice were stained with anti-GS antibodies (One representative of n=6 is shown, Scale bar = 25μm). (B) GS activity was measured in liver tissue (left panel, n=6), and whole brain tissue (right panel, n=3) from WT and *Tnfa*$^{-/-}$ mice. (C) Sections from snap frozen liver tissue from WT and *Tnfa*$^{-/-}$ mice were stained with anti-GLT1 (left panels, scale bar = 25μm), anti-RhBG (middle panels, scale bar = 100μm), and OAT1 (right panels, scale bar = 100μm). One representative out of n=6 is shown. (D) RNA expression levels of *Cps-1*(n=9), *Otc* (n=6), *Ass* (n=6), *Asl* (n=6), and *Arg* (n=6) were determined in liver tissue from WT and *Tnfa*$^{-/-}$ mice.

TNFα deficiency does not affect tyrosine nitration and RNA oxidation of brain tissues.

Ammonia can cause tyrosine nitration and oxidation of RNA, which can be assessed using anti-nitrotyrosine antibodies and 8-OH-guanosine, respectively. [218] Ammonia can reach brain tissue by passive diffusion or by passing through aquaporins 8 and 9. Additionally, aquaporin 4 is known to be induced by ammonia and promote cerebral edema.[245,247] We found no difference in the expression of aquaporin coding genes Aqp4, Aqp8, and Aqp9 in the cerebellum or cortex of WT and TNFα knockout animals (Figure 3.14 A, B).

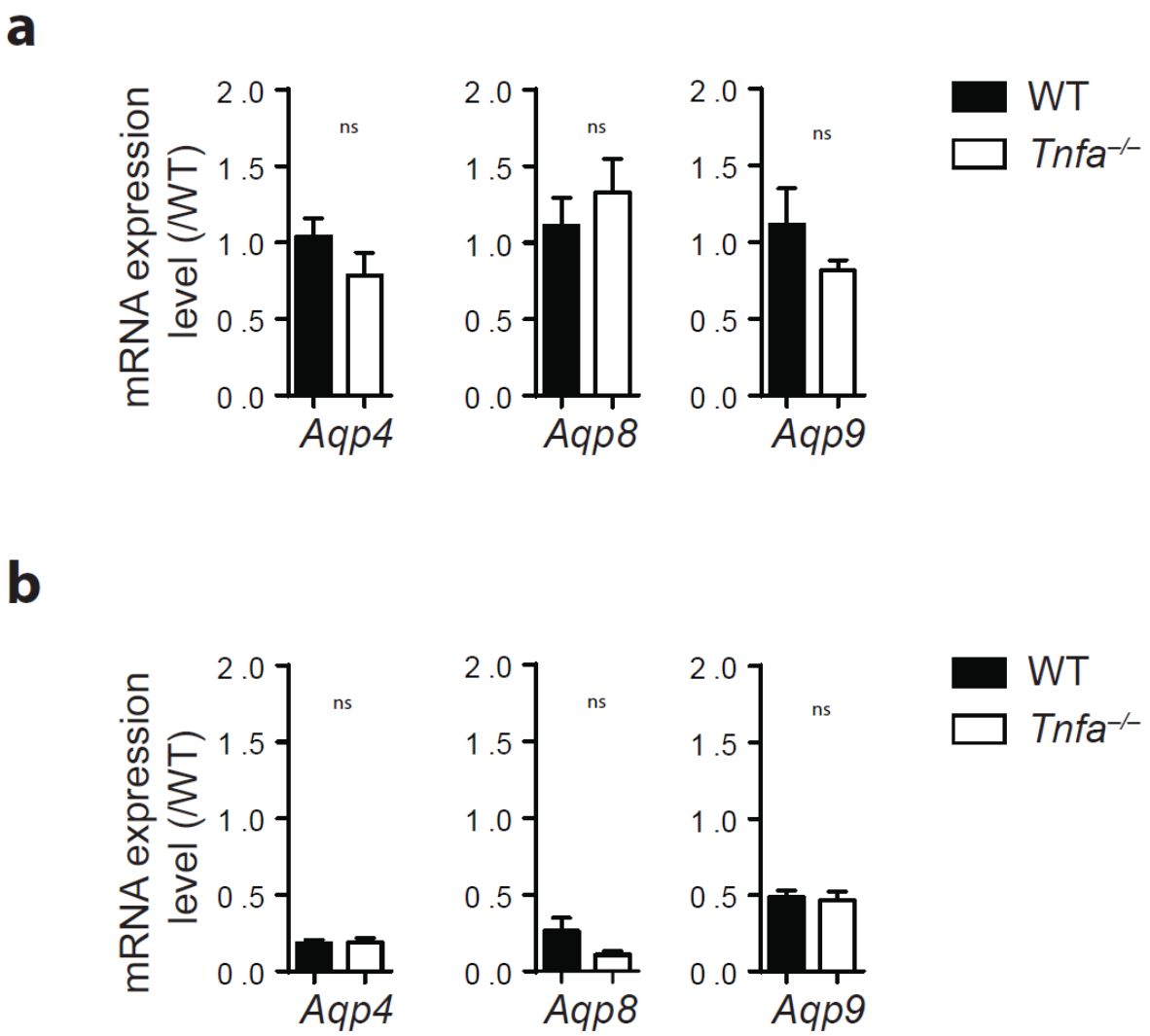

Figure 3.14 TNFα is dispensable for aquaporin expression. (A) RNA expression levels of Aqp4 (left panel), Aqp8 (middle panel), and Aqp9 (right panel) were measured in the cerebellum of WT and TNFα deficient animals (n=6). (B) RNA expression levels of Aqp4 (left panel), Aqp8 (middle panel), and Aqp9 (right panel) were measured in the cortex of WT and TNFα deficient animals (n=6-7).

Ammonia levels in the cerebrospinal fluid of WT and *Tnfa*$^{-/-}$ knockout mice were not altered (Figure 3.15 A). We also observed no difference in protein tyrosine nitration in the cerebellum and cortex of WT and TNFα-deficient animals by western blot (Figure 3.15 B) or by histological analysis (Figure 3.15 C, D). Consequently, no difference in the RNA oxidation was observed between WT and *Tnfa*$^{-/-}$ mice (Figure 3.15 E, F).

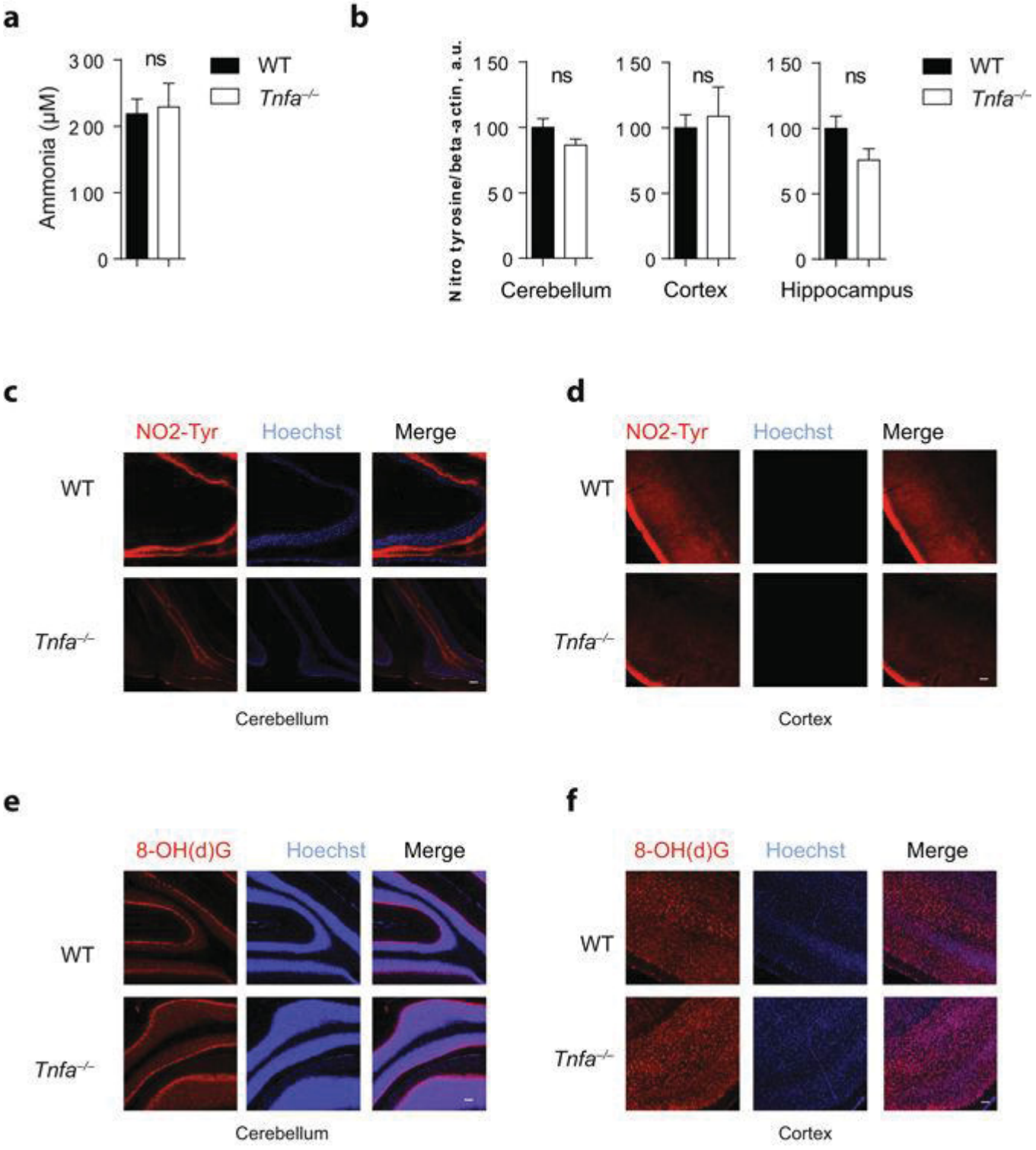
a
b
Ammonia (μM)
3 00
2 00
1 00
0
ns
WT
Tnfa−/−
N itro tyr os ine/ beta -a ctin , a.u.
1 50
1 00
5 0
0
ns
Cerebellum
Cortex
Hippocampus
c
d
NO2-Tyr
Hoechst
Merge
WT
Tnfa−/−
Cerebellum
Cortex
e
f
8-OH(d)G
Hoechst
Merge
WT
Tnfa−/−
Cerebellum
Cortex

Figure 3.15 Normal tyrosine nitration and RNA oxidation in brain tissues from *Tnfa*$^{-/-}$ mice. **(a)** Ammonia levels were measured in cerebrospinal fluid samples of WT and *Tnfa*$^{-/-}$ mice (n = 4–6). **(b)** Protein lysates harvested from the cerebellum of WT and *Tnfa*$^{-/-}$ mice were blotted and stained using anti-nitrotyrosine and anti-beta-actin antibodies, panel illustrates the densitometric analysis of nitrotyrosine/beta-actin (n = 17). **(c–d)** Sections from snap frozen (**c**) cerebellum or (**d**) cortex of WT and TNFα deficient mice were stained with anti-nitrotyrosine antibodies (red) and Hoechst (blue). One representative of n = 6 is shown, scale bar = 100 µm. **(e–f)** Sections from snap frozen (**e**) cerebellum or (**f**) cortex of WT and TNFα deficient mice were stained with anti-8-OH(d)G antibodies (red) and Hoechst (blue). One representative of n = 6 is shown, scale bar = 100 µm.

Tnfa$^{-/-}$ mice are protected against acute ammonia intoxication.

Glutamine synthetase is important for maintaining ammonia homeostasis *in vivo*. Mice lacking hepatic glutamine synthetase, as well as TNFα-deficient mice, demonstrate hyperammonemia. Consequently, during the challenge with sub-lethal doses of ammonia, *Glul*$^{fl/fl}$ *x Alb-Cre*$^{+}$ mice demonstrated high susceptibility towards ammonia intoxication compared with WT mice (Figure 3.16 A). After 15 minutes of ammonia intoxication, significantly higher levels of ammonia were observed in the peripheral blood of *Glul*$^{fl/fl}$ *x Alb-Cre*$^{+}$ mice, suggesting delayed ammonia clearance (Figure 3.16 B). An opposite effect of ammonia was observed in TNFα-deficient animals, when we challenged *Tnfa*$^{-/-}$ mice and WT with a lethal dose of ammonia, *Tnfa*$^{-/-}$ mice appeared to be protected against acute ammonia intoxication (Figure 3.16 C).

We also investigated whether TNFα triggers ammonia toxicity in the brain, specifically through one TNFR. When we challenged WT, TNFR1 and TNFR2 deficient mice with ammmonia, only TNFR1-deficient mice were protected from intoxication, while WT and TNFR2-deficient mice died in a similar manner (Figure 3.16 D). Interestingly, no significant differences in ammonia concentration in the blood were observed between WT and *Tnfa*$^{-/-}$ mice (Figure 3.16 E) or between WT, TNFR1-, and TNFR2-deficient mice (Figure 3.16 F). Taken together, these data indicate that TNFα enhances ammonia toxicity *in vivo* via TNFR1.

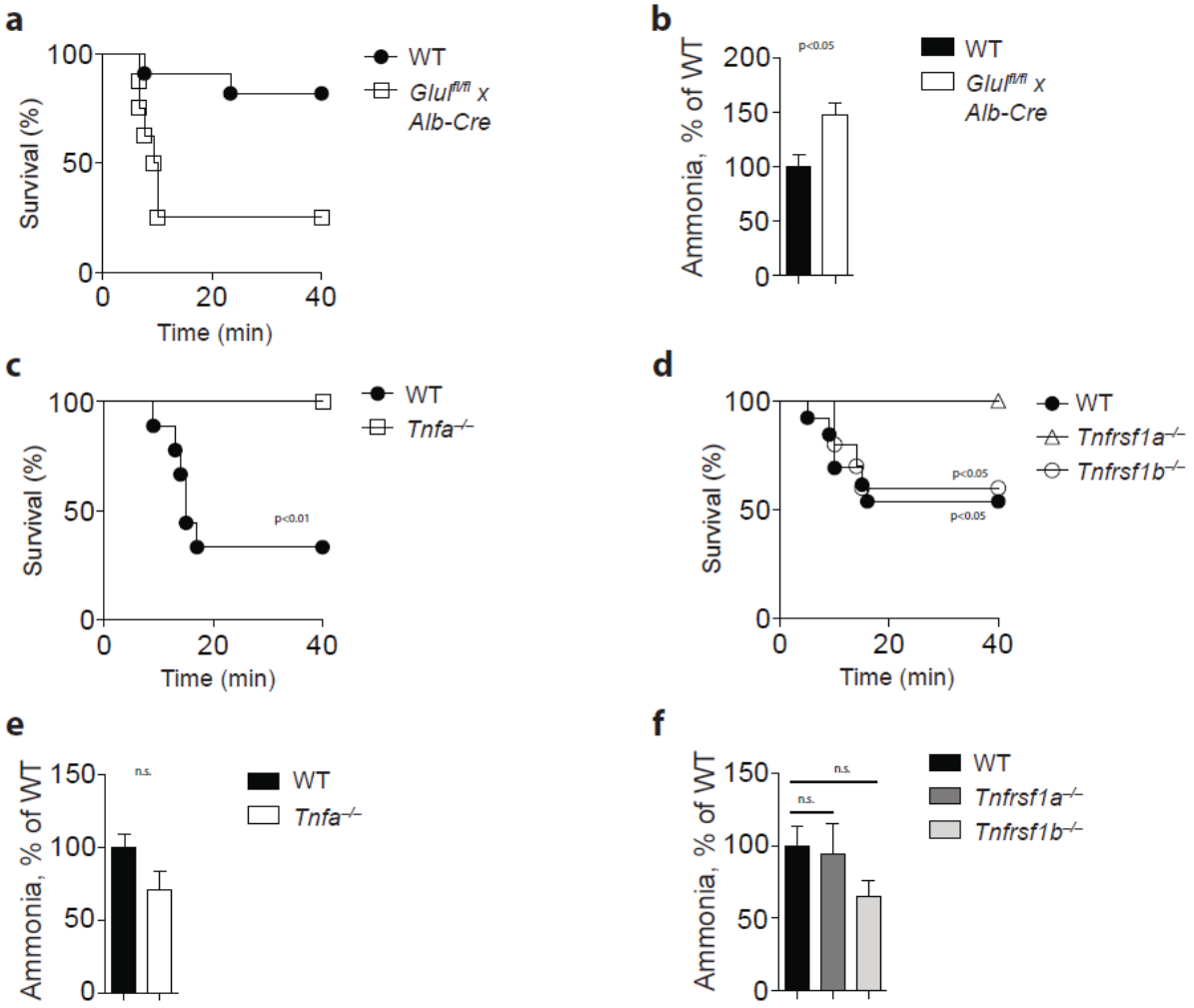
a
Survival (%)
100
50
0
0
20
40
Time (min)
WT
Glulfl/fl x
Alb-Cre
b
Ammonia, % of WT
200
150
100
50
0
p<0.05
WT
Glulfl/fl x
Alb-Cre
c
Survival (%)
100
50
0
0
20
40
Time (min)
p<0.01
WT
Tnfa−/−
d
Survival (%)
100
50
0
0
20
40
Time (min)
p<0.05
p<0.05
WT
Tnfrsf1a−/−
Tnfrsf1b−/−
e
Ammonia, % of WT
150
100
50
0
n.s.
WT
Tnfa−/−
f
Ammonia, % of WT
150
100
50
0
n.s.
n.s.
WT
Tnfrsf1a−/−
Tnfrsf1b−/−

Figure 3.16 *Tnfa*$^{-/-}$ mice are protected against acute ammonia intoxication. (a) WT and Glul$^{fl/fl}$ × Alb-Cre^{+} mice were challenged with 12 mmol/kg ammonium acetate in PBS following monitoring of survival (n = 8–11). (b) WT and Glul$^{fl/fl}$ × Alb-Cre $^{+}$ mice were challenged with 8 mmol/kg ammonium acetate in PBS, ammonia levels were measured in blood samples harvested from the retro-orbital venous sinus (n = 5–6). (c) Survival was monitored in WT and Tnfa$^{-/-}$ mice after challenge with 14 mmol/kg ammonium acetate in PBS (n = 8–9). (d) WT, Tnfrsf1a −/−, and Tnfrsf1b −/− mice were challenged with 14 mmol/kg ammonium acetate in PBS following monitoring of their survival (n = 10–13). (e) WT and Tnfa$^{-/-}$ mice were challenged with 8 mmol/kg ammonium acetate in PBS and ammonia levels were measured in blood samples harvested from the retro-orbital venous sinus (n = 9). (f) WT, Tnfrsf1a $^{-/-}$, and Tnfrsf1b $^{-/-}$ mice were challenged with 8 mmol/kg ammonium acetate in PBS and ammonia levels were measured in blood samples harvested from the retro-orbital venous sinus (n = 7–9).

To further investigate the role of TNFα during ammonia toxicity, we injected TNFα or PBS in WT mice and after three hours challenged these mice with ammonia. TNFα alone without D-Gal did not induce liver damage and did not affect ammonia concentration in the blood (Figure 3.17 A).

However, mice treated with TNFα spent a significantly longer time in coma after the ammonia acetate administration compared with the PBS-treated group (Figure 3.17 B). When we challenged WT animals with TNFα and D-Gal followed by the ammonia acetate challenge, we observed high susceptibility of these animals to ammonia toxicity compared with PBS-treated animals (Figure 3.17 C).

The TNFα effect was transient and after 24 hours, mice treated with TNFα demonstrated similar coma duration after the ammonia acetate challenge as the PBS-treated group (Figure 3.18).

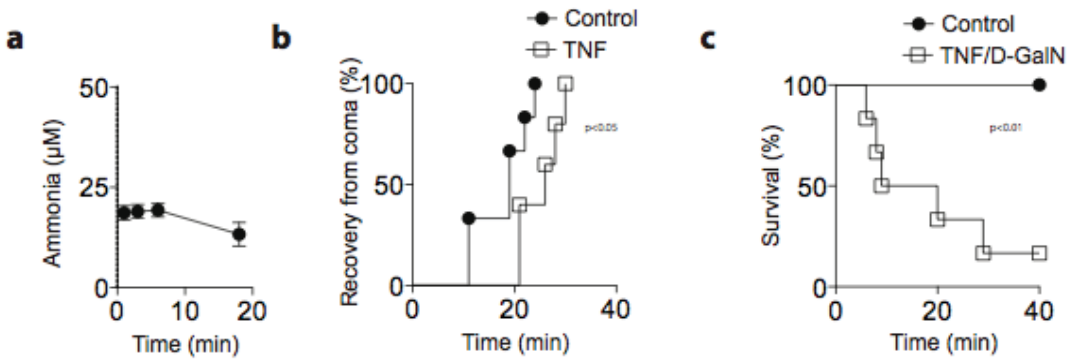

Figure 3.17 TNFα increases susceptibility towards ammonia toxicity. (A) Ammonia concentrations were measured from retro-orbital venous sinus after i.v. injection of 200ng TNFα (n=3). (B) C57Bl/6 animals were challenged intravenously with either 200ng TNFα or vehicle. After 3 hours 12 mmol/kg ammonium acetate in PBS was injected intraperitoneally followed by measurement of the coma time (n=5-6). (C) C57Bl/6 mice were injected with D- Gal and after 15 minutes with 200ng TNF. After 3 hours animals were challenged with 12 mmol/kg ammonium acetate in PBS along with a control group (n=6).

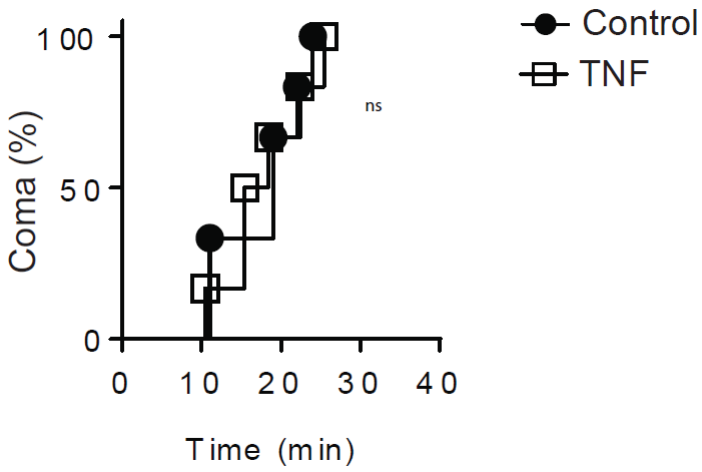

Figure 3.18 TNFα transiently promotes ammonia toxicity. C57Bl/6 animals were challenged intravenously with either 200ng TNFα or vehicle. After 24 hours 12 mmol/kg ammonium acetate in PBS was injected intraperitoneally following measurement of the coma time (n=6).

TNFα regulates expression of NKCC1 in brain tissue.

NKCC1 can transport ammonia[334] and regulate ammonia toxicity *in vivo* by regulating buffering of extracellular potassium by astrocytes.[244]

We investigated whether TNFα can affect NKCC1 expression in brain tissue. Findings revealed reduced expression of NKCC1 in the cerebellum of TNFα - deficient animals compared with the cerebellum from WT animals, using western-blot (Figure 3.19 A) and histological analysis (Figure 3.19 B). An opposite effect was observed after intravenous administration of TNFα, i.e., we observed a significant increase in NKCC1 expression in the cerebellum (Figure 3.19 C, D) and cerebral cortex (Figure 3.19 E, F) in TNFα-treated animals compared with PBS-treated mice. Taken together, these data indicate that TNFα regulates expression of NKCC1 in the brain.

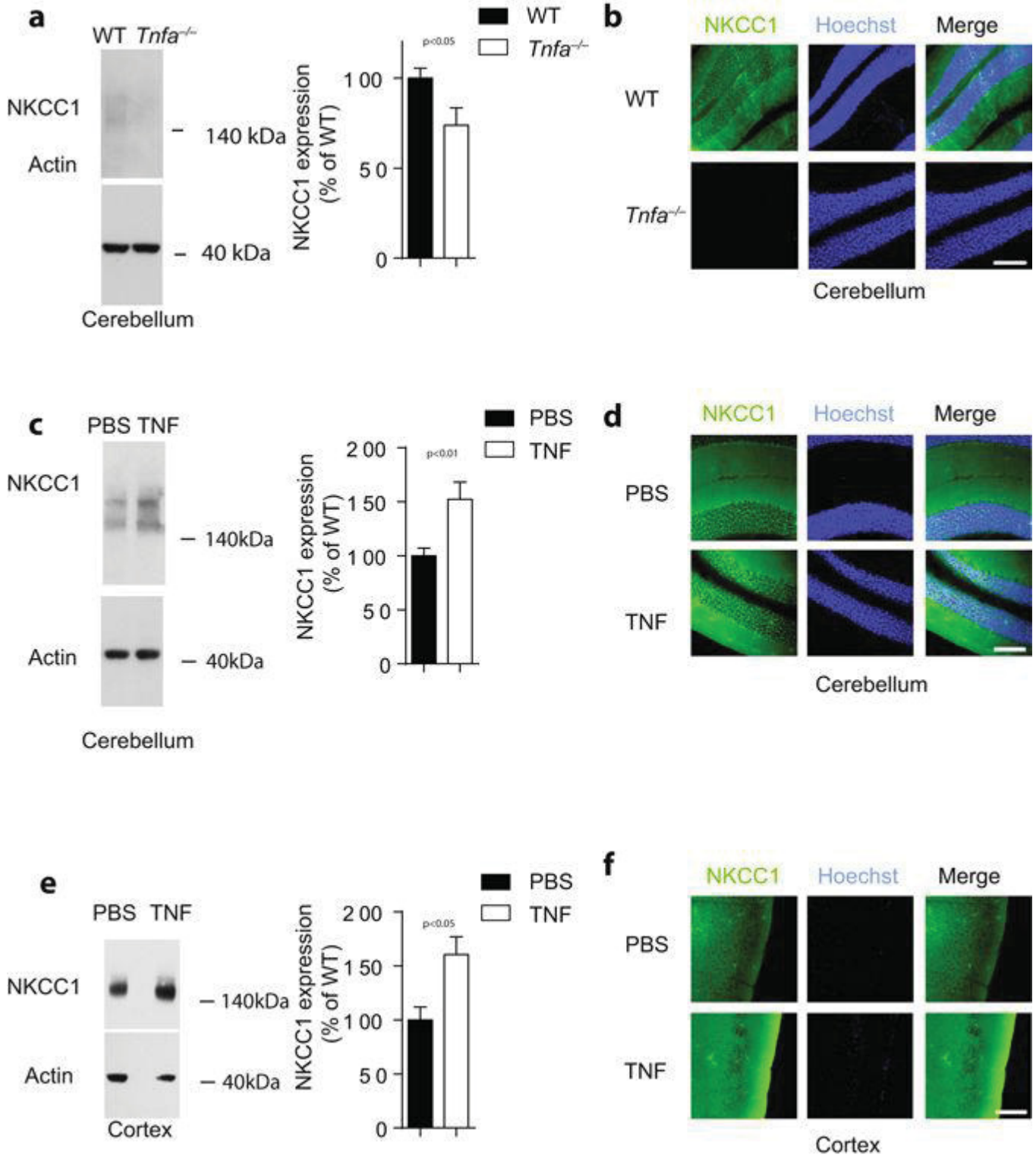
a
WT Tnfa-/-
NKCC1
Actin
140 kDa
40 kDa
Cerebellum
NKCC1 expression (% of WT)
p<0.05
WT
Tnfa-/-
b
NKCC1
Hoechst
Merge
WT
Tnfa-/-
Cerebellum
c
PBS TNF
NKCC1
Actin
140kDa
40kDa
Cerebellum
NKCC1 expression (% of WT)
p<0.01
PBS
TNF
d
NKCC1
Hoechst
Merge
PBS
TNF
Cerebellum
e
PBS TNF
NKCC1
Actin
140kDa
40kDa
Cortex
NKCC1 expression (% of WT)
p<0.05
PBS
TNF
f
NKCC1
Hoechst
Merge
PBS
TNF
Cortex

Figure 3.19. TNFα regulates expression of NKCC1 in brain tissue. (A) Protein lysates harvested from the cerebellum of WT and *Tnfa*$^{-/-}$ mice were blotted and stained using anti-NKCC1 (upper panel) and anti-beta- actin (lower panel) antibodies (One representative of n=12 is shown). Right panel illustrates the densitometrie of NKCC1/beta-actin (n=12). (B) Sections from snap frozen cerebellum of WT and TNFα deficient mice were stained with anti-NKCC1 antibodies (green) and Hoechst (blue). One representative of n=6 is shown, scale bar=100μm. (C-D) C57Bl/6 mice were treated with 200ng TNF. After 3h, protein lysates from (C) cerebellum or (D) cortex were blotted and stained with anti- NKCC1 and anti-beta- actin antibodies (left panels, one representative of n=8 is shown). Right panels illustrate the mean ± S.E.M. of the densitometric analysis of NKCC1/beta-actin (n=8). (E-F) After 3h, sections from snap frozen (E) cerebellum or (F) cortex were stained with anti-NKCC1 (green) and Hoechst (blue, n=6).

Pharmacological blockade of NKCC1 decreases severity of acute ammonia intoxication and does not affect ammonia levels in the blood.

We investigated whether pharmacological blockade of NKCC1 could modulate the toxic effects of ammonia *in vivo*. NKCC1 inhibitor (bumetanide) was used for the *in vivo* blockade of NKCC1 and when we administrated 30 mg/kg of bumetanide in DMSO, we observed no changes in ammonia levels in the peripheral blood of mice after 15 minutes and 60 minutes after administration (Figure 3.20 A). However, when bumetanide or DMSO was administrated together with 14 mmol/kg of ammonia acetate, we observed reduced coma duration in the bumetanide-treated group (Figure 3.20 B). These data demonstrate that pharmacological blockade of NKCC1 could decrease the toxic effects of acute ammonia intoxication.

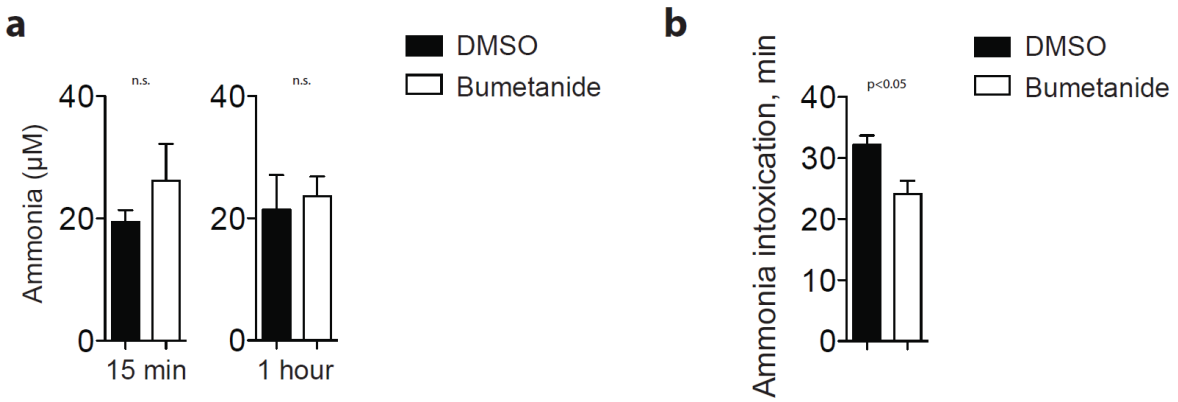

Figure 3.20 Inhibition of NKCC1 alleviates acute ammonia toxicity. (a) Ammonia concentrations were measured from retro-orbital venous sinus after i.p. injection of 30 mg/kg bumetanide (n = 5). (b) C57Bl/6 animals were treated intraperitoneally with either 30 mg/kg Bumetanide or vehicle. After 5 minutes 14 mmol/kg ammonium acetate in PBS was injected intraperitoneally followed by measurement of the duration of intoxication (time until recovery from coma) (n = 5–7).

4. Discussion

As identified by autopsy studies, the prevalence of cirrhosis is 4.5-9.5% in the general human population.[335] More specifically, liver cirrhosis is responsible for 2% of deaths worldwide, which consisted of and 771,000 deaths in 2001 and 722,000 deaths in 2015.[335,336] More than 60% of patients with cirrhosis have symptoms of hepatic encephalopathy.[175] It is therefore important to gain knowledge about mechanisms involved in the pathogenesis of hepatic encephalopathy in order to effectively treat and prevent the disease.

In the present studies, we dissect the role of hepatic glutamine synthetase and TNFα in ammonia metabolism and the pathogenesis of hepatic encephalopathy. We found that deletion of hepatic glutamine synthetase is sufficient to trigger hyperammonemia and symptoms of hepatic encephalopathy. Also, excess ammonia causes oxidative stress and oxidation of RNA in the brain tissue. We also found that deficiency in hepatic glutamine synthetase cannot be compensated by the urea cycle or extrahepatic glutamine synthetase. Additionally, our studies revealed that basal expression of TNFα drives expression of the *Cps-1* gene, which is necessary for urea cycle function. *Tnfa*$^{-/-}$ mice demonstrate hyperammonemia, but at the same time are protected against acute ammonia intoxication. TNFα is regulating expression of Na-K-Cl cotransporter (NKCC1), which can transport ammonia and mediate ammonia toxicity. Therefore, TNFα can promote susceptibility of mice to ammonia toxicity. Pharmacological inhibition of NKCC1 *in vivo* reduced coma duration after acute ammonia intoxication.

Hepatic detoxification of ammonia relies on two pathways: the urea cycle and glutamine synthetase.[17] The urea cycle is active in the periportal area of the liver acinus and requires activity of hepatic glutaminase. Hepatic glutaminase is needed to

produce glutamate and ammonia from glutamine and therefore increases local concentrations of ammonia to feed the urea cycle with ammonia. Ammonia spillover from the urea cycle is metabolized by hepatic GS, which combines ammonia and glutamate to glutamine. Hepatic glutamine synthetase is expressed in a small population of hepatocytes located in perivenous area of liver acinus and represent only 6-7% of hepatocytes.[16]

The importance of hepatic glutamine synthetase in the detoxification of ammonia and pathogenesis of hepatic encephalopathy has been discussed for decades, however, there has been no direct experimental *in vivo* evidence.[337,327] According to our observations, expression of hepatic glutamine synthetase appear to be vital in the prevention of systemic hyperammonemia. The present research used *Glul*$^{fl/fl}$ × *Alb-Cre*$^{+}$ mice, which lack GS only in the liver. The expression of glutamine synthetase in skeletal muscles and brain tissue was unaffected but insufficient to detoxify the excess of ammonia and prevent hyperammonemia. These data are supported by a study of muscle-specific GS knockout mice, which revealed no elevation of ammonia concentration in the arterial blood in naïve conditions.[183] Taken together, these phenotypes highlight the importance of hepatic glutamine synthetase in ammonia metabolism.

Patients with liver cirrhosis demonstrate reduced activity of the urea cycle and consequently, reduced excretion of nitrogen with urea.[338] Reduced activity of the urea cycle during chronic liver injury leads to compensatory up-regulation of glutaminase activity by 4-6 folds.[339] Increased glutaminase activity may contribute to further elevation of blood ammonia levels.

Hepatic glutamine synthetase represents the second mechanism of hepatic ammonia detoxification. Patients with hepatocellular carcinoma demonstrate significantly

reduced activity of hepatic GS.[340] Such reduced GS activity has also been observed *in vivo* in experimental model of rat cirrhosis.[341] During LPS induced liver injury, GS can undergo nitration in the catalytic center and such nitration leads to the inhibition of GS activity and can contribute to the onset of hyperammonemia and hepatic encephalopathy.[21]

Hepatic GS is expressed only in periveneous hepatocytes. Heterogenic distribution of hepatocytes function and liver zonation rely on WNT/β-catenin signaling.[34] Notably, our findings revealed that selective deletion of GS in *Glul*$^{fl/fl}$ × *Alb-Cre*$^{+}$ mice did not affect liver zonation, but was sufficient to trigger hyperammonemia.

Elevated concentrations of ammonia are not toxic to hepatocytes and in our study, we detected no significant elevation of transaminase activity in the serum from GS-deficient mice. However, the central nervous system is more sensitive to ammonia intoxication.[342]

Defects in the urea cycle lead to ammonia intoxication and the onset of neurological disorders such as mental status changes, brain edema, seizures, coma, and potentially death.[343]

Patients with mutations in the glutamine synthetase gene exhibit hyperammonemia, brain atrophy, epileptic encephalopathy, seizures, and multiple organ failure.[19,344]

After ammonia reaches the brain, it is metabolized to glutamine by astrocytes, which express glutamine synthetase.[185] Accumulation of glutamine cause astrocyte swelling and oxidative and nitrosative stress, which can be observed by protein nitration and RNA oxidation. Astrocyte swelling and oxidative and nitrosative stress impair astrocyte function and affect neurotransmission, synaptic plasticity, and oscillatory networks in the brain, leading to brain edema and manifestations of hepatic

encephalopathy symptoms.[173] Acute hyperammonemia leads to the activation of NMDA-receptors, which can cause neuronal death by exitoxicity. Importantly, a blockade of NMDA receptors has been shown to protect animals from ammonia intoxication and death.[345]

It has also been shown that ammonia intoxication triggers oxidative stress and oxidation of RNA in cultured astrocytes and in the brains of rats.[218] In our study, we observed region-specific expression of oxidative stress markers in brains of *Glul*$^{fl/fl}$ × *Alb-Cre*$^{+}$ mice. Increased RNA oxidation was observed in regions in which functions are impaired during HE, i.e., memory formation in the hippocampus, processing of sensory stimuli in the somatosensory cortex, and motor function in the cerebellum, and particularly Purkinje cells. [346,347,348] Interestingly, we did not observe a significant difference in RNA oxidation in the piriform cortex of *Glul*$^{fl/fl}$ × *Alb-Cre*$^{+}$ mice. Patients with HE demonstrate a variety of symptoms such as lethargy, fatigue, disorientation, and flapping tremors.[176] On a behavioral level, oxidative stress in cerebellum and Purkinje cells have been associated with alterations in motor functions. We observed increased motor activity of glutamine synthetase-deficient mice in comparison with WT mice. Moreover, *Glul*$^{fl/fl}$ × *Alb-Cre*$^{+}$ mice have been shown to have reduced learning ability and exploratory activity and delayed habituation to a novel environment, which are attributed to ammonia-induced alterations in synaptic plasticity and gene expression in the brain.[349] Interestingly, patients with hepatic encephalopathy demonstrate reduced locomotor activity and a similar phenotype was observed *in vivo* in models of bile duct ligation, portacaval shunting, and portal vein ligation. [348,350,351,352,353]

Such differences in observed phenotypes suggest involvement of other factors in addition to hyperammonemia. These factors may include neuroinflammation,

impaired hepatic metabolism of other than ammonia compounds, or adaptation mechanism involved in the compensation of chronic hypermmonemea.

In accordance with previous observations, in the BDL model and portocaval anastomosis, we observed no anxious behavior induced by hyperammonemia.[351,354]

Hyperammonemia was observed in *Glul*$^{fl/fl}$ × *Alb-Cre*$^{+}$ mice at a young age, e.g., 8 weeks, and this remained until at least 12 month. *Glul*$^{fl/fl}$ × *Alb-Cre*$^{+}$ mice have similar chronic hyperammonemia to the sparse-fur mice with a point mutation in the ornithine transcarbamoylase gene, which leads to reduction of OTC enzymatic activity.[355] Similar to *Glul*$^{fl/fl}$ × *Alb-Cre*$^{+}$ mice, sparse-fur mice have demonstrated impaired cognition abilities and reduced lifespan.[356,357]

The reduced ability to detoxify ammonia by *Glul*$^{fl/fl}$ × *Alb-Cre*$^{+}$ mice ultimately led to death during acute ammonia intoxication.

During acute liver failure, activation of microglia can be observed *in vivo* and in patients samples.[358,224] Activated microglia produce pro-inflammatory cytokines, e.g., TNFα, IL-6, and IL-1β. These cytokines promote the onset of hepatic encephalopathy. Notably, TNFα can directly induce astrocyte swelling and thereby contribute to the onset of hepatic encephalopathy.[212] Zemtsova et al. have reported up-regulation of the activation marker Iba1 *in vitro* in microglia cultured in the presence of ammonia. Microglia and astrocytes *in vitro* in the presence of ammonia up-regulate mRNA of pro-inflammatory cytokines. Interestingly, rats injected with ammonia acetate have showed activation of microglia and elevated expression of TNF, IL-1β, and IFNγ mRNA. However, in post-mortem samples of humans with cirrhosis with or without HE, only upregulation of Iba1 was reported during HE, but no significant difference was observed in the expression of pro-inflammatory cytokines

genes.[227] Post-mortem analysis of human brain samples with cirrhosis with or without HE have revealed significantly different expression of 1012 genes, which included genes related to oxidative stress, microglia activation, receptor signaling, inflammatory pathways, cell proliferation, and apoptosis.[228] HE during cirrhosis has been associated with increased expression of microglia activation markers gene, but no up-regulation of mRNA of pro-inflammatory cytokines has been observed. Moreover, HE is associated with increased expression of genes counteracting pro-inflammatory signaling and pro-inflammatory cytokine expression.[228]

We did not observe activation of microglia or production of pro-inflammatory cytokines in the brains of *Glul*$^{fl/fl}$ × *Alb-Cre*$^{+}$ mice. These data indicate that ammonia alone is not sufficient to trigger activation of microglia and induce neuroinflammation in a mouse model of chronic hyperammonemia. Such results could be explained by differences between species, possible compensatory mechanisms triggered by chronic exposure of animals to high levels of ammonia, and complexity of cirrhosis and liver-brain interplay. Interestingly, microglia co-cultured with astrocytes have demonstrate attenuated activation, specifically, reduced expression of CD14, Iba1, and pro-inflammatory cytokines after LPS and ammonia treatment.[359]

Ammonia is considered to be the main pathogenesis factor of hepatic encephalopathy; however, severity of HE does not always correlate with observed concentrations of ammonia in patients' blood. During HE stage I or II, no elevation of ammonia concentration in systemic circulation has been reported in patients with cirrhosis.[133] This observation suggests an involvement of other factors in HE pathogenesis.

Systemic inflammation is reported to play an important role in hepatic encephalopathy during acute liver failure and chronic liver failure.

Patients with acute liver failure with a secondary infection and higher systemic inflammation score progress to the higher grade of HE and typically have a worse prognosis.[360] Notably, pigs with acute liver failure caused by amatoxin with higher score of systemic inflammation demonstrate higher mortality during HE in acute liver falure.[361]

In patients with cirrhosis and minimal hepatic encephalopathy, ammonia concentration and liver parameters do not correlate with HE severity, but severity of HE does correlate with inflammation markers.[362]

The direct impact of systemic inflammation on brain function during hyperammonemia is indicated by prolonged sick behavior of sparse-fur mice after administration of LPS *in vivo*.[356] Importantly, TNFα alone can trigger oxidative stress in vital mouse brain slices and cause RNA oxidation, which is characteristic for HE.[218]

One of the central pro-inflammatory cytokines is TNFα. LPS-induced liver damage is mediated by TNFα and associated with nitration and reduced activity of hepatic glutamine synthetase.[21] Concentration of TNFα in the blood is also correlated with HE severity.[134]

These data suggest involvement of TNFα in the regulation of liver metabolic functions and HE. We observed increased blood concentration of ammonia in TNFα-deficient mice in peripheral and central blood; these data indicate the importance of basal expression of TNFα for effective ammonia detoxification by the liver. Basal ammonia metabolism requires TNFα signaling through both TNFα receptors.

In the present research, liver zonation was not affected by TNFα deficiency, expression of hepatic GS, OAT1, RhBg and GLT1 appears to be not altered between WT- and TNFα-deficient mice. We also observed enhanced activity of hepatic

glutamine synthetase in *Tnfa*$^{-/-}$ mice, but activity of GS in the brain was not affected. We can assume that activity of hepatic GS was upregulated as a compensatory mechanism counteracting chronic hyperammonemia.

We also found that basal expression of TNFα promoted expression of *Cps-1* and therefore, may promote activity of the urea cycle. However, TNFα can promote liver injury and consequently, cause hyperammonemia and HE.[363,364]

TNFR1-deficient mice and IL-1β-receptor-deficient mice are less susceptible to azoxymethane-induced coma and have shown reduced brain edema compared with WT mice.[135] A blockade of TNFα signaling during acute liver failure by etanercept alleviates liver injury, hyperammonemia, and the toxic effects of ammonia.[358]

Despite elevated ammonia concentration in the blood of TNFα-deficient mice, we did not observe increased expression of oxidative stress markers in their brains. Both RNA oxidation and protein tyrosine nitration appeared to be unaltered in TNFα-deficient mice. Observed blood ammonia concentrations in TNFα-deficient mice was lower than in *Glul*$^{fl/fl}$ × *Alb-Cre*$^{+}$ mice and could be not sufficiently high to trigger oxidative stress in the brain, or, unknown compensatory mechanisms may have prevented oxidative stress. Elevated ammonia and basal TNFα could act synergistically and trigger astrocyte swelling and oxidative stress. The importance of basal expression of TNFα for CNS function is indicated by behavioral alterations demonstrated by TNFα-deficient mice. *Tnfa*$^{-/-}$ mice have shown depression-like behavior associated with reduced exploratory behavior than WT mice.[365] Moreover, TNFα-deficient mice demonstrate impaired cognition compared with WT-, TNFR1-, or TNFR2-deficient mice. In addition, *Tnfa*$^{-/-}$ mice have demonstrated poorer spatial learning and learning effectiveness than WT mice.[366]

In our studies, we found that TNFα-deficient mice were protected from acute ammonia intoxication in a TNFR1-dependent manner.

Importantly, administration of TNFα alone did not cause elevation of ammonia concentration in the blood stream, however, TNFα alone did prolong coma duration after ammonia intoxication. Administration of D-galactosamine and TNFα sensitizes the liver to TNFα-induced apoptosis and induces liver damage. Mice treated with D-galactosamine and TNFα are more susceptible to acute ammonia intoxication and these phenotypes could be result of the effects of TNFα on both the liver and CNS.

Previously, it was thought that ammonia freely diffuses across blood brain barrier.[367] However, recent evidence suggests the participation of ammonia transporters in ammonia transport across the BBB. Ammonia transport across the BBB is significantly delayed at reduced temperatures, suggesting participation of protein transporters.[368] Notably, TNFα is known to significantly increase diffusion of ammonia across endothelial cells from the central nervous system.[369]

We found that TNFα drives expression of the ammonia permeable ion channel NKCC1, which is crucial for the ammonia toxic effect *in vivo*. NKCC1 is also involved in brain edema formation after ischemia and traumatic brain injury. [240,242] Jaykumar et al. have demonstrated that NKCC1 mediates ammonia-induced swelling of astrocytes. [243] Moreover, NKCC1 activity is up-regulated *in vitro* after ammonia treatment. Ammonia cause enhanced synthesis of NKCC1 protein.[243]

Interestingly, ammonia trigger oxidative and nitrosative stress and cause nitration and phosphorylation of NKCC1. Nitration and phosphorylation of NKCC1 increase its activity and therefore, may further promote astrocyte swelling and oxidative stress.

Antioxidants *N*-nitro-L-arginine methyl ester and uric acid reduce nitration and activity of NKCC1. [243]

NKCC1 expression, phosphorylation, and activity have also been shown to be elevated in the brains of thioacetamide-treated rats compared with control rats. [370]

Notably, we found that pharmacological inhibition of NKCC1 activity by bumetanide decreased coma duration after ammonia intoxication.

During acute ammonia intoxication, ammonia compromise potassium buffering by astrocytes, increasing extracellular potassium concentration and over-activating the NKCC1 in neurons. [244] Excess ammonia and potassium depolarize the neuronal GABA potential. Specific blockade of NKCC1 with bumetanide reduces the amount of ammonia-induced seizures and ultimately reduced death in animals from ammonia intoxication.[244]

TNFα and IL-1β contribute to the onset of cerebral edema by the up-regulation of NKCC1 expression in astrocytes during brain injury.[371]

TNFα can be produced by activated microglia within the CNS.[372] Also, TNFα from the blood stream can be actively transported across the blood brain barrier. This transport requires activity of both TNFR1 and TNFR2.[373]

TNFα, in addition to up-regulation of NKCC1 expression in the brain, could promote expression of aquaporins. Moreover, aquaporin 4 expression is induced *in vitro* in astrocytes directly by ammonia acetate and *in vivo* during endotoxin-induced liver damage.[247,248] Expression of aquaporin 4 correlates with the severity of brain edema in ischemia and traumatic brain injury.[251,252,253] Aquaporin 3, 8, and 9 can transport ammonia.[246,374] We did not observe significant difference of aquaporins mRNA

expression in the brain between WT and *Tnfa*$^{-/-}$ mice. However, we cannot exclude potential regulation of aquaporins expression on the protein level.

TNFα can activate glutaminase in microglia and thereby promote glutamate release.[375,376,372] An excess of extracellular TNFα promotes accumulation of glutamate and can induce excitotoxicity, inhibit synaptic activity, or kill neurons.[375] Excess of cerebral TNFα is associated with neuronal death in several diseases including post-stroke syndrome, Alzheimer's disease, traumatic brain injury, and Parkinson's disease.[377]

TNFα can also potentiate glutamate-induced excitotoxicity and neuron death by direct activation of NMDA receptor via TNFRII.[378] Ammonia toxicity *in vivo* is mediated through NMDA receptor and can be prevented by selective NMDA receptor antagonist MK-801. [379],[380]

Observed chronic hyperammonemia in TNFα-deficient mice can trigger adaptation, for example, rats with chronic hyperammonemia are protected against acute ammonia intoxication due to enhanced ammonia clearance and reduced activity of the NMDA-NO-cGMP pathway.[381,382]

Our findings are further supported by the work of Bemeur et al. in which TNFR1- and IL-1R1-deficient mice were shown to have an advantage over WT during acute liver failure caused by azoxymetane.[135] A blockade of TNFα signaling by etanercept decreased liver damage, serum activity of ALT and AST, and circulating ammonia levels. Notably, effects of etanercept treatment make it difficult to conclude if the observed delay in coma and reduced oxidative stress in brains were due to improved liver function or the blockade of the direct effects of TNFα on the CNS.[383] Anti- TNFα antibody Infliximab has been shown to reduce peripheral inflammation and

neuroinflammation and improve learning ability and motor coordination in rats with portocaval shunts. [384] Since antibodies cannot pass through blood brain barrier, positive effects on cognition and reduced activation of microglia can be attributed to reduced peripheral inflammation.[384] Our findings suggest that blocking of NKCC1 or TNFR1 could be beneficial for patients with hepatic encephalopathy. However, currently used TNFα blockers (etanercept or infliximab) bind directly to TNFα molecules and therefore block signaling through both receptors TNFR1 and TNFR2. According to our findings, a blockade of TNFα could lead to the hyperammonemia and down-regulation of NKCC1 expression. However, selective blockade of TNFR1 could desynthesize the brain to toxic effects of ammonia by the down-regulation of NKCC1 expression and would therefore not promote alterations in hepatic ammonia metabolism.

5. References

1. Hollander, C. F., van Bezooijen, C. F. & Solleveld, H. a. Anatomy, function and aging in the mouse liver. *Arch. Toxicol. Suppl.* **10,** 244–50 (1987).
2. Cook, M. J. The anatomy of the laboratory mouse. *Food and Cosmetics Toxicology* **4,** 371–372 (1966).
3. Kmieć, Z. Cooperation of liver cells in health and disease. *Adv. Anat. Embryol. Cell Biol.* **161,** III–XIII, 1-151 (2001).
4. Krishna, M. Microscopic anatomy of the liver. *Clinical Liver Disease* **2,** (2013).
5. Wisse, E. *et al.* Structure and function of sinusoidal lining cells in the liver. *Toxicol. Pathol.* **24,** 100–111 (1996).
6. Jungermann, K. & Keitzmann, T. Zonation of Parenchymal and Nonparenchymal Metabolism in Liver. *Annu. Rev. Nutr.* **16,** 179–203 (1996).
7. Haussinger, D. Nitrogen metabolism in liver: structural and functional organization and physiological relevance. *Biochem. J.* **267,** 281–290 (1990).
8. Haussinger, D., Lamers, W. H. & Moorman, A. F. Hepatocyte heterogeneity in the metabolism of amino acids and ammonia. *Enzyme* **46,** 72–93 (1992).
9. Walker, V. Ammonia metabolism and hyperammonemic disorders. *Adv. Clin. Chem.* **67,** 71–150 (2014).
10. Camacho, J. A. *et al.* Clinical and functional characterization of a human ORNT1 mutation (T32R) in the hyperornithinemia-hyperammonemia-homocitrullinuria (HHH) syndrome. *Pediatr. Res.* **60,** 423–429 (2006).
11. Saheki, T. & Kobayashi, K. Mitochondrial aspartate glutamate carrier (citrin) deficiency as the cause of adult-onset type II citrullinemia (CTLN2) and idiopathic neonatal hepatitis (NICCD). *Journal of Human Genetics* **47,** 333–341 (2002).
12. Stewart, P. M. & Walser, M. Short term regulation of ureagenesis. *J. Biol. Chem.* **255,** 5270–5280 (1980).
13. Beliveau, C. G., Cheung, C., Cohen, N., Brusilow, S. & Raijman, L. Regulation of urea and citrulline synthesis under physiological conditions. *Biochem. J.* **292,** 241–247 (1993).
14. Curthoys, N. P. & Watford, M. Regulation of Glutaminase Activity and Glutamine Metabolism. *Annu. Rev. Nutr.* **15,** 133–159 (1995).
15. Sidney, M. & Morris, J. Regulation of enzymes of the urea cycle and arginine metabolism. *Annu. Rev. Nutr.* **12,** 81–101 (1992).
16. Gebhardt, R. & Mecke, D. Heterogeneous distribution of glutamine synthetase among rat liver parenchymal cells in situ and in primary culture. *EMBO J.* **2,** 567–70 (1983).
17. Häussinger, D. Regulation of hepatic ammonia metabolism: The intercellular glutamine cycle. *Adv. Enzyme Regul.* **25,** 159–180 (1986).

18. Summar, M. Current strategies for the management of neonatal urea cycle disorders. *J. Pediatr.* **138,** S30–S39 (2001).

19. Häberle, J. *et al.* Congenital glutamine deficiency with glutamine synthetase mutations. *N. Engl. J. Med.* **353,** 1926–1933 (2005).

20. Häussinger, D., Sies, H. & Gerok, W. Functional hepatocyte heterogeneity in ammonia metabolism. The intercellular glutamine cycle. *J. Hepatol.* **1,** 3–14 (1985).

21. Görg, B., Wettstein, M., Metzger, S., Schliess, F. & Häussinger, D. Lipopolysaccharide-induced tyrosine nitration and inactivation of hepatic glutamine synthetase in the rat. *Hepatology* **41,** 1065–1073 (2005).

22. Nielsen, S. S., Grøfte, T., Tygstrup, N. & Vilstrup, H. Cirrhosis and endotoxin decrease urea synthesis in rats. *Hepatol. Res.* **37,** 540–547 (2007).

23. Ramadori, G., Rasokat, H., Burger, R., Meyer Zum Büschenfelde, K. H. & Bitter-Suermann, D. Quantitative determination of complement components produced by purified hepatocytes. *Clin. Exp. Immunol.* **55,** 189–96 (1984).

24. Ramadori, G., Tedesco, F., Bitter-Suermann, D. & Meyer zum Buschenfelde, K. H. Biosynthesis of the third (C3), eighth (C8), and ninth (C9) complement components by guinea pig hepatocyte primary cultures. *Immunobiology* **170,** 203–210 (1985).

25. Levitt, D. G. & Levitt, M. D. Human serum albumin homeostasis: A new look at the roles of synthesis, catabolism, renal and gastrointestinal excretion, and the clinical value of serum albumin measurements. *International Journal of General Medicine* **9,** 229–255 (2016).

26. Strnad, P., Tacke, F., Koch, A. & Trautwein, C. Liver-guardian, modifier and target of sepsis. *Nature Reviews Gastroenterology and Hepatology* **14,** 55–66 (2017).

27. Kaminsky, L. S. & Zhang, Q. Y. The small intestine as a xenobiotic-metabolizing organ. *Drug Metabolism and Disposition* **31,** 1520–1525 (2003).

28. Lock, E. a & Reed, C. J. Xenobiotic metabolizing enzymes of the kidney. *Toxicol. Pathol.* **26,** 18–25 (1998).

29. Monga, S. P. S. *Molecular Pathology of Liver Diseases*. (2011).

30. Curtis D. Klaassen. *Toxicology - The Basic Science of Poisons*. *Toxicology* **12,** (2008).

31. Peter Guengerich, F. *et al.* Twenty years of biochemistry of human p450s. Purification, expression, mechanism, and relevance to drugs. *Drug Metabolism and Disposition* **26,** 1175–1178 (1998).

32. Ziegler, D. M. An overview of the mechanism, substrate specificities, and structure of FMOs. *Drug Metab. Rev.* **34,** 503–511 (2002).

33. Nassir, F., Rector, R. S., Hammoud, G. M. & Ibdah, J. A. Pathogenesis and Prevention of Hepatic Steatosis. *Gastroenterol. Hepatol. (N. Y).* **11,** 167–175 (2015).

34. Sekine, S., Lan, B. Y., Bedolli, M., Feng, S. & Hebrok, M. Liver-specific loss of beta-catenin blocks glutamine synthesis pathway activity and cytochrome p450 expression in mice. *Hepatology* **43,** 817–825 (2006).

35. Benhamouche, S. *et al.* Apc Tumor Suppressor Gene Is the 'Zonation-Keeper' of Mouse Liver. *Dev. Cell* **10,** 759–770 (2006).

36. Racanelli, V. & Rehermann, B. The liver as an immunological organ. *Hepatology* **43,** (2006).

37. Wisse, E., De Zanger, R. B., Charels, K., Van Der Smissen, P. & McCuskey, R. S. The liver sieve: considerations concerning the structure and function of endothelial fenestrae, the sinusoidal wall and the space of Disse. *Hepatology* **5,** 683–692 (1985).

38. Tavassoli, M., Kishimoto, T. & Kataoka, M. Liver endothelium mediates the hepatocyte's uptake of ceruloplasmin. *J. Cell Biol.* **102,** 1298–1303 (1986).

39. Warren, A. *et al.* T lymphocytes interact with hepatocytes through fenestrations in murine liver sinusoidal endothelial cells. *Hepatology* **44,** 1182–90 (2006).

40. Wu, J. *et al.* Toll-like receptor-induced innate immune responses in non-parenchymal liver cells are cell type-specific. *Immunology* **129,** 363–374 (2010).

41. Knolle, P. a & Limmer, A. Control of immune responses by savenger liver endothelial cells. *Swiss Med. Wkly. Off. J. Swiss Soc. Infect. Dis. Swiss Soc. Intern. Med. Swiss Soc. Pneumol.* **133,** 501–506 (2003).

42. Knolle, P. A. *et al.* IL-10 down-regulates T cell activation by antigen-presenting liver sinusoidal endothelial cells through decreased antigen uptake via the mannose receptor and lowered surface expression of accessory molecules. *Clin. Exp. Immunol.* **114,** 427–433 (1998).

43. Lohse, A. W. *et al.* Antigen-presenting function and B7 expression of murine sinusoidal endothelial cells and Kupffer cells. *Gastroenterology* **110,** 1175–1181 (1996).

44. Steffan, A. -M, Gendrault, J. -L, McCuskey, R. S., McCuskey, P. A. & Kirn, A. Phagocytosis, an unrecognized property of murine endothelial liver cells. *Hepatology* **6,** 830–836 (1986).

45. Sorensen, K. K. *et al.* The scavenger endothelial cell: a new player in homeostasis and immunity. *AJP Regul. Integr. Comp. Physiol.* **303,** R1217–R1230 (2012).

46. Limmer, a *et al.* Efficient presentation of exogenous antigen by liver endothelial cells to CD8(+) T cells results in antigen-specific T-cell tolerance. *Nat. Med.* **6,** 1348–1354 (2000).

47. Berg, M. *et al.* Cross-presentation of antigens from apoptotic tumor cells by liver sinusoidal endothelial cells leads to tumor-specific CD8+ T cell tolerance. *Eur. J. Immunol.* **36,** 2960–2970 (2006).

48. Limmer, A. *et al.* Cross-presentation of oral antigens by liver sinusoidal endothelial cells leads to CD8 T cell tolerance. *Eur. J. Immunol.* **35,** 2970–2981 (2005).

49. Diehl, L. *et al.* Tolerogenic maturation of liver sinusoidal endothelial cells promotes B7-homolog 1-dependent CD8+ T cell tolerance. *Hepatology* **47,** 296–305 (2008).

50. Knolle, P. a *et al.* Endotoxin down-regulates T cell activation by antigen-

presenting liver sinusoidal endothelial cells. *J. Immunol.* **162,** 1401–7 (1999).

51. Knoll, P. *et al.* Human Kupffer cells secrete IL-10 in response to lipopolysaccharide (LPS) challenge. *J. Hepatol.* **22,** 226–229 (1995).
52. Schildberg, F. a *et al.* Liver sinusoidal endothelial cells veto CD8 T cell activation by antigen-presenting dendritic cells. *Eur. J. Immunol.* **38,** 957–67 (2008).
53. Bilzer, M., Roggel, F. & Gerbes, A. L. Role of Kupffer cells in host defense and liver disease. *Liver International* **26,** 1175–1186 (2006).
54. Miura, K. *et al.* Toll-like receptor 9 promotes steatohepatitis by induction of interleukin-1beta in mice. *Gastroenterology* **139,** 323–34.e7 (2010).
55. Miura, K. *et al.* Toll-like receptor 2 and palmitic acid cooperatively contribute to the development of nonalcoholic steatohepatitis through inflammasome activation in mice. *Hepatology* **57,** 577–589 (2013).
56. van Egmond, M. *et al.* FcαRI-positive liver Kupffer cells: reappraisal of the function of immunoglobulin A in immunity. *Nat. Med.* **6,** 680–685 (2000).
57. Schieferdecker, H. L., Schlaf, G., Jungermann, K. & Götze, O. Functions of anaphylatoxin C5a in rat liver: Direct and indirect actions on nonparenchymal and parenchymal cells. in *International Immunopharmacology* **1,** 469–481 (2001).
58. Helmy, K. Y. *et al.* CRIg: A macrophage complement receptor required for phagocytosis of circulating pathogens. *Cell* **124,** 915–927 (2006).
59. He, J. Q. *et al.* CRIg mediates early Kupffer cell responses to adenovirus. *J. Leukoc. Biol.* **93,** 301–306 (2013).
60. Ju, C. *et al.* Protective role of kupffer cells in acetaminophen-induced hepatic injury in mice. *Chem. Res. Toxicol.* **15,** 1504–1513 (2002).
61. Chen, Y. *et al.* Induction of immune hyporesponsiveness after portal vein immunization with ovalbumin. *Surgery* **129,** 66–75 (2001).
62. Burgio, V. L. *et al.* Expression of co-stimulatory molecules by Kupffer cells in chronic hepatitis of hepatitis C virus etiology. *Hepatology* **27,** 1600–6 (1998).
63. You, Q., Cheng, L., Kedl, R. M. & Ju, C. Mechanism of T cell tolerance induction by murine hepatic Kupffer cells. *Hepatology* **48,** 978–990 (2008).
64. Lee, W.-Y. *et al.* An intravascular immune response to Borrelia burgdorferi involves Kupffer cells and iNKT cells. *Nat. Immunol.* **11,** 295–302 (2010).
65. Geerts, A. History, heterogeneity, developmental biology, and functions of quiescent hepatic stellate cells. *Seminars in Liver Disease* **21,** 311–335 (2001).
66. Friedman, S. L. Hepatic stellate cells: protean, multifunctional, and enigmatic cells of the liver. *Physiol. Rev.* **88,** 125–72 (2008).
67. Li, J.-T., Liao, Z.-X., Ping, J., Xu, D. & Wang, H. Molecular mechanism of hepatic stellate cell activation and antifibrotic therapeutic strategies. *J. Gastroenterol.* **43,** 419–428 (2008).
68. Baroni, G. S. *et al.* Interferon gamma decreases hepatic stellate cell activation and extracellular matrix deposition in rat liver fibrosis. *Hepatology* **23,** 1189–99 (1996).

69. Saile, B., Eisenbach, C., Dudas, J., El-Armouche, H. & Ramadori, G. Interferon-gamma acts proapoptotic on hepatic stellate cells (HSC) and abrogates the antiapoptotic effect of interferon-alpha by an HSP70-dependant pathway. *Eur. J. Cell Biol.* **83,** 469–76 (2004).

70. Chen, M. *et al.* Adeno-associated virus mediated interferon-gamma inhibits the progression of hepatic fibrosis in vitro and in vivo. *World J. Gastroenterol.* **11,** 4045–4051 (2005).

71. Viñas, O. *et al.* Human hepatic stellate cells show features of antigen-presenting cells and stimulate lymphocyte proliferation. *Hepatology* **38,** 919–29 (2003).

72. Winau, F. *et al.* Ito Cells Are Liver-Resident Antigen-Presenting Cells for Activating T Cell Responses. *Immunity* **26,** 117–129 (2007).

73. Muhanna, N., Horani, A., Doron, S. & Safadi, R. Lymphocyte-hepatic stellate cell proximity suggests a direct interaction. *Clin. Exp. Immunol.* **148,** 338–347 (2007).

74. Prickett, T. C., McKenzie, J. L. & Hart, D. N. Characterization of interstitial dendritic cells in human liver. *Transplantation* **46,** 754–761 (1988).

75. Lautenschlager, I., Halttunen, J. & Hayry, P. Characteristics of dendritic cells in rat liver. *Transplantation* **45,** 936–939 (1988).

76. Steiniger, B., Klempnauer, J. & Wonigeit, K. *Phenotype and histological distribution of interstitial dendritic cells in the rat pancreas, liver, heart, and kidney*. *Transplantation.* **38,** 169–174 (1984).

77. Yoneyama, H. & Ichida, T. Recruitment of dendritic cells to pathological niches in inflamed liver. in *Medical Molecular Morphology* **38,** 136–141 (2005).

78. Matsuno, K., Nomiyama, H., Yoneyama, H. & Uwatoku, R. Kupffer cell-mediated recruitment of dendritic cells to the liver crucial for a host defense. in *Developmental Immunology* **9,** 143–149 (2002).

79. Lutz, M. B. & Schuler, G. Immature, semi-mature and fully mature dendritic cells: Which signals induce tolerance or immunity? *Trends in Immunology* **23,** 445–449 (2002).

80. Jomantaite, I. *et al.* Hepatic dendritic cell subsets in the mouse. *Eur. J. Immunol.* **34,** 355–365 (2004).

81. Thomson, A. W., O'Connell, P. J., Steptoe, R. J. & Lu, L. Immunobiology of liver dendritic cells. *Immunology and Cell Biology* **80,** 65–73 (2002).

82. Wu, L. & Dakic, A. Development of dendritic cell system. *Cell. Mol. Immunol.* **1,** 112–118 (2004).

83. Hemmi, H. & Akira, S. TLR signalling and the function of dendritic cells. *Chem. Immunol. Allergy* **86,** 120–135 (2005).

84. Goddard, S., Youster, J., Morgan, E. & Adams, D. H. Interleukin-10 Secretion Differentiates Dendritic Cells from Human Liver and Skin. *Am. J. Pathol.* **164,** 511–519 (2004).

85. Tokita, D. *et al.* Poor allostimulatory function of liver plasmacytoid DC is associated with pro-apoptotic activity, dependent on regulatory T cells. *J. Hepatol.* **49,** 1008–1018 (2008).

86. Pillarisetty, V. G., Shah, A. B., Miller, G., Bleier, J. I. & DeMatteo, R. P. Liver Dendritic Cells Are Less Immunogenic Than Spleen Dendritic Cells because of Differences in Subtype Composition. *J. Immunol.* **172,** 1009–1017 (2004).

87. Vivier, E., Tomasello, E., Baratin, M., Walzer, T. & Ugolini, S. Functions of natural killer cells. *Nat. Immunol.* **9,** 503–510 (2008).

88. Giroux, M., Schmidt, M. & Descoteaux, A. IFN-gamma-induced MHC class II expression: transactivation of class II transactivator promoter IV by IFN regulatory factor-1 is regulated by protein kinase C-alpha. *J. Immunol.* **171,** 4187–4194 (2003).

89. Hart, O. M., Athie-Morales, V., O'Connor, G. M. & Gardiner, C. M. TLR7/8-Mediated Activation of Human NK Cells Results in Accessory Cell-Dependent IFN-{gamma} Production. *J. Immunol.* **175,** 1636–1642 (2005).

90. Horras, C. J., Lamb, C. L. & Mitchell, K. A. Regulation of hepatocyte fate by interferon-?? *Cytokine and Growth Factor Reviews* **22,** 35–43 (2011).

91. Lang, P. A. *et al.* Natural killer cell activation enhances immune pathology and promotes chronic infection by limiting CD8+ T-cell immunity. *Proc. Natl. Acad. Sci.* **109,** 1210–1215 (2012).

92. Brennan, P. J., Brigl, M. & Brenner, M. B. Invariant natural killer T cells: an innate activation scheme linked to diverse effector functions. *Nat. Rev. Immunol.* **13,** 101–117 (2013).

93. Swain, M. G. Hepatic NKT cells: friend or foe? *Clin. Sci.* **114,** 457–466 (2008).

94. Kakimi, K., Guidotti, L. G., Koezuka, Y. & Chisari, F. V. Natural killer T cell activation inhibits hepatitis B virus replication in vivo. *J. Exp. Med.* **192,** 921–30 (2000).

95. Albarran, B. *et al.* Profiles of NK, NKT cell activation and cytokine production following vaccination against hepatitis B. *APMIS* **113,** 526–535 (2005).

96. Miyagi, T. *et al.* CD1d-mediated stimulation of natural killer T cells selectively activates hepatic natural killer cells to eliminate experimentally disseminated hepatoma cells in murine liver. *Int. J. Cancer* **106,** 81–89 (2003).

97. Margalit, M. *et al.* Suppression of hepatocellular carcinoma by transplantation of ex-vivo immune-modulated NKT lymphocytes. *Int. J. Cancer* **115,** 443–449 (2005).

98. Nakashima, H. *et al.* Activation of Mouse Natural Killer T Cells Accelerates Liver Regeneration After Partial Hepatectomy. *Gastroenterology* **131,** 1573–1583 (2006).

99. Dong, Z., Zhang, J., Sun, R., Wei, H. & Tian, Z. Impairment of liver regeneration correlates with activated hepatic NKT cells in HBV transgenic mice. *Hepatology* **45,** 1400–1412 (2007).

100. Wieczorek, M. *et al.* Major histocompatibility complex (MHC) class I and MHC class II proteins: Conformational plasticity in antigen presentation. *Frontiers in Immunology* **8,** (2017).

101. Crispe, I. N. Hepatic T cells and liver tolerance. *Nature Reviews Immunology* **3,** 51–62 (2003).

102. Raphael, I., Nalawade, S., Eagar, T. N. & Forsthuber, T. G. T cell subsets and

their signature cytokines in autoimmune and inflammatory diseases. *Cytokine* **74,** 1043–4666 (2014).

103. Zhu, J., Yamane, H. & Paul, W. E. Differentiation of Effector CD4 T Cell Populations. *Annu. Rev. Immunol.* **28,** 445–489 (2010).
104. Biedermann, T., Röcken, M. & Carballido, J. M. TH1 and TH2 lymphocyte development and regulation of TH cell-mediated immune responses of the skin. *J. Investig. Dermatol. Symp. Proc.* **9,** 5–14 (2004).
105. Semmo, N. & Klenerman, P. CD4+ T cell responses in hepatitis C virus infection. *World J. Gastroenterol.* **13,** 4831–8 (2007).
106. Schulze zur Wiesch, J. *et al.* Broadly directed virus-specific CD4 $^{+}$ T cell responses are primed during acute hepatitis C infection, but rapidly disappear from human blood with viral persistence. *J. Exp. Med.* **209,** 61–75 (2012).
107. Lemmers, A. *et al.* The interleukin-17 pathway is involved in human alcoholic liver disease. *Hepatology* **49,** 646–657 (2009).
108. Bao, S., Zheng, J. & Shi, G. The role of T helper 17 cells in the pathogenesis of hepatitis B virus-related liver cirrhosis (Review). *Molecular Medicine Reports* **16,** 3713–3719 (2017).
109. Lee, H. C. *et al.* Hepatitis C virus promotes t-helper (Th)17 responses through thymic stromal lymphopoietin production by infected hepatocytes. *Hepatology* **57,** 1314–1324 (2013).
110. Kägi, D. *et al.* Fas and perforin pathways as major mechanisms of T cell-mediated cytotoxicity. *Science* **265,** 528–530 (1994).
111. Zhang, N. & Bevan, M. J. CD8+ T Cells: Foot Soldiers of the Immune System. *Immunity* **35,** 161–168 (2011).
112. Thimme, R. *et al.* CD8(+) T cells mediate viral clearance and disease pathogenesis during acute hepatitis B virus infection. *J. Virol.* **77,** 68–76 (2003).
113. Shoukry, N. H. *et al.* Memory CD8+ T cells are required for protection from persistent hepatitis C virus infection. *J Exp Med* **197,** 1645–1655 (2003).
114. Grüner, N. H. *et al.* Association of hepatitis C virus-specific CD8+ T cells with viral clearance in acute hepatitis C. *J. Infect. Dis.* **181,** 1528–1536 (2000).
115. Wherry, E. J. T cell exhaustion. *Nature Immunology* **12,** 492–499 (2011).
116. Rehermann, B. Pathogenesis of chronic viral hepatitis: Differential roles of T cells and NK cells. *Nature Medicine* **19,** 859–868 (2013).
117. Shin, E.-C., Sung, P. S. & Park, S.-H. Immune responses and immunopathology in acute and chronic viral hepatitis. *Nat. Rev. Immunol.* **16,** 509–523 (2016).
118. Pennington, H. L., Wilce, P. A. & Worrall, S. Chemokine and cell adhesion molecule mRNA expression and neutrophil infiltration in lipopolysaccharide-induced hepatitis in ethanol-fed rats. *Alcohol. Clin. Exp. Res.* **22,** 1713–1718 (1998).
119. Lalor, P. F., Shields, P., Grant, A. & Adams, D. H. Recruitment of lymphocytes to the human liver. *Immunol. Cell Biol.* **80,** 52–64 (2002).
120. Oo, Y. H. & Adams, D. H. The role of chemokines in the recruitment of

lymphocytes to the liver. *J. Autoimmun.* **34,** 45–54 (2010).

121. Schwabe, R. F., Bataller, R. & Brenner, D. a. Human hepatic stellate cells express CCR5 and RANTES to induce proliferation and migration. *Am. J. Physiol. Gastrointest. Liver Physiol.* **285,** G949-58 (2003).
122. Seki, E. *et al.* CCR1 and CCR5 promote hepatic fibrosis in mice. *J. Clin. Invest.* **119,** 1858–1870 (2009).
123. Seki, E. *et al.* CCR2 promotes hepatic fibrosis in mice. *Hepatology* **50,** 185–197 (2009).
124. Tacke, F., Luedde, T. & Trautwein, C. Inflammatory pathways in liver homeostasis and liver injury. *Clinical Reviews in Allergy and Immunology* **36,** 4–12 (2009).
125. Czaja, M. J. *et al.* Expression of tumor necrosis factor-alpha and transforming growth factor-beta 1 in acute liver injury. *Growth Factors* **1,** 219–226 (1989).
126. Czaja, M. J., Xu, J. & Alt, E. Prevention of carbon tetrachloride-induced rat liver injury by soluble tumor necrosis factor receptor. *Gastroenterology* **108,** 1849–54 (1995).
127. Morio, L. a *et al.* Distinct roles of tumor necrosis factor-alpha and nitric oxide in acute liver injury induced by carbon tetrachloride in mice. *Toxicol. Appl. Pharmacol.* **172,** 44–51 (2001).
128. Pfeffer, K. *et al.* Mice deficient for the 55 kd tumor necrosis factor receptor are resistant to endotoxic shock, yet succumb to L. monocytogenes infection. *Cell* **73,** 457–467 (1993).
129. Yin, M. *et al.* Essential role of tumor necrosis factor alpha in alcohol-induced liver injury in mice. *Gastroenterology* **117,** 942–952 (1999).
130. McClain, C. J., Hill, D. B., Song, Z., Deaciuc, I. & Barve, S. Monocyte activation in alcoholic liver disease. *Alcohol* **27,** 53–61 (2002).
131. Tomita, K. *et al.* Tumour necrosis factor alpha signalling through activation of Kupffer cells plays an essential role in liver fibrosis of non-alcoholic steatohepatitis in mice. *Gut* **55,** 415–24 (2006).
132. Wigg, A. J. *et al.* The role of small intestinal bacterial overgrowth, intestinal permeability, endotoxaemia, and tumour necrosis factor alpha in the pathogenesis of non-alcoholic steatohepatitis. *Gut* **48,** 206–11 (2001).
133. Ong, J. P. *et al.* Correlation between ammonia levels and the severity of hepatic encephalopathy. *Am. J. Med.* **114,** 188–193 (2003).
134. Odeh, M., Sabo, E., Srugo, I. & Oliven, A. Relationship between tumor necrosis factor-alpha and ammonia in patients with hepatic encephalopathy due to chronic liver failure. *Ann. Med.* **37,** 603–12 (2005).
135. Bémeur, C., Qu, H., Desjardins, P. & Butterworth, R. F. IL-1 or TNF receptor gene deletion delays onset of encephalopathy and attenuates brain edema in experimental acute liver failure. *Neurochem. Int.* **56,** 213–215 (2010).
136. Gabay, C. & Kushner, I. Acute-Phase Proteins and Other Systemic Responses to Inflammation. *N. Engl. J. Med.* **340,** 448–454 (1999).
137. Schmidt-Arras, D. & Rose-John, S. IL-6 pathway in the liver: From physiopathology to therapy. *Journal of Hepatology* **64,** 1403–1415 (2016).

138. Aparicio-Siegmund, S., Deseke, M., Lickert, A. & Garbers, C. Trans-signaling of interleukin-6 (IL-6) is mediated by the soluble IL-6 receptor, but not by soluble CD5. *Biochem. Biophys. Res. Commun.* **484,** 808–812 (2017).

139. Kopf, M. *et al.* Impaired immune and acute-phase responses in interleukin-6-deficient mice. *Nature* **368,** 339–342 (1994).

140. Taub, R. Liver regeneration: from myth to mechanism. *Nat. Rev. Mol. Cell Biol.* **5,** 836–847 (2004).

141. Cressman, D. E. *et al.* Liver Failure and Defective Hepatocyte Regeneration in Interleukin-6-Deficient Mice. *Science (80-.).* **274,** 1379–1383 (1996).

142. Gewiese-Rabsch, J., Drucker, C., Malchow, S., Scheller, J. & Rose-John, S. Role of IL-6 trans-signaling in CCl_4induced liver damage. *Biochim. Biophys. Acta* **1802,** 1054–61 (2010).

143. Sun, Y., Tokushige, K., Isono, E., Yamauchi, K. & Obata, H. Elevated serum interleukin-6 levels in patients with acute hepatitis. *J. Clin. Immunol.* **12,** 197–200 (1992).

144. Deviere, J. *et al.* High interleukin-6 serum levels and increased production by leucocytes in alcoholic liver cirrhosis. Correlation with IgA serum levels and lymphokines production. *Clin. Exp. Immunol.* **77,** 221–5 (1989).

145. Aleksandrova, K. *et al.* Inflammatory and metabolic biomarkers and risk of liver and biliary tract cancer. *Hepatology* **60,** 858–71 (2014).

146. Nakatsukasa, H. *et al.* Cellular distribution of transforming growth factor-beta 1 and procollagen types I, III, and IV transcripts in carbon tetrachloride-induced rat liver fibrosis. *J. Clin. Invest.* **85,** 1833–43 (1990).

147. Dooley, S. & Ten Dijke, P. TGF-β in progression of liver disease. *Cell and Tissue Research* **347,** 245–256 (2012).

148. Oberhammer, F. *et al.* Effect of transforming growth factor beta on cell death of cultured rat hepatocytes. *Cancer Res* **51,** 2478–2485 (1991).

149. Gressner, A. M., Lahme, B., Mannherz, H. G. & Polzar, B. TGF-beta-mediated hepatocellular apoptosis by rat and human hepatoma cells and primary rat hepatocytes. *J. Hepatol.* **26,** 1079–92 (1997).

150. Fausto, N. *et al.* Proto-oncogene expression and growth factors during liver regeneration. *Symposium on Fundamental Cancer Research* **39,** 69–86 (1986).

151. Gressner, A. M., Weiskirchen, R., Breitkopf, K. & Dooley, S. Roles of TGF-beta in hepatic fibrosis. *Front. Biosci.* **7,** d793–d807 (2002).

152. World Health Organization. Global health estimates 2015 summary tables: deaths by cause, age and sex. *World Health Organization* (2015). Available at: http://www.who.int/healthinfo/global_burden_disease/estimates/en/index1.html.

153. Gower, E., Estes, C., Blach, S., Razavi-Shearer, K. & Razavi, H. Global epidemiology and genotype distribution of the hepatitis C virus infection. *J. Hepatol.* **61,** S45–S57 (2014).

154. Ott, J. J., Stevens, G. A., Groeger, J. & Wiersma, S. T. Global epidemiology of hepatitis B virus infection: New estimates of age-specific HBsAg seroprevalence and endemicity. *Vaccine* **30,** 2212–2219 (2012).

155. Trépo, C., Chan, H. L. Y. & Lok, A. Hepatitis B virus infection. *Lancet* **384,**

2053–2063 (2014).

156. Di Bisceglie, A. M. Hepatitis B and hepatocellular carcinoma. *Hepatology* **49,** (2009).
157. Zhao, L. H. *et al.* Genomic and oncogenic preference of HBV integration in hepatocellular carcinoma. *Nat. Commun.* **7,** (2016).
158. Lindenbach, B. D. & Rice, C. M. Unravelling hepatitis C virus replication from genome to function. *Nature* **436,** 933–938 (2005).
159. Ringelhan, M., McKeating, J. A. & Protzer, U. Viral hepatitis and liver cancer. *Philos. Trans. R. Soc. Lond. B. Biol. Sci.* **372,** (2017).
160. Chen, S. L. & Morgan, T. R. The natural history of hepatitis C virus (HCV) infection. *International Journal of Medical Sciences* **3,** 47–52 (2006).
161. Manns, M. P. *et al.* Hepatitis C virus infection. *Nat. Rev. Dis. Prim.* **3,** 17006 (2017).
162. de Oliveria Andrade, L. J. *et al.* Association between hepatitis C and hepatocellular carcinoma. *J. Glob. Infect. Dis.* **1,** 33–37 (2009).
163. Koike, K. Hepatitis C virus contributes to hepatocarcinogenesis by modulating metabolic and intracellular signaling pathways. in *Journal of Gastroenterology and Hepatology (Australia)* **22,** (2007).
164. Lazo, M. *et al.* Prevalence of nonalcoholic fatty liver disease in the United States: The third national health and nutrition examination survey, 1988-1994. *American Journal of Epidemiology* **178,** 38–45 (2013).
165. Clark, J. M., Brancati, F. L. & Diehl, A. M. The prevalence and etiology of elevated aminotransferase levels in the United States. *Am. J. Gastroenterol.* **98,** 960–967 (2003).
166. Tilg, H. & Moschen, A. R. Evolution of inflammation in nonalcoholic fatty liver disease: The multiple parallel hits hypothesis. *Hepatology* **52,** 1836–1846 (2010).
167. McCullough, A. J. The clinical features, diagnosis and natural history of nonalcoholic fatty liver disease. *Clinics in Liver Disease* **8,** 521–533 (2004).
168. Schuppan, D. & Afdhal, N. H. Liver cirrhosis. *Lancet (London, England)* **371,** 838–51 (2008).
169. Tsochatzis, E. A., Bosch, J. & Burroughs, A. K. Liver cirrhosis. in *The Lancet* **383,** 1749–1761 (2014).
170. Ge, P. S. & Runyon, B. A. Treatment of Patients with Cirrhosis. *N. Engl. J. Med.* **375,** 767–777 (2016).
171. Häussinger, D. & Sies, H. Editorial: Hepatic encephalopathy: Clinical aspects and pathogenetic concept. *Archives of Biochemistry and Biophysics* **536,** 97–100 (2013).
172. Norenberg, M. D. *et al.* Ammonia-induced astrocyte swelling in primary culture. *Neurochem. Res.* **16,** 833–836 (1991).
173. Häussinger, D. & Schliess, F. Pathogenetic mechanisms of hepatic encephalopathy. *Gut* **57,** 1156–1165 (2008).
174. Bajaj, J. S. *et al.* Persistence of Cognitive Impairment After Resolution of Overt

Hepatic Encephalopathy. *Gastroenterology* **138,** 2332–2340 (2010).

175. Das, A., Dhiman, R. K., Saraswat, V. A., Verma, M. & Naik, S. R. Prevalence and natural history of subclinical hepatic encephalopathy in cirrhosis. *J. Gastroenterol. Hepatol.* **16,** 531–535 (2001).
176. Blei, A. T. & Cordoba, J. Hepatic encephalopathy. *Am J Gastroenterol* **96,** 1968–1976 (2001).
177. Kappus, M. R. & Bajaj, J. S. Assessment of Minimal Hepatic Encephalopathy (with Emphasis on Computerized Psychometric Tests). *Clinics in Liver Disease* **16,** 43–55 (2012).
178. Bajaj, J. S. Review article: the modern management of hepatic encephalopathy. *Aliment. Pharmacol. Ther.* **31,** 537–47 (2010).
179. Häussinger, D., Wettstein, M., Kircheis, G., Schnitzler, A. & Timmermann, L. Critical flicker frequency for quantification of low-grade hepatic encephalopathy. *Hepatology* **35,** 357–366 (2002).
180. Norenberg, M. D. Astrocytic-ammonia interactions in hepatic encephalopathy. *Semin. Liver Dis.* **16,** 245–253 (1996).
181. Aldridge, D. R., Tranah, E. J. & Shawcross, D. L. Pathogenesis of hepatic encephalopathy: Role of ammonia and systemic inflammation. *Journal of Clinical and Experimental Hepatology* **5,** S7–S20 (2015).
182. PHILLIPS, G. B., SCHWARTZ, R., GABUZDA, G. J. J. & DAVIDSON, C. S. The syndrome of impending hepatic coma in patients with cirrhosis of the liver given certain nitrogenous substances. *N. Engl. J. Med.* **247,** 239–246 (1952).
183. He, Y. *et al.* Glutamine synthetase in muscle is required for glutamine production during fasting and extrahepatic ammonia detoxification. *J. Biol. Chem.* **285,** 9516–9524 (2010).
184. Verlander, J. W., Chu, D., Lee, H.-W., Handlogten, M. E. & Weiner, I. D. Expression of glutamine synthetase in the mouse kidney: localization in multiple epithelial cell types and differential regulation by hypokalemia. *AJP Ren. Physiol.* **305,** F701–F713 (2013).
185. Suárez, I., Bodega, G. & Fernández, B. Glutamine synthetase in brain: Effect of ammonia. *Neurochem. Int.* **41,** 123–142 (2002).
186. Bernal, W. *et al.* Arterial ammonia and clinical risk factors for encephalopathy and intracranial hypertension in acute liver failure. *Hepatology* **46,** 1844–1852 (2007).
187. Clemmesen, J. O., Larsen, F. S., Kondrup, J., Hansen, B. a & Ott, P. Cerebral herniation in patients with acute liver failure is correlated with arterial ammonia concentration. *Hepatology* **29,** 648–653 (1999).
188. Walz, W. Role of astrocytes in the clearance of excess extracellular potassium. in *Neurochemistry International* **36,** 291–300 (2000).
189. Santello, M. & Volterra, A. Synaptic modulation by astrocytes via Ca2+-dependent glutamate release. *Neuroscience* **158,** 253–259 (2009).
190. Martinez-Hernandez, A., Bell, K. P. & Norenberg, M. D. Glutamine synthetase: glial localization in brain. *Science* **195,** 1356–8 (1977).
191. Rao, K. V. R., Panickar, K. S., Jayakumar, A. R. & Norenberg, M. D. Astrocytes

protect neurons from ammonia toxicity. *Neurochem. Res.* **30,** 1311–1318 (2005).

192. Kato, M., Hughes, R. D., Keays, R. T. & Williams, R. Electron microscopic study of brain capillaries in cerebral edema from fulminant hepatic failure. *Hepatology* **15,** 1060–6 (1992).
193. Norenberg, M. D. A light and electron microscopic study of experimental portal-systemic (ammonia) encephalopathy. Progression and reversal of the disorder. *Lab Invest* **36,** 618–627 (1977).
194. Gregorios, J. B., Mozes, L. W., Norenberg, L. O. & Norenberg, M. D. Morphologic effects of ammonia on primary astrocyte cultures. I. Light microscopic studies. *J. Neuropathol. Exp. Neurol.* **44,** 397–403 (1985).
195. Görg, B., Karababa, A., Shafigullina, A., Bidmon, H. J. & Häussinger, D. Ammonia-induced senescence in cultured rat astrocytes and in human cerebral cortex in hepatic encephalopathy. *Glia* **63,** 37–50 (2015).
196. Rovira, a, Alonso, J. & Córdoba, J. MR imaging findings in hepatic encephalopathy. *Am. J. Neuroradiol.* **29,** 1612–1621 (2008).
197. Tanigami, H. *et al.* Effect of glutamine synthetase inhibition on astrocyte swelling and altered astroglial protein expression during hyperammonemia in rats. *Neuroscience* **131,** 437–449 (2005).
198. Huang, D. Y. *et al.* Impaired ability to increase water excretion in mice lacking the taurine transporter gene TAUT. *Pflugers Arch. Eur. J. Physiol.* **451,** 668–677 (2006).
199. Shawcross, D. L. *et al.* Low myo-inositol and high glutamine levels in brain are associated with neuropsychological deterioration after induced hyperammonemia. *Am. J. Physiol. Gastrointest. Liver Physiol.* **287,** G503-9 (2004).
200. Albrecht, J. & Norenberg, M. D. Glutamine: A Trojan horse in ammonia neurotoxicity. *Hepatology* **44,** 788–794 (2006).
201. Rao, K. V. R. & Norenberg, M. D. Cerebral energy metabolism in Hepatic Encephalopathy and hyperammonemia. *Metabolic Brain Disease* **16,** 67–78 (2001).
202. Bernal, W., Donaldson, N., Wyncoll, D. & Wendon, J. Blood lactate as an early predictor of outcome in paracetamol-induced acute liver failure: A cohort study. *Lancet* **359,** 558–563 (2002).
203. Murthy, C. R., Rama Rao, K. V, Bai, G. & Norenberg, M. D. Ammonia-induced production of free radicals in primary cultures of rat astrocytes. *J. Neurosci. Res.* **66,** 282–8 (2001).
204. Schliess, F., Foster, N., Görg, B., Reinehr, R. & Häussinger, D. Hypoosmotic swelling increases protein tyrosine nitration in cultured rat astrocytes. *Glia* **47,** 21–29 (2004).
205. Görg, B. *et al.* Benzodiazepine-induced protein tyrosine nitration in rat astrocytes. *Hepatology* **37,** 334–342 (2003).
206. Reinehr, R. *et al.* Hypoosmotic swelling and ammonia increase oxidative stress by NADPH oxidase in cultured astrocytes and vital brain slices. *Glia* **55,** 758–771 (2007).

207. Schliess, F. *et al.* Ammonia induces MK-801-sensitive nitration and phosphorylation of protein tyrosine residues in rat astrocytes. *FASEB J.* **16,** 739–741 (2002).

208. Schliess, F., Görg, B. & Häussinger, D. Pathogenetic interplay between osmotic and oxidative stress: The hepatic encephalopathy paradigm. in *Biological Chemistry* **387,** 1363–1370 (2006).

209. Stewart, V. C., Sharpe, M. A., Clark, J. B. & Heales, S. J. R. Astrocyte-derived nitric oxide causes both reversible and irreversible damage to the neuronal mitochondrial respiratory chain. *J. Neurochem.* **75,** 694–700 (2000).

210. Radi, R. Protein tyrosine nitration: Biochemical mechanisms and structural basis of functional effects. *Acc. Chem. Res.* **46,** 550–559 (2013).

211. Görg, B. *et al.* Inflammatory cytokines induce protein tyrosine nitration in rat astrocytes. *Arch. Biochem. Biophys.* **449,** 104–114 (2006).

212. Lachmann, V., Görg, B., Bidmon, H. J., Keitel, V. & Häussinger, D. Precipitants of hepatic encephalopathy induce rapid astrocyte swelling in an oxidative stress dependent manner. *Arch. Biochem. Biophys.* **536,** 143–151 (2013).

213. Häussinger, D., Görg, B., Reinehr, R. & Schliess, F. Protein tyrosine nitration in hyperammonemia and hepatic encephalopathy. in *Metabolic Brain Disease* **20,** 285–294 (2005).

214. Görg, B. *et al.* Reversible inhibition of mammalian glutamine synthetase by tyrosine nitration. *FEBS Lett.* **581,** 84–90 (2007).

215. Buchczyk, D. P., Briviba, K., Hartl, F. U. & Sies, H. Responses to peroxynitrite in yeast: glyceraldehyde-3-phosphate dehydrogenase (GAPDH) as a sensitive intracellular target for nitration and enhancement of chaperone expression and ubiquitination. *Biol. Chem.* **381,** 121–126 (2000).

216. Görg, B. *et al.* Oxidative stress markers in the brain of patients with cirrhosis and hepatic encephalopathy. *Hepatology* **52,** 256–265 (2010).

217. Nunomura, A. *et al.* Oxidative damage to RNA in neurodegenerative diseases. *Journal of Biomedicine and Biotechnology* **2006,** (2006).

218. Görg, B. *et al.* Ammonia induces RNA oxidation in cultured astrocytes and brain in vivo. *Hepatology* **48,** 567–579 (2008).

219. Kruczek, C. *et al.* Hypoosmotic swelling affects zinc homeostasis in cultured rat astrocytes. *Glia* **57,** 79–92 (2009).

220. Kruczek, C. *et al.* Ammonia increases nitric oxide, free Zn 2+, and metallothionein mRNA expression in cultured rat astrocytes. *Biol. Chem.* **392,** 1155–1165 (2011).

221. Aschner, M. The functional significance of brain metallothioneins. *FASEB J.* **10,** 1129–1136 (1996).

222. Aschner, M., Conklin, D. R., Yao, C. P., Allen, J. W. & Tan, K. H. Induction of astrocyte metallothioneins (MTs) by zinc confers resistance against the acute cytotoxic effects of methylmercury on cell swelling, Na+ uptake, and K+ release. *Brain Res.* **813,** 254–261 (1998).

223. Giatzakis, C. & Papadopoulos, V. Differential Utilization of the Promoter of Peripheral-Type Benzodiazepine Receptor by Steroidogenic Versus

Nonsteroidogenic Cell Lines and the Role of Sp1 and Sp3 in the Regulation of Basal Activity. *Endocrinology* **145,** 1113–1123 (2004).

224. Wright, G., Shawcross, D., Olde Damink, S. W. M. & Jalan, R. Brain cytokine flux in acute liver failure and its relationship with intracranial hypertension. in *Metabolic Brain Disease* **22,** 375–388 (2007).
225. Jiang, W., Desjardins, P. & Butterworth, R. F. Cerebral inflammation contributes to encephalopathy and brain edema in acute liver failure: Protective effect of minocycline. *J. Neurochem.* **109,** 485–493 (2009).
226. Rodrigo, R. *et al.* Hyperammonemia induces neuroinflammation that contributes to cognitive impairment in rats with hepatic encephalopathy. *Gastroenterology* **139,** 675–684 (2010).
227. Zemtsova, I. *et al.* Microglia activation in hepatic encephalopathy in rats and humans. *Hepatology* **54,** 204–15 (2011).
228. Görg, B., Bidmon, H.-J. & Häussinger, D. Gene expression profiling in the cerebral cortex of patients with cirrhosis with and without hepatic encephalopathy. *Hepatology* **57,** 2436–47 (2013).
229. Traber, P. G., Canto, M. D., Ganger, D. R. & Blei, A. T. Electron microscopic evaluation of brain edema in rabbits with galactosamine-induced fulminant hepatic failure: Ultrastructure and integrity of the blood-brain barrier. *Hepatology* **7,** 1272–1277 (1987).
230. Gove, C. D., Hughes, R. D., Ede, R. J. & Williams, R. Regional cerebral edema and chloride space in galactosamine-induced liver failure in rats. *Hepatology* **25,** 295–301 (1997).
231. Lv, S. *et al.* Tumour necrosis factor-alpha affects blood-brain barrier permeability and tight junction-associated occludin in acute liver failure. *Liver Int.* **30,** 1198–1210 (2010).
232. Argaw, A. T. *et al.* IL-1 Regulates Blood-Brain Barrier Permeability via Reactivation of the Hypoxia-Angiogenesis Program. *J. Immunol.* **177,** 5574–5584 (2006).
233. Yang, Y., Estrada, E. Y., Thompson, J. F., Liu, W. & Rosenberg, G. A. Matrix Metalloproteinase-Mediated Disruption of Tight Junction Proteins in Cerebral Vessels is Reversed by Synthetic Matrix Metalloproteinase Inhibitor in Focal Ischemia in Rat. *J. Cereb. Blood Flow Metab.* **27,** 697–709 (2007).
234. Lee, I.-T., Lin, C.-C., Wu, Y.-C. & Yang, C.-M. TNF-alpha induces matrix metalloproteinase-9 expression in A549 cells: role of TNFR1/TRAF2/PKCalpha-dependent signaling pathways. *J. Cell. Physiol.* **224,** 454–64 (2010).
235. Nguyen, J. H. *et al.* Matrix metalloproteinase-9 contributes to brain extravasation and edema in fulminant hepatic failure mice. *J. Hepatol.* **44,** 1105–1114 (2006).
236. Hooper, D. C. *et al.* Uric acid, a peroxynitrite scavenger, inhibits CNS inflammation, blood-CNS barrier permeability changes, and tissue damage in a mouse model of multiple sclerosis. *FASEB J.* **14,** 691–8 (2000).
237. Kean, R. B., Spitsin, S. V, Mikheeva, T., Scott, G. S. & Hooper, D. C. The peroxynitrite scavenger uric acid prevents inflammatory cell invasion into the

central nervous system in experimental allergic encephalomyelitis through maintenance of blood-central nervous system barrier integrity. *J. Immunol.* **165,** 6511–8 (2000).

238. Orlov, S. N., Koltsova, S. V., Kapilevich, L. V., Gusakova, S. V. & Dulin, N. O. NKCC1 and NKCC2: The pathogenetic role of cation-chloride cotransporters in hypertension. *Genes and Diseases* **2,** 186–196 (2015).
239. Haas, M. & Forbush, B. The Na-K-Cl cotransporters. *Journal of Bioenergetics and Biomembranes* **30,** 161–172 (1998).
240. O'Donnell, M. E., Tran, L., Lam, T. I., Liu, X. B. & Anderson, S. E. Bumetanide inhibition of the blood-brain barrier Na-K-Cl cotransporter reduces edema formation in the rat middle cerebral artery occlusion model of stroke. *J. Cereb. Blood Flow Metab.* **24,** 1046–1056 (2004).
241. Staub, F., Stoffel, M., Berger, S., Eriskat, J. & Baethmann, A. Treatment of vasogenic brain edema with the novel Cl- transport inhibitor torasemide. *J. Neurotrauma* **11,** 679–90 (1994).
242. Lu, K.-T. *et al.* Inhibition of the Na+ -K+ -2Cl- -cotransporter in choroid plexus attenuates traumatic brain injury-induced brain edema and neuronal damage. *Eur. J. Pharmacol.* **548,** 99–105 (2006).
243. Jayakumar, A. R. *et al.* Na-K-Cl Cotransporter-1 in the mechanism of ammonia-induced astrocyte swelling. *J. Biol. Chem.* **283,** 33874–33882 (2008).
244. Rangroo Thrane, V. *et al.* Ammonia triggers neuronal disinhibition and seizures by impairing astrocyte potassium buffering. *Nat. Med.* **19,** 1643–8 (2013).
245. Agre, P. Molecular physiology of water transport: Aquaporin nomenclature workshop. Mammalian aquaporins. in *Biology of the Cell* **89,** 255–257 (1997).
246. Holm, L. M. *et al.* NH3 and NH4+ permeability in aquaporin-expressing Xenopus oocytes. *Pflugers Arch. Eur. J. Physiol.* **450,** 415–428 (2005).
247. Rama Rao, K. V, Chen, M., Simard, J. M. & Norenberg, M. D. Increased aquaporin-4 expression in ammonia-treated cultured astrocytes. *Neuroreport* **14,** 2379–82 (2003).
248. Eefsen, M. *et al.* Brain expression of the water channels aquaporin-1 and -4 in mice with acute liver injury, hyperammonemia and brain edema. *Metab. Brain Dis.* **25,** 315–323 (2010).
249. Manley, G. T. *et al.* Aquaporin-4 deletion in mice reduces brain edema after acute water intoxication and ischemic stroke. *Nat. Med.* **6,** 159–163 (2000).
250. Amiry-Moghaddam, M. *et al.* An -syntrophin-dependent pool of AQP4 in astroglial end-feet confers bidirectional water flow between blood and brain. *Proc. Natl. Acad. Sci.* **100,** 2106–2111 (2003).
251. Taniguchi, M. *et al.* Induction of aquaporin-4 water channel mRNA after focal cerebral ischemia in rat. *Mol. Brain Res.* **78,** 131–137 (2000).
252. Sun, M.-C., Honey, C. R., Berk, C., Wong, N. L. M. & Tsui, J. K. C. Regulation of aquaporin-4 in a traumatic brain injury model in rats. *J. Neurosurg.* **98,** 565–569 (2003).
253. Amorini, A. M., Dunbar, J. G. & Marmarou, A. Modulation of aquaporin-4 water transport in a model of TBI. *Acta Neurochir. Suppl.* **86,** 261–263 (2003).

254. Suraweera, D., Sundaram, V. & Saab, S. Evaluation and management of hepatic encephalopathy: Current status and future directions. *Gut and Liver* **10,** 509–519 (2016).

255. Chadalavada, R., Sappati Biyyani, R. S., Maxwell, J. & Mullen, K. Nutrition in hepatic encephalopathy. *Nutr. Clin. Pract.* **25,** 257–264 (2010).

256. Rombouts, K., Bémeur, C. & Rose, C. F. Targeting the muscle for the treatment and prevention of hepatic encephalopathy. *Journal of Hepatology* **65,** 876–878 (2016).

257. Patil, D. H. *et al.* Comparative modes of action of lactitol and lactulose in the treatment of hepatic encephalopathy. *Gut* **28,** 255–9 (1987).

258. Bass, N. M. *et al.* Rifaximin Treatment in Hepatic Encephalopathy. *N. Engl. J. Med.* **362,** 1071–1081 (2010).

259. Sharma, B. C. *et al.* A Randomized, Double-Blind, Controlled Trial Comparing Rifaximin Plus Lactulose With Lactulose Alone in Treatment of Overt Hepatic Encephalopathy. *Am. J. Gastroenterol.* **108,** 1458–1463 (2013).

260. Rockey, D. C. *et al.* Randomized, double-blind, controlled study of glycerol phenylbutyrate in hepatic encephalopathy. *Hepatology* **59,** 1073–83 (2014).

261. Ventura-Cots, M. *et al.* Safety of ornithine phenylacetate in cirrhotic decompensated patients: an open-label, dose-escalating, single-cohort study. *J. Clin. Gastroenterol.* **47,** 881–7 (2015).

262. Rose, C. *et al.* L-ornithine-L-aspartate in experimental portal-systemic encephalopathy: Therapeutic efficacy and mechanism of action. *Metab. Brain Dis.* **13,** 147–157 (1998).

263. Bai, M., Yang, Z., Qi, X., Fan, D. & Han, G. L-Ornithine-L-Aspartate for Hepatic Encephalopathy in Patients With Cirrhosis: a Meta-Analysis of Randomized Controlled Trials. *J. Gastroenterol. Hepatol.* **28,** 783–92 (2013).

264. Rahimi, R. S., Singal, A. G., Cuthbert, J. A. & Rockey, D. C. Lactulose vs Polyethylene Glycol 3350-Electrolyte Solution for Treatment of Overt Hepatic Encephalopathy. *JAMA Intern. Med.* **174,** 1727 (2014).

265. Agrawal, A., Sharma, B. C., Sharma, P. & Sarin, S. K. Secondary Prophylaxis of Hepatic Encephalopathy in Cirrhosis: An Open-Label, Randomized Controlled Trial of Lactulose, Probiotics, and No Therapy. *Am. J. Gastroenterol.* **107,** 1043–1050 (2012).

266. Zhao, L. N. *et al.* Probiotics can improve the clinical outcomes of hepatic encephalopathy: An update meta-analysis. *Clin. Res. Hepatol. Gastroenterol.* **39,** 674–682 (2015).

267. Chen, G., Shi, J., Hu, Z. & Hang, C. Inhibitory effect on cerebral inflammatory response following traumatic brain injury in rats: A potential neuroprotective mechanism of N-Acetylcysteine. *Mediators Inflamm.* **2008,** (2008).

268. Bemeur, C., Vaquero, J., Desjardins, P. & Butterworth, R. F. N-acetylcysteine attenuates cerebral complications of non-acetaminophen-induced acute liver failure in mice: antioxidant and anti-inflammatory mechanisms. *Metab Brain Dis.* **25,** 241–249 (2010).

269. Catalina, M.-V. *et al.* Hepatic and systemic haemodynamic changes after MARS in patients with acute on chronic liver failure. *Liver Int.* **23 Suppl 3,** 39–

43 (2003).

270. Laleman, W. *et al.* Effect of the molecular adsorbent recirculating system and Prometheus devices on systemic haemodynamics and vasoactive agents in patients with acute-on-chronic alcoholic liver failure. *Crit. Care* **10,** R108 (2006).

271. Sen, S. *et al.* Albumin dialysis reduces portal pressure acutely in patients with severe alcoholic hepatitis. *J. Hepatol.* **43,** 142–148 (2005).

272. Guo, L. M. *et al.* Application of Molecular Adsorbents Recirculating System to remove NO and cytokines in severe liver failure patients with multiple organ dysfunction syndrome. *Liver Int* **23 Suppl 3,** 16–20 (2003).

273. Stirling, D. P., Koochesfahani, K. M., Steeves, J. D. & Tetzlaff, W. Minocycline as a Neuroprotective Agent. *Neurosci.* **11,** 308–322 (2005).

274. Jiang, W., Desjardins, P. & Butterworth, R. F. Minocycline attenuates oxidative/nitrosative stress and cerebral complications of acute liver failure in rats. *Neurochem. Int.* **55,** 601–605 (2009).

275. Renehan, A. G., Booth, C. & Potten, C. S. What is apoptosis, and why is it important? *BMJ* **322,** 1536–8 (2001).

276. Elmore, S. Apoptosis: A Review of Programmed Cell Death. *Toxicologic Pathology* **35,** 495–516 (2007).

277. Trauth, B. *et al.* Monoclonal antibody-mediated tumor regression by induction of apoptosis. *Science (80-.).* **245,** 301–305 (1989).

278. Kojima, Y. *et al.* Localization of Fas ligand in cytoplasmic granules of CD8+ cytotoxic T lymphocytes and natural killer cells: Participation of Fas ligand in granule exocytosis model of cytotoxicity. *Biochem. Biophys. Res. Commun.* **296,** 328–336 (2002).

279. Muschen, M. *et al.* Involvement of CD95 (Apo-1/Fas) ligand expressed by rat Kupffer cells in hepatic immunoregulation. *Gastroenterology* **116,** 666–677 (1999).

280. Feldstein, A. E. *et al.* Hepatocyte apoptosis and Fas expression are prominent features of human nonalcoholic steatohepatitis. *Gastroenterology* **125,** 437–443 (2003).

281. Ueno, Y. *et al.* Fas-mediated cholangiopathy in the murine model of graft versus host disease. *Hepatology* **31,** 966–74 (2000).

282. Saile, B., Knittel, T., Matthes, N., Schott, P. & Ramadori, G. CD95/CD95L-mediated apoptosis of the hepatic stellate cell. A mechanism terminating uncontrolled hepatic stellate cell proliferation during hepatic tissue repair. *Am. J. Pathol.* **151,** 1265–72 (1997).

283. Wallach, D. *et al.* Tumor necrosis factor receptor and Fas signaling mechanisms. *Annu. Rev. Immunol.* **17,** 331–67 (1999).

284. Hao, Z. & Mak, T. W. Type I and type II pathways of Fas-mediated apoptosis are differentially controlled by XIAP. *J. Mol. Cell Biol.* **2,** 63–64 (2010).

285. Luo, X., Budihardjo, I., Zou, H., Slaughter, C. & Wang, X. Bid, a Bcl2 interacting protein, mediates cytochrome c release from mitochondria in response to activation of cell surface death receptors. *Cell* **94,** 481–490 (1998).

286. Li, H., Zhu, H., Xu, C. & Yuan, J. Cleavage of BID by Caspase 8 Mediates the Mitochondrial Damage in the Fas Pathway of Apoptosis. *Cell* **94,** 491–501 (1998).

287. Zou, H., Li, Y., Liu, X. & Wang, X. An APAf-1 · cytochrome C multimeric complex is a functional apoptosome that activates procaspase-9. *J. Biol. Chem.* **274,** 11549–11556 (1999).

288. Scaffidi, G. *et al.* Differential modulation of apoptosis sensitivity in CD95 type I and type II cells. *J. Biol. Chem.* **274,** 22532–22538 (1999).

289. Ogasawara, J. *et al.* Lethal effect of the anti-Fas antibody in mice. *Nature* **364,** 806–809 (1993).

290. Higaki, K., Yano, H. & Kojiro, M. Fas antigen expression and its relationship with apoptosis in human hepatocellular carcinoma and noncancerous tissues. *Am. J. Pathol.* **149,** 429–37 (1996).

291. Natori, S. *et al.* Hepatocyte apoptosis is a pathologic feature of human alcoholic hepatitis. *J. Hepatol.* **34,** 248–253 (2001).

292. Strand, S. *et al.* Hepatic failure and liver cell damage in acute Wilson's disease involve CD95 (APO-1/Fas) mediated apoptosis. *Nat. Med.* **4,** 588–593 (1998).

293. Feldstein, A. E. *et al.* Diet associated hepatic steatosis sensitizes to Fas mediated liver injury in mice. *J. Hepatol.* **39,** 978–983 (2003).

294. Hayashi, N. & Mita, E. Involvement of Fas system-mediated apoptosis in pathogenesis of viral hepatitis. *Journal of Viral Hepatitis* **6,** 357–365 (1999).

295. Luo, K. X. *et al.* In situ investigation of Fas/FasL expression in chronic hepatitis B infection and related liver diseases. *J. Viral Hepat.* **4,** 303–7 (1997).

296. Sedger, L. M. & McDermott, M. F. TNF and TNF-receptors: From mediators of cell death and inflammation to therapeutic giants - past, present and future. *Cytokine and Growth Factor Reviews* **25,** 453–472 (2014).

297. Loffreda, S., Rai, R., Shi Qi Yang, Hui Zhi Lin & Diehl, A. M. Bile ducts and portal and central veins are major producers of tumor necrosis factor ?? in regenerating rat liver. *Gastroenterology* **112,** 2089–2098 (1997).

298. McIlwain, D. R. *et al.* iRhom2 Regulation of TACE Controls TNF-Mediated Protection Against Listeria and Responses to LPS. *Science (80-.).* **335,** 229–232 (2012).

299. Wajant, H., Pfizenmaier, K. & Scheurich, P. Tumor necrosis factor signaling. *Cell Death.Differ.* **10,** 45–65 (2003).

300. Grell, M. *et al.* The transmembrane form of tumor necrosis factor is the prime activating ligand of the 80 kDa tumor necrosis factor receptor. *Cell* **83,** 793–802 (1995).

301. Puimège, L., Libert, C. & Van Hauwermeiren, F. Regulation and dysregulation of tumor necrosis factor receptor-1. *Cytokine and Growth Factor Reviews* **25,** 285–300 (2014).

302. Franzoso, G., Zazzeroni, F. & Papa, S. JNK: a killer on a transcriptional leash. *Cell Death Differ.* **10,** 13–15 (2003).

303. Rothe, M., Sarma, V., Dixit, V. M. & Goeddel, D. V. TRAF2-mediated activation of NF-kappa B by TNF receptor 2 and CD40. *Science* **269,** 1424–1427 (1995).

304. Hsu, H., Huang, J., Shu, H. B., Baichwal, V. & Goeddel, D. V. TNF-dependent recruitment of the protein kinase RIP to the TNF receptor-1 signaling complex. *Immunity* **4,** 387–396 (1996).

305. Ting, A. T., Pimentel-Muiños, F. X. & Seed, B. RIP mediates tumor necrosis factor receptor 1 activation of NF-κB but not Fas/APO-1-initiated apoptosis. *EMBO J.* **15,** 6189–96 (1996).

306. Hsu, H., Shu, H. B., Pan, M. G. & Goeddel, D. V. TRADD-TRAF2 and TRADD-FADD interactions define two distinct TNF receptor 1 signal transduction pathways. *Cell* **84,** 299–308 (1996).

307. Micheau, O. & Tschopp, J. Induction of TNF receptor I-mediated apoptosis via two sequential signaling complexes. *Cell* **114,** 181–190 (2003).

308. Ea, C. K., Deng, L., Xia, Z. P., Pineda, G. & Chen, Z. J. Activation of IKK by TNFα Requires Site-Specific Ubiquitination of RIP1 and Polyubiquitin Binding by NEMO. *Mol. Cell* **22,** 245–257 (2006).

309. Israël, A. The IKK Complex, a Central Regulator of NF-κB Activation. *Cold Spring Harb. Perspect. Biol.* **2,** 14 (2010).

310. Brenner, D., Blaser, H. & Mak, T. W. Regulation of tumour necrosis factor signalling: live or let die. *Nat. Rev. Immunol.* **15,** 362–74 (2015).

311. Van Antwerp, D. J., Martin, S. J., Kafri, T., Green, D. R. & Verma, I. M. Suppression of TNF-a-induced apoptosis by NF-κB. *Science (80-.).* **274,** 787–9 (1996).

312. Micheau, O., Lens, S., Gaide, O., Alevizopoulos, K. & Tschopp, J. NF-kappaB signals induce the expression of c-FLIP. *Mol. Cell. Biol.* **21,** 5299–305 (2001).

313. Pop, C. *et al.* FLIP(L) induces caspase 8 activity in the absence of interdomain caspase 8 cleavage and alters substrate specificity. *Biochem J* **433,** 447–457 (2011).

314. Oberst, A. *et al.* Catalytic activity of the caspase-8–FLIPL complex inhibits RIPK3-dependent necrosis. *Nature* **471,** 363–367 (2011).

315. Deng, Y., Ren, X., Yang, L., Lin, Y. & Wu, X. A JNK-dependent pathway is required for TNFα-induced apoptosis. *Cell* **115,** 61–70 (2003).

316. Wang, S. & El-Deiry, W. S. TRAIL and apoptosis induction by TNF-family death receptors. *Oncogene* **22,** 8628–8633 (2003).

317. Ichikawa, K. *et al.* Tumoricidal activity of a novel anti-human DR5 monoclonal antibody without hepatocyte cytotoxicity. *Nat. Med.* **7,** 954–60 (2001).

318. Koschny, R., Walczak, H. & Ganten, T. M. The promise of TRAIL--potential and risks of a novel anticancer therapy. *J. Mol. Med. (Berl).* **85,** 923–935 (2007).

319. Malhi, H., Barreyro, F. J., Isomoto, H., Bronk, S. F. & Gores, G. J. Free fatty acids sensitise hepatocytes to TRAIL mediated cytotoxicity. *Gut* **56,** 1124–1131 (2007).

320. Higuchi, H. *et al.* The Bile Acid Glycochenodeoxycholate Induces TRAIL-Receptor 2/DR5 Expression and Apoptosis. *J. Biol. Chem.* **276,** 38610–38618 (2001).

321. Zheng, S. J., Wang, P., Tsabary, G. & Chen, Y. H. Critical roles of TRAIL in hepatic cell death and hepatic inflammation. *J. Clin. Invest.* **113,** 58–64 (2004).

322. Zheng, S.-J., Jiang, J., Shen, H. & Chen, Y. H. Reduced apoptosis and ameliorated listeriosis in TRAIL-null mice. *J. Immunol.* **173,** 5652–8 (2004).

323. Kahraman, A. *et al.* TRAIL mediates liver injury by the innate immune system in the bile duct-ligated mouse. *Hepatology* **47,** 1317–1330 (2008).

324. Dunn, C. *et al.* Cytokines induced during chronic hepatitis B virus infection promote a pathway for NK cell–mediated liver damage. *J. Exp. Med.* **204,** 667–680 (2007).

325. Postic, C. *et al.* Dual roles for glucokinase in glucose homeostasis as determined by liver and pancreatic β cell-specific gene knock-outs using Cre recombinase. *J. Biol. Chem.* **274,** 305–315 (1999).

326. Hof PR, Young WG, Bloom FL, Belichenko PV, C. M. *Comparative Cytoarchitectonic Atlas of the C57BL/6 and 129/Sv Mouse Brains*. (2000).

327. Häussinger, D. & Gerok, W. Hepatocyte heterogeneity in ammonia metabolism: Impairment of glutamine synthesis in CCl4 induced liver cell necrosis with no effect on urea synthesis. *Chem. Biol. Interact.* **48,** 191–194 (1984).

328. Bode, J. G., Peters-Regehr, T., Kubitz, R. & Häussinger, D. Expression of glutamine synthetase in macrophages. *J. Histochem. Cytochem.* **48,** 415–22 (2000).

329. Kuo, F. C., Hwu, W. L., Valle, D. & Darnell, J. E. Colocalization in pericentral hepatocytes in adult mice and similarity in developmental expression pattern of ornithine aminotransferase and glutamine synthetase mRNA. *Proc. Natl. Acad. Sci. U. S. A.* **88,** 9468–72 (1991).

330. Weiner, I. D., Miller, R. T. & Verlander, J. W. Localization of the ammonium transporters, Rh B glycoprotein and Rh C glycoprotein, in the mouse liver. *Gastroenterology* **124,** 1432–1440 (2003).

331. Barski, J. J. *et al.* Calbindin in Cerebellar Purkinje Cells Is a Critical Determinant of the Precision of Motor Coordination. *J. Neurosci.* **23,** 3469–3477 (2003).

332. Glass, C. K., Saijo, K., Winner, B., Marchetto, M. C. & Gage, F. H. Mechanisms Underlying Inflammation in Neurodegeneration. *Cell* **140,** 918–934 (2010).

333. Odeh, M., Sabo, E., Srugo, I. & Oliven, a. Serum levels of tumor necrosis factor-alpha correlate with severity of hepatic encephalopathy due to chronic liver failure. *Liver Int.* **24,** 110–6 (2004).

334. Bachmann, O. *et al.* Expression and regulation of the Na+-K+-2Cl- cotransporter NKCC1 in the normal and CFTR-deficient murine colon. *J. Physiol.* **549,** 525–536 (2003).

335. Lim, Y.-S. & Kim, W. R. The Global Impact of Hepatic Fibrosis and End-Stage Liver Disease. *Clin. Liver Dis.* **12,** 733–746 (2008).

336. Mokdad, A. A. *et al.* Liver cirrhosis mortality in 187 countries between 1980 and 2010: a systematic analysis. *BMC Med.* **12,** 145 (2014).

337. Haüssinger, D. Nitrogen metabolism in liver: structural and functional organization and physiological relevance. *Biochem. J.* **267,** 281–290 (1990).

338. Bianchi, G. *et al.* Hepatic amino-nitrogen clearance to urea-nitrogen in control subjects and in patients with cirrhosis: A simplified method. *Hepatology* **13,**

460–466 (1991).

339. Kaiser, S., Gerok, W. & Häussinger, D. Ammonia and glutamine metabolism in human liver slices: new aspects on the pathogenesis of hyperammonaemia in chronic liver disease. *Eur. J. Clin. Invest.* **18,** 535–542 (1988).

340. Matsuno, T. Glutaminase and Glutamine Synthetase Activities in Human Cirrhotic Liver and Hepatocellular Carcinoma. *Cancer Res.* **52,** 1192–1194 (1992).

341. Gebhardt, R. & Reichen, J. Changes in distribution and activity of glutamine synthetase in carbon tetrachloride-induced cirrhosis in the rat: potential role in hyperammonemia. *Hepatology* **20,** 684–691 (1994).

342. Braissant, O., McLin, V. A. & Cudalbu, C. Ammonia toxicity to the brain. *Journal of Inherited Metabolic Disease* **36,** 595–612 (2013).

343. Gropman, A. L., Summar, M. & Leonard, J. V. Neurological implications of urea cycle disorders. *Journal of Inherited Metabolic Disease* **30,** 865–879 (2007).

344. Häberle, J., Shahbeck, N., Ibrahim, K., Hoffmann, G. F. & Ben-Omran, T. Natural course of glutamine synthetase deficiency in a 3year old patient. *Mol. Genet. Metab.* **103,** 89–91 (2011).

345. Kosenko, E., Kaminski, Y., Lopata, O., Muravyov, N. & Felipo, V. Blocking NMDA receptors prevents the oxidative stress induced by acute ammonia intoxication. *Free Radic. Biol. Med.* **26,** 1369–1374 (1999).

346. Weissenborn, K., Heidenreich, S., Giewekemeyer, K., Rückert, N. & Hecker, H. Memory function in early hepatic encephalopathy. *J. Hepatol.* **39,** 320–325 (2003).

347. Brenner, M. *et al.* Patients with manifest hepatic encephalopathy can reveal impaired thermal perception. *Acta Neurol. Scand.* **132,** 156–163 (2015).

348. Butz, M. *et al.* Motor impairment in liver cirrhosis without and with minimal hepatic encephalopathy. *Acta Neurol. Scand.* **122,** 27–35 (2010).

349. Chepkova, A. N. *et al.* Impaired novelty acquisition and synaptic plasticity in congenital hyperammonemia caused by hepatic glutamine synthetase deficiency. *Sci. Rep.* **7,** 40190 (2017).

350. Brück, J. *et al.* Locomotor impairment and cerebrocortical oxidative stress in portal vein ligated rats in vivo. *J. Hepatol.* **54,** 251–257 (2011).

351. Leke, R. *et al.* Impairment of the organization of locomotor and exploratory behaviors in bile duct-ligated rats. *PLoS One* **7,** (2012).

352. Magen, I. *et al.* Cannabidiol ameliorates cognitive and motor impairments in mice with bile duct ligation. *J. Hepatol.* **51,** 528–534 (2009).

353. Cauli, O., Llansola, M., Erceg, S. & Felipo, V. Hypolocomotion in rats with chronic liver failure is due to increased glutamate and activation of metabotropic glutamate receptors in substantia nigra. *J. Hepatol.* **45,** 654–661 (2006).

354. Sergeeva, O. A. *et al.* Deficits in cortico-striatal synaptic plasticity and behavioral habituation in rats with portacaval anastomosis. *Neuroscience* **134,** 1091–1098 (2005).

355. Veres, G., Gibbs, R. a, Scherer, S. E. & Caskey, C. T. The molecular basis of

the sparse fur mouse mutation. *Science* **237,** 415–7 (1987).

356. Marini, J. C. & Broussard, S. R. Hyperammonemia increases sensitivity to LPS. *Mol. Genet. Metab.* **88,** 131–137 (2006).
357. Batshaw, M. L. *et al.* The sparse fur mouse as a model for gene therapy in ornithine carbamoyltransferase deficiency. *Gene Ther.* **2,** 743–749 (1995).
358. Chastre, A. *et al.* Inflammatory cascades driven by tumor necrosis factor-alpha play a major role in the progression of acute liver failure and its neurological complications. *PLoS One* **7,** e49670 (2012).
359. Karababa, A. *et al.* Ammonia Attenuates LPS-Induced Upregulation of Pro-Inflammatory Cytokine mRNA in Co-Cultured Astrocytes and Microglia. *Neurochem. Res.* **42,** 737–749 (2017).
360. Vaquero, J. *et al.* Infection and the progression of hepatic encephalopathy in Acute Liver Failure. *Gastroenterology* **125,** 755–764 (2003).
361. Rolando, N. *et al.* The systemic inflammatory response syndrome in acute liver failure. *Hepatology* **32,** 734–9 (2000).
362. Shawcross, D. L., Wright, G., Olde Damink, S. W. M. & Jalan, R. Role of ammonia and inflammation in minimal hepatic encephalopathy. *Metab. Brain Dis.* **22,** 125–138 (2007).
363. Rothe, J. *et al.* Mice lacking the tumour necrosis factor receptor 1 are resistant to TNF-mediated toxicity but highly susceptible to infection by Listeria monocytogenes. *Nature* **364,** 798–802 (1993).
364. Pfeffer, K. *et al.* Mice deficient for the 55 kd tumor necrosis factor receptor are resistant to endotoxic shock, yet succumb to L. monocytogenes infection. *Cell* **73,** 457–467 (1993).
365. Camara, M. Lou *et al.* Tumor necrosis factor alpha and its receptors in behaviour and neurobiology of adult mice, in the absence of an immune challenge. *Behav. Brain Res.* **290,** 51–60 (2015).
366. Baune, B. T. *et al.* Cognitive dysfunction in mice deficient for TNF- and its receptors. *Am. J. Med. Genet. Part B Neuropsychiatr. Genet.* **147,** 1056–1064 (2008).
367. Cooper, A. J. & Plum, F. Biochemistry and physiology of brain ammonia. *Physiol. Rev.* **67,** 440–519 (1987).
368. Ott, P. & Larsen, F. S. Blood-brain barrier permeability to ammonia in liver failure: A critical reappraisal. *Neurochemistry International* **44,** 185–198 (2004).
369. Duchini, A., Govindarajan, S., Santucci, M., Zampi, G. & Hofman, F. M. Effects of tumor necrosis factor-α and interleukin-6 on fluid-phase permeability and ammonia diffusion in CNS-derived endothelial cells. *J. Investig. Med.* **44,** 474–82 (1996).
370. Jayakumar, A. R., Valdes, V. & Norenberg, M. D. The Na-K-Cl cotransporter in the brain edema of acute liver failure. *J. Hepatol.* **54,** 272–278 (2011).
371. Huang, L.-Q. *et al.* Hypertonic saline alleviates cerebral edema by inhibiting microglia-derived TNF-α and IL-1β-induced Na-K-Cl Cotransporter up-regulation. *J. Neuroinflammation* **11,** 102 (2014).
372. Hernández-Rabaza, V. *et al.* Hyperammonemia induces glial activation,

neuroinflammation and alters neurotransmitter receptors in hippocampus, impairing spatial learning: reversal by sulforaphane. *J. Neuroinflammation* **13,** 41 (2016).

373. Pan, W. & Kastin, A. J. TNFalpha transport across the blood-brain barrier is abolished in receptor knockout mice. *Exp. Neurol.* **174,** 193–200 (2002).
374. Assentoft, M. *et al.* Aquaporin 4 as a NH3 channel. *J. Biol. Chem.* **291,** 19184–19195 (2016).
375. Takeuchi, H. *et al.* Tumor necrosis factor-?? induces neurotoxicity via glutamate release from hemichannels of activated microglia in an autocrine manner. *J. Biol. Chem.* **281,** 21362–21368 (2006).
376. Hernandez-Rabaza, V. *et al.* Neuroinflammation increases GABAergic tone and impairs cognitive and motor function in hyperammonemia by increasing GAT-3 membrane expression. Reversal by sulforaphane by promoting M2 polarization of microglia. *J. Neuroinflammation* **13,** 83 (2016).
377. Clark, I. A. *et al.* Excess cerebral TNF causing glutamate excitotoxicity rationalizes treatment of neurodegenerative diseases and neurogenic pain by anti-TNF agents. *J. Neuroinflammation* **13,** 236 (2016).
378. Jara, J. H., Singh, B. B., Floden, A. M. & Combs, C. K. Tumor necrosis factor alpha stimulates NMDA receptor activity in mouse cortical neurons resulting in ERK-dependent death. *J. Neurochem.* **100,** 1407–1420 (2007).
379. Hermenegildo, C. *et al.* NMDA Receptor antagonists prevent acute ammonia toxicity in mice. *Neurochem. Res.* **21,** 1237–1244 (1996).
380. Hermenegildo, C., Monfort, P. & Felipo, V. Activation of N-methyl-D-aspartate receptors in rat brain in vivo following acute ammonia intoxication: characterization by in vivo brain microdialysis. *Hepatology* **31,** 709–715 (2000).
381. Azor??n, I., Mi??ana, M. ???D, Felipo, V. & Grisol??a, S. A simple animal model of hyperammonemia. *Hepatology* **10,** 311–314 (1989).
382. Hermenegildo, C. Chronic hyperammonemia impairs the glutamate-nitric oxide-cyclic GMP pathway in cerebellar neurons in culture and in the rat in vivo. *Eur. J. Neurosci.* **10,** 3201–3209 (1998).
383. Chastre, A. *et al.* Inflammatory Cascades Driven by Tumor Necrosis Factor-Alpha Play a Major Role in the Progression of Acute Liver Failure and Its Neurological Complications. *PLoS One* **7,** (2012).
384. Dadsetan, S. *et al.* Infliximab reduces peripheral inflammation, neuroinflammation, and extracellular GABA in the cerebellum and improves learning and motor coordination in rats with hepatic encephalopathy. *J Neuroinflammation* **13,** 245 (2016).

List of Publications

1. TNF-mediated survival of CD169 + cells promotes immune activation during vesicular stomatitis virus infection.

Shinde PV, Xu HC, Maney SK, Kloetgen A, Namineni S, Zhuang Y, Honke N, Shaabani N, Bellora N, Doerrenberg M, Trilling M, **Pozdeev VI**, van Rooijen N, Scheu S, Pfeffer K, Crocker PR, Tanaka M, Duggimpudi S, Knolle P, Heikenwalder M, Ruland J, Mak TW, Brenner D, Pandyra AA, Hoell JI, Borkhardt A, Häussinger D, Lang KS, Lang PA

J Virol. 2017 Nov 15. pii: JVI.01637-17. doi: 10.1128/JVI.01637-17

2. TNFα induced up-regulation of Na+,K+,2Cl- cotransporter NKCC1 in hepatic ammonia clearance and cerebral ammonia toxicity.

Pozdeev VI*, Lang E*, Görg B, Bidmon HJ, Shinde PV, Kircheis G, Herebian D, Pfeffer K, Lang F, Häussinger D, Lang KS, Lang PA.

Sci Rep. 2017 Aug 11;7(1):7938. doi: 10.1038/s41598-017-07640-8.

3. RAIDD Mediates TLR3 and IRF7 Driven Type I Interferon Production.

Maney SK, Xu HC, Huang J, Pandyra AA, Ehlting C, Aguilar-Valenzuela R, **Pozdeev VI**, McIlwain DR, Zimmermann A, Bode JG, Hengel H, Kirschning CJ, Kim IR, Hiscott J, Brenner D, Häussinger D, Ohashi PS, Mak TW, Lang KS, Lang PA.

Cell Physiol Biochem. 2016;39(4):1271-80. doi: 10.1159/000447832. Epub 2016 Sep 8.

4. Storage of erythrocytes induces suicidal erythrocyte death.

Lang E*, **Pozdeev VI***, Xu HC, Shinde PV, Behnke K, Hamdam JM, Lehnert E, Scharf RE, Lang F, Häussinger D, Lang KS, Lang PA

Cell Physiol Biochem, 2016 Jul 21 ;39(2):668-76. doi: 10.1159/000445657.

5. Bile acid-induced suicidal erythrocyte death.

Lang E*, **Pozdeev VI***, Gatidis S, Qadri SM, Häussinger D, Kubitz R, Herebian D, Mayatepek E, Lang F, Lang KS, Lang PA.

Cell Physiol Biochem : 2016 April 07;38:1500-1509, DOI: 10.1159/000443091

6. Hyperammonemia in gene-targeted mice lacking functional hepatic glutamine synthetase.

Qvartskhava N, Lang PA, Görg B, **Pozdeev VI**, Ortiz MP, Lang KS, Bidmon HJ, Lang E, Leibrock CB, Herebian D, Bode JG, Lang F, Häussinger D.

Proc Natl Acad Sci U S A. 2015 Apr 28;112(17):5521-6. doi: 10.1073/pnas.1423968112.

7. CEACAM1 induces B-cell survival and is essential for protective antiviral antibody production.

Khairnar V, Duhan V, Maney SK, Honke N, Shaabani N, Pandyra AA, Seifert M, **Pozdeev V**, Xu HC, Sharma P, Baldin F, Marquardsen F, Merches K, Lang E, Kirschning C, Westendorf AM, Häussinger D, Lang F, Dittmer U, Küppers R, Recher M, Hardt C, Scheffrahn I, Beauchemin N, Göthert JR, Singer BB, Lang PA, Lang KS.

Nat Commun. 2015 Feb 18;6:6217. doi: 10.1038/ncomms7217.

8. T-cell STAT3 is required for the maintenance of humoral immunity to LCMV.

McIlwain DR, Grusdat M, **Pozdeev VI**, Xu HC, Shinde P, Reardon C, Hao Z, Beyer M, Bergthaler A, Häussinger D, Nolan GP, Lang KS, Lang PA

Eur J Immunol. 2015 Feb;45(2):418-27. doi: 10.1002/eji.201445060.

9. Involvement of Toso in activation of monocytes, macrophages, and granulocytes.

Lang KS, Lang PA, Meryk A, Pandyra AA, Boucher LM, **Pozdeev VI**, Tusche MW, Göthert JR, Haight J, Wakeham A, You-Ten AJ, McIlwain DR, Merches K, Khairnar

V, Recher M, Nolan GP, Hitoshi Y, Funkner P, Navarini AA, Verschoor A, Shaabani N, Honke N, Penn LZ, Ohashi PS, Häussinger D, Lee KH, Mak TW

Proc Natl Acad Sci U S A. 2013 Feb 12;110(7):2593-8. doi: 10.1073/pnas.1222264110. 2013 Jan 28.

10. IRF4 and BATF are critical for $CD8^+$ T-cell function following infection with LCMV.

Lang KS, Lang PA, Meryk A, Pandyra AA, Boucher LM, **Pozdeev VI**, Tusche MW, Göthert JR, Haight J, Wakeham A, You-Ten AJ, McIlwain DR, Merches K, Khairnar V, Recher M, Nolan GP, Hitoshi Y, Funkner P, Navarini AA, Verschoor A, Shaabani N, Honke N, Penn LZ, Ohashi PS, Häussinger D, Lee KH, Mak TW

Cell Death Differ. 2014 Jul;21(7):1050-60. doi: 10.1038/cdd.2014.19.

11. Reactive oxygen species delay control of lymphocytic choriomeningitis virus.

Lang PA, Xu HC, Grusdat M, McIlwain DR, Pandyra AA, Harris IS, Shaabani N, Honke N, Kumar Maney S, Lang E, **Pozdeev VI**, Recher M, Odermatt B, Brenner D, Häussinger D, Ohashi PS, Hengartner H, Zinkernagel RM, Mak TW, Lang KS.

Cell Death Differ. 2013 Jan 18. doi: 10.1038/cdd.2012.167.

12. Dynein light chain roadblock-type 1(DYNLRB1) interact with NDP-kinase from bovine retina.

Pagaev RM, Kakuev DL, **Pozdeev VI**, Kutuzov MA, Rakitina TV, Lipkin VM

Doklady Biochemistry and Biophysics, Vol 447, Issue 4, p.601-604 2012

13. Comparative studies in vivo of free and liposomal forms of photosensitizer on a base of hydrophilic derivative of chlorin e6.

Chan Thi Xai Ien, I.G. Meerovich, G.A. Meerovich, **Pozdeev VI**, S.Sh. Karshieva, O.L. Orlova, A.P. Polozkova, N.A. Oborotova

J. DRUG DEL. SCI. TECH., 22 (4) p.291-294 2012

14. Liposomal form of photoditazine.

Chan Thi Xai Ien, **Pozdeev VI**, G.A. Meerovich, S.Sh. Karshieva, L.M. Borisova, O.L. Orlova, A.P. Polozkova, G.V. Ramenskaya, N.A. Oborotova.

Russian journal of biotherapy Vol. 9, No. 2, 2010: p.105-107

15. Haponin (EIF1AD) Interacts with Glyceraldehyde 3-Phosphatedehydrohenase in CHO-K1 Cell Line

Rakitina TV, Bogatova OV, Smirnova EV, **Pozdeev VI**, Kostanian IA, Lipkin VM

Bioorg Khim, Moscow Vol. 36, No. 3, 2010: p.312-318

16. Medication for photodynamic therapy, method of obtaining claimed medication and method of carrying out photodynamic therapy with application of claimed medication.

Baryshnikov AJ, Loshchenov VB, Meerovich GA, Orlova OL, Oborotova NA, **Pozdeev VI**, Polozkova AP

Patent: RU 2428981 C1

*contributed equally and thus share first authorship

Curriculum vitae

Education

2012- 2016	**PhD student**, Institute of Molecular Medicine II	Heinrich-Heine-University Duesseldorf, Germany
2008 - 2010	**Master of Science** in Chemical Technology and Biotechnology "Synthesis and studying of biological properties of infrared photosensitizers based on alcoxybacteriopurpurinimides"	Moscow State Academy of Fine Chemical Technology Moscow, Russia;
2004 - 2008	**Bachelor of Science** in Chemical Technology and Biotechnology "Synthesis and in vivo studying of Bacteriochlorin p N-ethoxycycloimide alcoxyoxymemethyl ester"	Moscow State Academy of Fine Chemical Technology, Moscow, Russia

Research and working Experience

01.2012-10.2016	**PhD student,** Institute of molecular medicine II	Heinrich-Heine-University Duesseldorf, Germany
07.2011-11.2011	**Laboratory Assistant,** Department of combinatorial chemistry and chromatography	Chembridge corp., Moscow Russia
01.2008-12.2011	**Research Assistant,** Laboratory of Hormonal Reception Proteins	Institute of Bioorganic Chemistry, Moscow, Russia
01.2008-10.2010	**Research Assistant,** Laboratory of new drug formulations	Russian Cancer Research Center, Moscow, Russia

Eidesstattliche Erklärung

Ich versichere an Eides Statt, dass die Dissertation von mir selbstständig und ohne unzulässige fremde Hilfe unter Beachtung der „Grundsätze zur Sicherung guter wissenschaftlicher Praxis an der Heinrich-Heine-Universität Düsseldorf“ erstellt worden ist. Die Dissertation wurde in der vorgelegten oder in ähnlicher Form noch bei keiner anderen Institution eingereicht. Ich habe bisher keine erfolglosen Promotionsversuche unternommen.

Düsseldorf, den

Vitaly Pozdeev